FEDERAL UNIVERSITY OF PARANÁ

ANDRÉ LUIZ LANGNER

OBSERVABILITY ANALYSIS FOR POWER SYSTEMS MODELED AT THE SUBSTATION LEVEL INCLUDING PMU

CURITIBA

2016

ANDRÉ LUIZ LANGNER

OBSERVABILITY ANALYSIS FOR POWER SYSTEMS MODELED AT THE SUBSTATION LEVEL INCLUDING PMU

Dissertation submitted to the Graduate Program in Electrical Engineering from Federal University of Paraná, as partial fulfillment of the requirements for the degree of Master of Science in Electrical Engineering

Supervisor: Prof. Dr. Elizete Maria Lourenço

CURITIBA

2016

L283o Langner, André Luiz
Observability analysis for power systems modeled at the substation level including PMU/ André Luiz Langner. – Curitiba, 2016.
114 f. : il. color. ; 30 cm.

Dissertação - Universidade Federal do Paraná, Setor de Tecnologia, Programa de Pós-graduação em Engenharia Elétrica, 2016.

Orientador: Elizete Maria Lourenço .
Bibliografia: p. 97-101.

1. Rede elétrica. 2. Disjuntores elétricos. 3. Algoritmos. I. Universidade Federal do Paraná. II.Lourenço, Elizete Maria. III. Título.

CDD: 621.3192

STATEMENT OF APPROVAL

André Luiz Langner

Observability Analysis for Power Systems Modeled at the Substation Level Including PMU

Dissertation presented as partial fulfillment of the requirements for the degree of Master of Science of the Graduate Program in Electrical Engineering of the Federal University of Paraná.

Examination Board:

Prof. Dr. Elizete Maria Lourenço – Supervisor
Federal University of Paraná

Prof. Dr. Djalma Mosqueira Falcão – Guest
Federal University of Rio de Janeiro

Prof. Dr. Thelma Solange Piazza Fernandes – Guest
Federal University of Paraná

Prof. Dr. Alexandre Rasi Aoki – Guest
Federal University of Paraná

Curitiba, February 24th of 2016

Acknowledgements

First and foremost, I would like to express my deepest gratitude to my advisor, Professor Elizete Maria Lourenço, for her guidance, support, and patience throughout this M.S. study. It has been an honor and a great pleasure to be her research student.

I would like to extend my gratitude to Professors Djalma Mosqueira Falcão, Thelma Solange Piazza Fernandes and Alexandre Rasi Aoki for serving as my master's thesis committee members.

I also would express my gratitude to Professor Ali Abur, from Northeastern University, for his dedication with me during the time I have spent as visiting scholar at his laboratory. I am indebted to express my gratitude to my friend Murat Gol, who also contributed to this work.

Finally, I would like to give special thanks to my parents Edilson and Maristela Langner, and my beloved wife Simone Pontarolo Langner, for their endless love and support.

RESUMO

O Estimador de Estados tem papel fundamental no monitoramento e controle em tempo real de grandes sistemas de potência, sendo capaz de prover informações a respeito do mais provável estado de operação da rede. Os primeiros algoritmos de estimação de estados foram concebidos considerando o sistema inteiro modelado no nível barra-ramo, uma vez que o processador de topologia reduz o sistema em um modelo simplificado. Sendo assim, o presente trabalho foca na Estimação de Estados Generalizada, na qual chaves e disjuntores são considerados no modelo da rede, tendo seus respectivos estados estimados. A aplicação de medidas sincrofasoriais no processo de Estimação de Estados e nas análises de observabildiade e criticidade de medidas também fazem parte deste estudo. Neste trabalho são apresentadas duas formulações para o uso de medidas sincrofasoriais na Estimação de Estados Generalizada, bem como resultados que comprovam a aplicação das mesmas. Dentro da proposta principal, está o desenvolvimento de um algoritmo numérico para análise de observabilidade e criticidade de medidas em sistemas modelados no nível de subestação. Testes são conduzidos no sistema de 14 barras dos IEEE, considerando a modelagem explícita de algumas subestações, com diferentes configurações, e simulando situações de falha na comunicação de medidas e do status dos disjuntores. Os resultados mostram que os métodos implementados permitem a determinação da observabildiade do sistema além da deteção de medidas e restrições críticas. Casos de falha da método também são mostrados, bem como meios de mitigá-los. Uma importante constação é sobre a vantagem do uso das medidas sincrofasoriais na Estimação de Estados Generalizada, no qual sua aplicação elimina a criticidade de restrições operacionais, as quais são crítitas devido a topologia da rede e não pela quantidade e alocação de medidas.

Palavras chaves: Estimação de Estados. Generalizada. Análise de Observabilidade. Medidas Sincrofasoriais.

ABSTRACT

State Estimation (SE) plays a vital role in real-time monitoring and controlling of larger power systems, as it provides the most likely operation state, and helps to keep it working in a secure mode. The first SE algorithms were developed considering the entire system modeled at the bus-branch level since the topology processor reduces it in a simplified way. Having that in mind, this work is focused on the Generalized State Estimation approach, in which switches and circuit breakers are considered in the network model, with their status being estimated. The application of synchrophasor measurements in the process of State Estimation, observability and measurement criticality analyses, are also part of this study. This Master's thesis presents two formulations of using phasor measurements in the Generalized State Estimation, as well as the results of such approaches, ensuring their application. The main proposal is the development and deployment of a numerical algorithm to perform the observability and criticality analyses in power systems modeled at the bus-section level. Test are conducted over the IEEE 14 bus system considering the explicit modeling of three substations, with different layouts, and simulating situations of measurement and switch status failure. The results show that the deployed methods allow the determination of the system observability besides the detection of critical measurements and constraints. Cases where the method fails to provide desirable results as also discussed, as well as ways of mitigating them. An important statement regards the advantage of using synchrophasor measurements in the Generalized State Estimation, in which their application eliminates critical operational constraints, which are associated with the network topology, irrespectively of the measurement quantity and allocation.

Keywords: Generalized State Estimation. Observability Analysis. Synchrophasor Measurements.

LIST OF FIGURES

LIST OF ACRONYMS

CB - Circuit Breaker

EMS - Energy Management Systems

GPS - Global Positioning System

GSE - Generalized State Estimation

NTP - Network Topology Processor

OST - Observable Spanning Tree

PET - Power Education Toolbox

PMU - Phasor Measurement Unit

SE - State Estimation

TOA - Traditional Observability Analysis

TSE - Traditional State Estimation

TSO - Transmission System Operators

RTU - Remote Terminal Units

SCADA - Supervisory Control and Data Acquisition

WLS - Weighted Least Squares

CONTENTS

1 INTRODUCTION

Since the power systems have developed larger and more complex, and due to the growing demand for reliability and security, the usage of real-time monitoring and controlling of the entire system has become a necessity. Within that context, the State Estimation plays a vital role as it gathers snap shots from remote terminal units (RTU), via Supervisory Control and Data Acquisition (SCADA) system, which provides visualization from the power plants to great load centers.

On account of it, the State Estimation method for Power System operation, introduced by Fred Schweppe at the beginning of 70´s (SCHWEPPE, F.; WILDES, 1970), have been benefiting a great number of theoretical advances and practical applications. Nowadays, SE is the backbone of modern Energy Management Systems (EMS), and it provides the most likely state of operation.

Most of the commercial State Estimators (SE) adopt the so-called bus-branch model of SE formulation. In such approach, a network topology processor (NTP) reduces the system assuming correct information regarding switches and circuit breaker status. Hence, it avoids the physical representation of switches and circuit breakers, scaling down the size and complexity of the network.

In spite of the advantages of using the bus-branch model, there might occur some drawbacks. For instance, it does not allow a detailed representation of substations arrangements; switches and circuit breakers measurements may be lost, as well as topology errors cannot be detectable.

To cope with such problems, Monticelli and Garcia (1991) proposed a new way of modeling switches and breakers in order to have more information acquired from SE algorithms, allowing the processing of topology erros. With the Generalized State Estimation (GSE) it was possible not only estimate the conventional states (voltage phasors of all buses) but also the switches and circuit breakers status, as much as the power flow through them.

More recently, the advent of synchronized phasor measurements has also aided the power system operation area, since such devices provide timestamp in

Global Positioning Systems (GPS) synchronized measurements with a high accuracy and precision.

These being said, the main motivation of this work is to explore the use of synchronized phasor measurements in the Generalized State Estimation, as such field of research has not been fully studied yet. Although other works have demonstrated that Phasor Measurement Units (PMU) can benefit the observability and criticality analysis, most of them focus in power systems modeled at the bus-branch level. Therefore, there is a lot to be explored when the modeling of switches and circuit breakers comes out.

This first chapter presents a state of the review, by briefly showing the advances in the area of Power System State Estimation, the evolution of Observability methods as well as the advent of synchronized phasor measurements. Along with that, it also depicts the objectives and an outline of this work.

1.1 STATE OF THE ART REVIEW

The State Estimation technique was first introduced in the Power System area by Schweppe in the 70’s, in a series of three papers that presented the Exact Model (SCHWEPPE, F.; WILDES, 1970), the approximate model (SCHWEPPE; ROM, 1970), and implementation issues regarding computational limitations (SCHWEPPE, 1970). Although the problem of observability had not been formally recognized in the former papers, the authors addressed questions about the meter placement in the estimator performance.

1.1.1 Observability Analysis

Observability issues started to gain more attention after 1973 when many researchers addressed efforts to consolidate methods to perform such analyses. In the 80’s, selected research groups published a variety of papers establishing methodologies to determine the system observability. They proposed algorithms to determine the system observability, and along with those when the network is found

unobservable, methods of finding observable islands and placing measurements to restate the system observability.

One of these research groups, compounded by Krumpholz, Clements and Davis, focused on the Topological methodology to assess the system observability. One of their papers (KRUMPHOLZ; CLEMENTS; DAVIS, 1980), discloses a practical algorithm using the network topology to find a full rank spanning tree, which renders the system observable. The algorithm finds such a spanning tree using a combinatorial method and the graphs theory, which firstly processes the lines flow measurements. Then, it processes the boundary injections, aiming at finding the so-called spanning three, in an iterative manner. Besides evaluating the network observability, the algorithm also identifies observable islands, for unobservable systems, and it makes use of pseudo measurements to make the system observable.

In another paper, Clements, Davis and Krumpholz, (1981) emphasized the problem of identification of critical measurements, which directly affects the detection and identification of Bad Data. Other papers from this group disclosed modified algorithms as a means to deal with measurement deficiency (CLEMENTS; KRUMPHOLZ; DAVIS, 1982) so as to find maximal observable sub networks, as well as to place measurements to recover the network observability (CLEMENTS; KRUMPHOLZ; DAVIS, 1983).

Quintana, Simões Costa and Mandel (1982) propose a method to determine the network observability through a Topological approach. In this paper, they used the Graph Theory approach over Matroid Intersections. In the first place, the algorithm finds an observable spanning tree processing the flow measurements, and so it does with the injection measurements afterwards, by making use of a color scheme. They also present the method results through tests in a realistic model of the Brazilian Power System with 121 buses. In addition to that, the same researchers have also investigated the critical measurements and the detectability of measurements errors over their proposed algorithm (SIMÕES COSTA; PIAZZA; MANDEL, 1990).

The work of Nucera and Gilles (1991) have also focused on the Topological approach by employing an optimal combinatorial algorithm. They compared their

developments to the Krumpholz; Clements and Davis (1980)' algorithms, which revealed good advances in the computing process time.

Back in the 80's, other researchers laid efforts on another approach to carry out observability analysis. Monticelli and Wu have worked with the numerical methods, and in two papers they explained the methodology used (MONTICELLI; WU, 1985a, 1985b). The first paper presents a complete theory about observability, with definitions, theorems and proofs of the determination of network observability, unobservable states, and identification of observable islands. The second one depicts the deployment of the algorithms to determine the system observability and to identify observable islands, by using the Jacobian and Gain matrix of the measurements. The algorithms are iterative and both discuss the effects of irrelevant injection measurements. A third paper from Monticelli and Wu proposed the orthogonal transformations, as a means to circumvent ill-conditioning problems faced by numerical methods (MONTICELLI; WU, 1986).

Falcão and Arias (1994) describe a numerical method through the factorization of the linearized models in the echelon form, representing an evolution of the least absolute value state estimation method. Along with that, they present a discussion regarding critical measurements and Bad Data processing. Expósito, Abur and Ramos (1995) investigate the use of loop equations as an alternative to traditional formulation of the State Estimation, as well for observability purposes. They also explore the use of current measurements (more abundant in distribution networks) which causes multiple solutions due to the unlikelihood of determining the current direction (ABUR; EXPÓSITO, 1997). After that, they use the loop equations to determine the network observability regarding current measurements (EXPÓSITO; ABUR, 1998).

More recently, Gou and Abur (2000) offer a direct method to carry out the observability analysis. The method consists of performing the triangular factorization of the Gain matrix, manipulating the resulting lower and diagonal matrices by making use of a numerical approach. The above-mentioned technique presents advantages as it does not require the elimination of both irrelevant branches and irrelevant injection measurements. The authors also suggest an algorithm for pseudo measurements placement in order to restore the system observability in an iterative manner. As a

matter of fact, in a second paper they propose an improved pseudo measurements placement algorithm through a direct way (GOU; ABUR, 2001). Gou (2006) also suggests a method for observability analysis based on the direct use of the Jacobian matrix.

London, Alberto and Bretas (2007) introduce a new tool for assessing measurement sets in the light of network observability, restoration, and identification of critical measurements and critical sets. The method finds the critical information using only the network-topology data over the concepts of the H_{Δ} matrix, which is processed by triangular factorization of the Jacobian matrix. Benedito *et al.* (2008) also use concepts of the H_{Δ} matrix, though for purposes of observability and identification of observable islands, based on path graphs.

Almeida, Asada and Garcia (2008) disclose a direct numerical method for observability analysis based on Gram matrix factorization, along with another method to identify observable islands based on minimum norm solutions. They argue that the method is easy of deploying thanks to its use for information already in State Estimation (SE) routines, as well as for its capability of dealing with irrelevant measurements and detecting observable islands. Another numerical method to determine the network observability and identify observable islands, based on a numerical approach was proposed by Silva, Simões Costa and Lourenço (2011) in which it uses orthogonal Givens rotation. The methodology does not account Gain matrix since it operates directly on the Jacobian matrix.

In summary, the Topological methods have advantages due to the fact that they do not use floating point calculations, what may cause round-off errors (NUCERA; GILLES, 1991). On the other hand, Numerical methods are easy to deploy as they allow the employment of an already existing subroutines in a State Estimation program (MONTICELLI; WU, 1985b). Aiming at taking advantage of the aforementioned approaches, Korres and Katsikas (2003) introduce an hybrid method for observability analysis. In short, the method firstly processes the flow measurements based on a topological approach, forming the observable islands. After that, the boundary injection measurements are retained for numerical analysis. Furthermore, in another paper,

they illustrate a numerical method for topological observability analysis, using concepts of the graph theory and echelon form (KORRES *et al.*, 2003).

1.1.2 Generalized State Estimation

All the foregoing methodologies were proposed considering the power system modeled at the so-called bus-branch level, in which the substations are modeled by buses and transmission lines and transformers by their equivalent PI model. According to Abur and Exposito (2004) the topology processor converts a bus section/switch detailed model into a compact bus-branch model. In other words, it determines the simplified model of the power system through the available data of measurements and circuit breaker (CB) statuses.

Irving and Sterling (1982) were the first to investigate the use of substation data for purposes of measurement error detection and correction, and Monticelli and Garcia (1991) propose a new approach to run State Estimation algorithms in networks modeled at the bus-section level. Their method allows the exact model of zero impedance branches, as it applies the power flows through circuit breakers as new state variables. Monticelli also published two more papers focusing on this approach (MONTICELLI, 1993a, 1993b), setting the basis of the so-called Generalized State Estimation (GSE) (ALSAC *et al.*, 1998).

The extension of the numerical observability analysis was addressed by Monticelli (1993b), in which the new state variables (the power flows through circuit breakers) are represented by extra columns in the measurement Jacobian matrix. The rank determination also provides information regarding the network observability. The observable islands are found by means of the same approach of Monticelli and Wu (1985b). Katsikas and Korres also worked with the numerical approach, unfolding a direct method (KATSIKAS; KORRES, 2003), along with a simplified model, whose purpose is to reduce the computation burden (KORRES; KATSIKAS, 2005).

The observability topological approach for systems modeled at the substation level (bus section/switch level) was investigated by Simões Costa, Lourenço and Clements (2002), as a means of extending the conventional method of graph theory.

Such method includes power flows through circuit breakers (switching branches) as new state variables, aiming at finding an observable spanning tree of full rank. In addition to it, the concept used to find critical measurements and critical constraints was extended.

1.1.3 Synchronized Phasor Measurement Units

The advent of GPS (Global Positioning System) synchronized measurements, along with the use of microprocessors into substations has allowed measuring positive sequence voltage phasors and positive sequence current phasors (PHADKE; THORP, 1986). Also known as PMU (Phasor Measurement Units), had its origin in the development of a Symmetrical Component Distance Relay (SCDR) in the 70´s for protection purposes (PHADKE; IBRAHIM; HLIBKA, 1977). Since then, it has enhanced the state estimation performance (THORP; PHADKE; KARIMI, 1985).

Thorp, Phadke and Karimi (1985) present the concepts of using synchronized measurements for state estimation purposes. It has been demonstrated that the capability of directly measuring a state, the voltage angle, was able to improve the convergence rates of the existing algorithms. Data reduction feature has also been reported, in which the flow measurements are replaced by angle measurements. However, such strategy has proven jeopardize the rejection of bad data. In another paper, the same authors depict an algorithm that incorporates phasor measurements in the state estimation problem (PHADKE; THORP, 1986).

Many researchers have presented different methodologies to use synchronized phasor measurements in conjunction with SCADA measurements in state estimation algorithms. Zhou *et al.* (2006) propose the use of phasor measurements in a post processing linear estimator. In this approach, the SCADA/conventional measurements are processed by a non-linear estimator, and the phasor measurements processed afterward, with the results of the first stage. Nuqui and Phadke (2007) have worked in the same way, presenting a hybrid linear state estimator. Manousakis *et al.* (2013), in turn, propose to process the phasor measurements first, in a linear estimator, and use the estimates as measurements with

high weights, or equality constraints, in a non-linear estimator. Another approach is to use SCADA/conventional measurements in conjunction with phasor measurements; converting current phasor measurements into power flow ones is also an alternative (ATANACKOVIC *et al.*, 2008).

Zhu and Abur (2007) investigate the effects of choosing a reference bus angle in the presence of PMU. They pointed out that if the slack bus has no PMU placed, it may cause inconsistencies during the state estimation process. On the other hand, if the slack bus has a PMU placed, it will have to provide accurate measurements. Otherwise, errors will not be detectable biasing the final estimate. Their proposal does not choose a reference bus in the presence of PMU, a fact that provides better results for bad data detectability purposes.

In the light of observability analysis, many researchers suggested techniques for optimal placement of PMU, in order to render a given power network fully observable with a minimum number of measurements. Baldwin *et al.* (1993) and Nuqui and Phadke (2005) have worked with the topological approach and a simulated annealing technique to find optimal measurement design. Xu and Abur (2004) use the numerical approach with the intent of finding an optimal meter placement, over an integer programming technique and so did Chen and Abur (2006), but for purposes of bad data detection. Koutsoukis *et al.* (2013) used a Recursive Tabu Search method for optimal placement.

Out of the optimal placement techniques, London *et al.* (2009) propose the use of the H_{Δ} for redundancy and observability purposes, regarding conventional and PMU measurements, and Korres and Manousakis (2012) use a hybrid algorithm for observability checking and restoration.

The majority of the methodologies that made usage of synchronized phasor measurements for purposes of SE and observability analysis have been carried out considering the PMU capable of measuring all the adjacent lines of a given bus, which means, unlimited channel numbers. However, the existing PMU come with a limited number of channels, as recognized by Korkali and Abur (2009), who proposed an optimal placement approach regarding this limitation. In the same way, Emami and Abur (2010) suggest a robust measurement design considering the PMU capable of

measuring the voltage phasor of a given bus, and only one adjacent line, called “branch PMU”.

Another possible drawback, such as the availability of only synchronized current phasor measurements was investigated by Gol and Abur (2013). They propose a new methodology to include voltage magnitude measurements in the observability and criticality analysis, in which PMU can only provide current phasor measurements. The method handles an incidence matrix, which relates the states to measurements by using the reduced echelon form for observability purposes, as well as to form a sensitivity matrix to find critical measurements.

Regarding modern substations, the use of PMU inside of it has been investigated by Jaén, Romero and Expósito (2005) whose work attempts to thoroughly measure the substation through intelligent electronic devices (IED). Such devices are effective for providing voltage and current magnitude, as well as angles. In this paper, a three-phase Generalized State Estimator (GSE) was recommended for validation of substation data.

On its turn, Yang, Sun and Bose (2011a, 2011b) also came up with a relevant paper using phasor measurements, in the context of substation level SE. It firstly processes current phasor measurements pondering current in CBs as states, and it aims at identifying CB status errors.

1.2 DISSERTATION OBJECTIVES

This Master’s work focus on the research field of Power System State Estimation, aiming to develop new techniques for real time modeling and analysis. This field involves studies of topology and measurements errors, as well as observability analysis in the generalized approach, considering the explicit modeling of switches and circuit breakers. Since the synchronized phasor measurements units have become a reality in power systems, and its benefits can boost the state estimation algorithms, the application of such devices for State Estimation purposes are also one of the major points of the research.

In the light of it, the main objective here is to further study the use of synchronized phasor measurements for observability and measurement criticality purposes, considering the power system modeled at the bus-section level. It also aims to propose a new technique to carry out such analyses considering modern methods, already applied to systems modeled at the bus-branch model.

The specific objectives are the following:

- To evaluate the main methods of observability analysis and computational algorithms, such as topological and numerical ones;
- To implement phasor measurements on the already developed Generalized State Estimator algorithm;
- To develop a suitable algorithm to provide observability and measurement criticality analysis in power system modeled at the bus-section level;
- To validate the developed algorithm over an IEEE benchmark test system.

1.3 DISSERTATION OUTLINE

This dissertation comprises six chapters and it is organized as follow: in the current chapter, it is presented an introduction of this work, a literature review, motivations for conducting such a research, and an outline regarding its contributions.

In the succeeding chapter, the methodology of State Estimation for power systems modeled at the bus-branch level, as well as for power systems modeled at the bus-section level is depicted. Furthermore, it also discusses the use of phasor measurements, and its implications.

Chapter 3 covers the methodology related to the Observability analysis. Consequently, the numerical approach is presented in details, as it is the method adopted in this work. A brief review of the topological approach is as well introduced. In addition, this chapter also presents both observability approaches for power systems modeled at the bus-branch level and bus-section level. Chapter 4 acknowledges the method of Observability and Criticality analysis for power systems modeled at the bus-section level, emphasizing the use of phasor measurements. Moreover, the method is

presented with tutorial examples in a small system and an algorithm summarizes the process at the end.

Chapter 5 reveals the results of the proposed method in the well-known IEEE 14 bus system, bearing in mind some substations modeled in detail. The test cases illustrate possible situations for system operators, and the results show the advantages of using phasor measurements inside the substations. Finally, in chapter 6, the main contributions are outlined and discussed, as well as possible further studies.

2 POWER SYSTEM STATE ESTIMATION

This chapter aims at presenting the concepts of the Traditional formulation of state estimation (TSE) in which the network is modeled by the bus-branch model; the Generalized State Estimation (GSE), where the bus section level or substation level of the network is also taken into account. In addition to those, the chapter also discusses and portrays two different approaches for the type of measurement processed by the state estimator. In the first instance, both TSE and GSE are formulated considering that the set of available measurements is composed only of conventional measurements, which are: power flow, power injection, and voltage magnitude measurements. In the second instance, the modifications required to include synchronized phasor measurements units (PMU) are deliberated and described.

2.1 TRADITIONAL STATE ESTIMATION

This section presents the formulation of Traditional State Estimation in which conventional measurements, such as power flow, power injections, and voltage magnitudes, are pondered.

2.1.1 SE with Conventional Measurements

Traditional State Estimation (TSE) refers to a procedure for obtaining all the voltage phasors of a given power network (ABUR; EXPÓSITO, 2004). The system is modeled by the bus-branch model; buses represent the substations, and PI models indicate the transmission lines and transformers. Figure 1 portrays a power system at the bus-branch model.

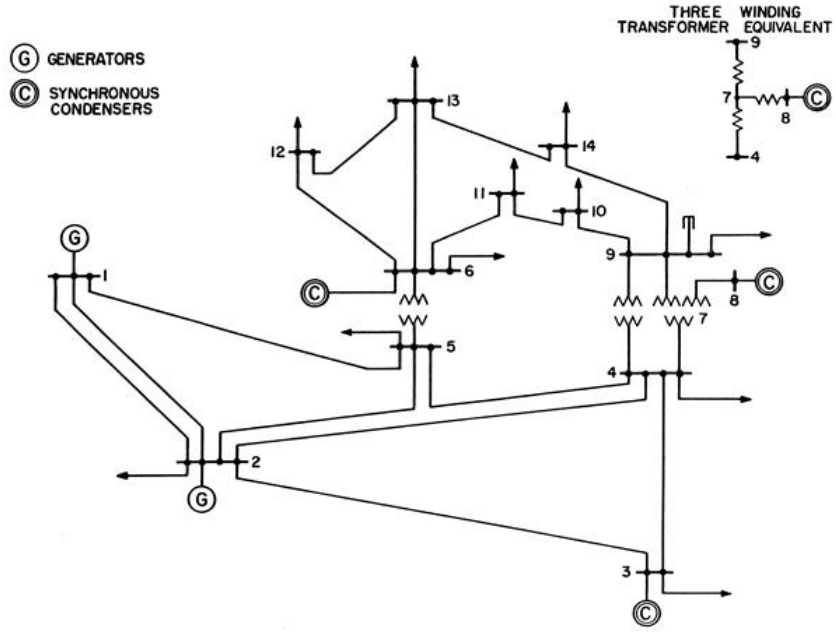

Figure 1 – IEEE 14 Bus System – Bus-branch Model
Source: University of Washington (2015)

In the TSE, SCADA system gathers all the real-time measurements spread all over the power system, and it process them in the control center. SE algorithms will provide the most likely estimated states of the entire network if the system is observable. Since real time measurements contain errors, and such errors have a Gaussian (Normal) distribution, its variance depends on the measuring device precision. Thus, the procedure for obtaining the estimated states uses a statistical approach.

The classical and established SE method is the Weighted Least Squares (WLS), which relies on the following measurement model, shown in Eq. (1).

$$z = h(x) + e \tag{1}$$

where:

z: is the measurement vector, with size m;

x: is the state vector, with size n;

$h(x)$: is the nonlinear function relating the measurements to the system states;

e: is the vector of measurements errors;

m: is the number of measurements;

n: is the number of states.

The state vector x has a dimension of $2N - 1$, where N is the number of the buses, and is given by Eq. (2).

$$x = [\ \theta_2 \quad \theta_3 \quad \dots \quad \theta_n \quad V_1 \quad V_2 \quad V_3 \quad \dots \quad V_n]^T. \tag{2}$$

In Eq. (2) the bus 1 is chosen as the slack bus, with the phase angle set to zero, what provides a system reference. Eq. (3) represents the measurement function $h(x)$ vector, which relates each measurement to the state variables:

$$h(x) = \begin{bmatrix} P_{km} \\ P_k \\ Q_{km} \\ Q_k \\ V_k \end{bmatrix}. \tag{3}$$

where:

P_{km}: refers to active power flow measurements from a generic bus k to bus m;

P_k: refers to active power injection measurements at a generic bus k;

Q_{km}: refers to reactive power flow measurements from a generic bus k to bus m;

Q_k: refers to reactive power injection measurements at a generic bus k;

V_k: refers to voltage magnitude measurements at a generic bus k;[1].

[1]Please refer to Appendix A for further description of all measurement equations.

The purpose of the WLS SE is to obtain the state variables, which minimizes the following objective function, presented in the Eq. (4) (ABUR; EXPÓSITO, 2004; SCHWEPPE, FRED C; WILDES, 1970):

$$J(x) = \sum_{i=1}^{m} (z_i - h_i(x))^2 \Big/ R_{ii} = [z - h(x)]^T R^{-1} [z - h(x)] \quad (4)$$

where:

R: is a diagonal covariance matrix, given by $R = diag\{\sigma_1^2, \sigma_2^2, \dots, \sigma_m^2\}$.

In others words, the WLS SE aims at minimizing the sum of weighted measurement residues.

A minimum is found once the first-order optimality conditions are satisfied (ABUR; EXPÓSITO, 2004), and it is achieved by a first-order approximation, given in Eq. (5):

$$g(x) = \frac{\partial J(x)}{\partial x} = -H^T(x) R^{-1} [z_i - h_i(x)] = 0 \quad (5)$$

where:

$H(x)$: is the Jacobian matrix, given by Eq. (6). [2]

[2] Please refer to Appendix A for further description of all Jacobian equations.

$$H(x) = {}^{\partial h(x)}/_{\partial x} = \begin{bmatrix} {}^{\partial P_{km}}/_{\partial \theta} & {}^{\partial P_{km}}/_{\partial V} \\ {}^{\partial P_{k}}/_{\partial \theta} & {}^{\partial P_{k}}/_{\partial V} \\ {}^{\partial Q_{km}}/_{\partial \theta} & {}^{\partial Q_{km}}/_{\partial V} \\ {}^{\partial Q_{k}}/_{\partial \theta} & {}^{\partial Q_{k}}/_{\partial V} \\ {}^{\partial V_{k}}/_{\partial \theta} & {}^{\partial V_{k}}/_{\partial V} \end{bmatrix}. \quad (6)$$

By expanding the nonlinear function $g(x)$ into its Taylor series around the state vector x^k, and by neglecting the higher order terms, it can lead to an iterative solution scheme, given in Eq. (7):

$$G(x^k)\Delta x^{k+1} = H^T(x^k)W[z - h(x^k)] \quad (7)$$

where:

$G(x^k) = H^T(x^k)WH(x^k)$: is the Gain matrix;

$W = R^{-1}$: is the weighting matrix;

$\Delta x^k = x^{k+1} - x^k$, being k the iteration index.

Abur and Expósito (2004) present a step by step algorithm to solve the traditional state estimation problem, which is summarized as follows:

1. Set iteration index k equal to zero;
2. Initialize the state vector x^k in a flat start (voltage magnitudes equal to one and voltage angle equal to zero);
3. Calculate the Gain matrix $G(x^k)$;
4. Calculate the equation $H^T(x)R^{-1}[z_i - h_i(x^k)]$;
5. Determine Δx^k;
6. Test for convergence, i.e. $\max|\Delta x^k| \leq \epsilon$, where ϵ is the tolerance;
7. If the tolerance is attained, stop. If not, update $x^{k+1} = x^k + \Delta x^k$, $k = k + 1$, and go back to step 3.

2.1.2 SE with Synchronized Phasor Measurements

The PMU advent recalls as a distance relay with symmetrical components, developed in the 70´s at Virginia Tech Laboratory (PHADKE; IBRAHIM; HLIBKA, 1977). The capability of obtaining synchronized measurements with GPS time stamp has developed important advances, for instance: PMU provides the magnitude and the angle of the voltage at the bus where it is connected; it is usable as a measurement in the state estimation equations and it does not required to set a slack bus, as reported in (ZHU; ABUR, 2007). Hence, the state vector must include all the voltage angles and magnitudes, with a dimension $2N$, as presented in Eq. (8).

$$x = [\,\theta_1 \quad \theta_2 \quad \theta_3 \quad \ldots \quad \theta_n \quad V_1 \quad V_2 \quad V_3 \quad \ldots \quad V_n]^T. \tag{8}$$

PMU not only provides the voltage phasors but it also can provide current phasor measurements of adjacent power lines, depending upon the number of channels (KORKALI; ABUR, 2009). This way, the current phasors may also be included as measurements in state estimation equations.

Considering the current flow from a bus to another, one can say that it is usually measured and transmitted in the polar form, i.e. current magnitude (I_{km}) and angle (δ_{km}). It is preferable, however, to use them in the rectangular form, due to numerical problems in case of either lightly load systems or flat start initialization (KORRES; MANOUSAKIS, 2011). Notwithstanding, the rectangular coordinates present disadvantage as it will amplify errors of PMU measurements (KORRES; MANOUSAKIS, 2011). Such conversion is simple to apply, as it can be seen at the set of Eq. (9).

$$\begin{aligned} I_{km}^{Re} &= I_{km}\cos(\delta_{km}) \\ I_{km}^{Im} &= I_{km}\sin(\delta_{km}) \end{aligned} \tag{9}$$

where:

I_{km}^{Re} and I_{km}^{Im}: refers to the real and imaginary parts of phasor current measurement;

I_{km}: refers to the phasor current magnitude, measured by PMU;

δ_{km}: refers to the phasor current angle, measured by PMU.

Thus, the measurement function equations and Jacobian matrix elements must be properly adapted to accommodate the new measurements, as follows:

$$h(x) = \begin{bmatrix} P_{km} \\ P_k \\ Q_{km} \\ Q_k \\ V_k \\ \theta_k \\ I_{km}^{Re} \\ I_{km}^{Im} \end{bmatrix} \tag{10}$$

$$H(x) = {\partial h(x)}/{\partial x} = \begin{bmatrix} {\partial P_{km}}/{\partial \theta} & {\partial P_{km}}/{\partial V} \\ {\partial P_k}/{\partial \theta} & {\partial P_k}/{\partial V} \\ {\partial Q_{km}}/{\partial \theta} & {\partial Q_{km}}/{\partial V} \\ {\partial Q_k}/{\partial \theta} & {\partial Q_k}/{\partial V} \\ {\partial V_k}/{\partial \theta} & {\partial V_k}/{\partial V} \\ {\partial \theta_k}/{\partial \theta} & {\partial \theta_k}/{\partial V} \\ {\partial I_{km}^{Re}}/{\partial \theta} & {\partial I_{km}^{Re}}/{\partial V} \\ {\partial I_{km}^{Im}}/{\partial \theta} & {\partial I_{km}^{Im}}/{\partial V} \end{bmatrix}. \tag{11}$$

By deriving the current phasor flow equations as a function of the power flows, it is possible to determine the partial derivatives of the Jacobian matrix, as follows:

$$I_{km}^{Re} = \frac{P_{km}\cos(\theta_k) + Q_{km}\sin(\theta_k)}{V_k}$$

$$I_{flow}^{Im} = \frac{P_{km}\sin(\theta_k) - Q_{km}\cos(\theta_k)}{V_k} \quad (12)$$

where:

V_k: refers to the voltage magnitude at the sending bus k, measured by the PMU;

θ_k: refers to the voltage angle at the sending bus k, measured by the PMU.

Having the above mentioned in mind, the partial derivatives of real part of the current phasor will be:

$$\frac{\partial I_{km}^{Re}}{\partial \theta_k} = \frac{1}{V_k}\left[\cos(\theta_k)\left(\frac{\partial P_{km}}{\partial \theta_k} + Q_{km}\right) - \sin(\theta_k)\left(\frac{\partial Q_{km}}{\partial \theta_k} - P_{km}\right)\right]$$

$$\frac{\partial I_{km}^{Re}}{\partial \theta_m} = \frac{1}{V_k}\left[\frac{\partial P_{km}}{\partial \theta_m}\cos(\theta_k) + \frac{\partial Q_{km}}{\partial \theta_m}\sin(\theta_k)\right] \quad (13)$$

$$\frac{\partial I_{km}^{Re}}{\partial V_k} = \frac{1}{V_k}\left[\frac{\partial P_{km}}{\partial V_k}\cos(\theta_k) + \frac{\partial Q_{km}}{\partial V_k}\sin(\theta_k)\right] - \frac{1}{V_k^2}\left[P_{km}\cos(\theta_k) + Q_{km}\sin(\theta_k)\right]$$

$$\frac{\partial I_{km}^{Re}}{\partial V_m} = \frac{1}{V_k}\left[\frac{\partial P_{km}}{\partial V_m}\cos(\theta_k) + \frac{\partial Q_{km}}{\partial \theta V_m}\sin(\theta_k)\right].$$

Considering partial derivatives of imaginary part of the current phasor:

$$\frac{\partial I_{km}^{Im}}{\partial \theta_k} = \frac{1}{V_k}\left[\cos(\theta_k)(P_{km} - \frac{\partial Q_{km}}{\partial \theta_k}) + \sin(\theta_k)(Q_{km} + \frac{\partial P_{km}}{\partial \theta_k})\right]$$

$$\frac{\partial I_{km}^{Im}}{\partial \theta_m} = \frac{1}{V_k}\left[\frac{\partial P_{km}}{\partial \theta_m}\sin(\theta_k) - \frac{\partial Q_{km}}{\partial \theta_m}\cos(\theta_k)\right] \quad (14)$$

$$\frac{\partial I_{km}^{Im}}{\partial V_k} = \frac{1}{V_k}\left[\frac{\partial P_{km}}{\partial V_k}\sin(\theta_k) - \frac{\partial Q_{km}}{\partial V_k}\cos(\theta_k)\right] - \frac{1}{V_k^2}[P_{km}\sin(\theta_k) - Q_{km}\cos(\theta_k)]$$

$$\frac{\partial I_{km}^{Im}}{\partial V_m} = \frac{1}{V_k}\left[\frac{\partial P_{km}}{\partial V_m}\sin(\theta_k) - \frac{\partial Q_{km}}{\partial \theta V_m}\cos(\theta_k)\right].$$

Moreover, there are the partial derivatives of voltage angle measurements, which are linearly related to the states, so that:

$$\frac{\partial \theta_k}{\partial \theta_k} = 1, \frac{\partial \theta_k}{\partial \theta_m} = 0, \frac{\partial \theta_k}{\partial V_k} = 0, \frac{\partial \theta_k}{\partial V_m} = 0 \quad (15)$$

After such modifications, the process for obtaining the states is the same as that one from the previous section, applying the normal equation and performing the previous algorithm.

2.2 GENERALIZED STATE ESTIMATION

Basically, there are three steps for real time modeling of a power network: (i) network configuration analysis; (ii) observability analysis; (iii) state estimation and bad data processing (MONTICELLI, 1993a). In the first one, a topology processor gathers all the logical information from switches and circuit breakers (CB) status, so that it forms the bus-branch model and it performs the next steps. In spite of it, the topology processor may create an incorrect network model if a wrong status of a CB arises, hampering all results obtained with such a model.

The generalized approach has been developed to circumvent topology problems that cannot be detected by the topology processor. As proposed by Monticelli and Garcia (1991), the switches and circuit breakers are modeled in conjunction with PI models of transmission lines and transformers, in the so-called bus-

section/switching-device level, or substation level model. Figure 2 shows the IEEE 14 bus system at the substation level.

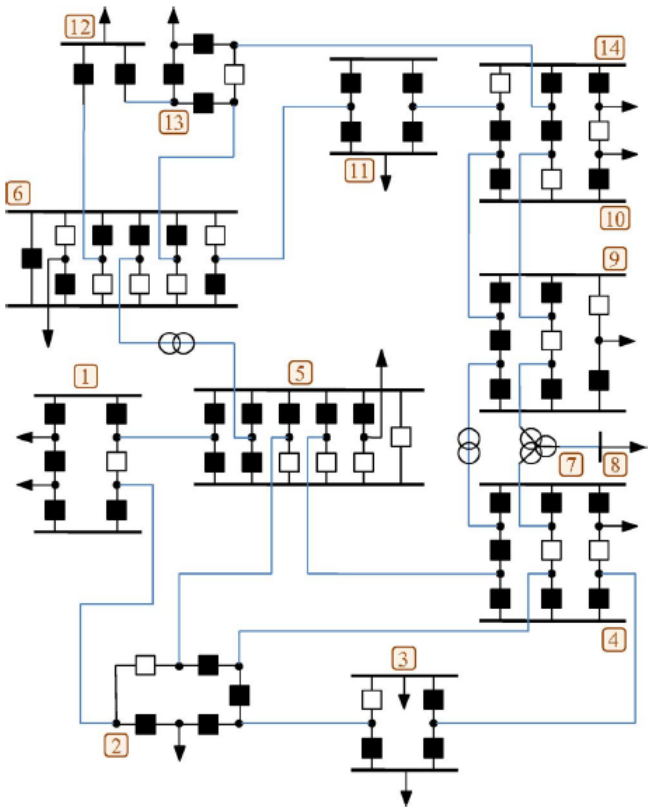

Figure 2 – IEEE 14 Bus System at the Substation Level
Source: (CARO; CONEJO; ABUR, 2010)

Furthermore, power flows through switches and circuit breakers (from now on referred to as *switching branches*) are treated as state variables to be estimated within such approach. Thus, the use of infinite and null values of impedances in the model might be disregarded, since they cause numerical ill-conditioning problems, as pointed out in Monticelli and Garcia (1991). Figure 3 shows a switching branch between buses *k* and *l.* In this case, the active and reactive power flow from bus *k* to *l* are included as new state variables.

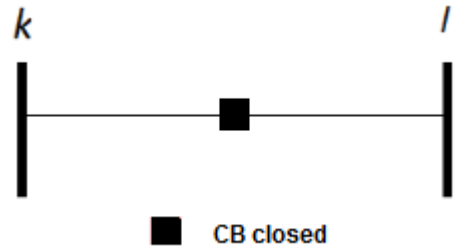

Figure 3 – Closed Switch/Breaker from Bus k to l

By doing so, the use of branches with atypical values is avoided, while the size of the state vector enlarges, as shown in Eq. (16).

$$x = [\theta_2 \quad \theta_3 \quad \dots \quad \theta_n \quad V_1 \quad V_2 \quad V_3 \quad \dots \quad V_n \ \dots \ t_{kl} \ u_{kl}]^T \tag{16}$$

where:

t_{kl}: indicates active power flow through switching branch $k - l$;

u_{kl}: indicates reactive power flow through switching branch $k - l$.

So far it has been discussed the inclusion of switches and circuit breakers in the network model for state estimation purposes. The following subsections depict two different formulations of the GSE: one that uses conventional measurements, and another one that combines the use of conventional and synchronized phasor measurements.

2.2.1 GSE with Conventional Measurements

Taken into account only conventional measurements, the available power flow measurements on switching branches are no longer modeled as a function of voltage phasors. Instead, they are directly related to the new state variables. Referring to Figure 4, Eq. (17) and (18) demonstrate the GSE approach when it comes to power flow measurement through a switching branch.

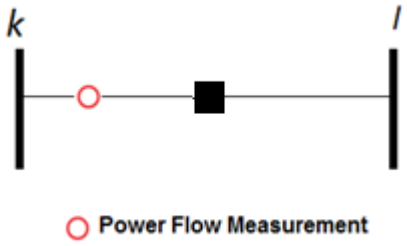

Figure 4 – Power flow measurements on a switching branch

$$z_{t_{kl}} = t_{kl} + \varepsilon_{t_{kl}} \tag{17}$$

$$z_{u_{kl}} = u_{kl} + \varepsilon_{u_{kl}} \tag{18}$$

Injection measurements on boundary buses, i.e. buses connecting switching branches with transmission lines, must consider the sum of power flows in conventional branches and the power flows through switching branches. Referring to Figure 5, Eq. (19) and (20) demonstrate the formulation. The ticker line is a conventional branch, with a PI model.

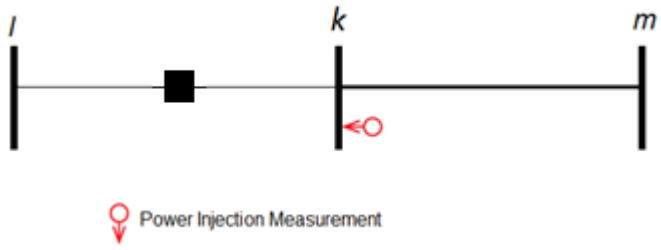

Figure 5 – Power Injection Measurement in a boundary bus

$$z_{P_k} = \sum_{m \in \Omega_k} P_{km}(\theta_k, \theta_m, V_k, V_m) + \sum_{l \epsilon \Gamma_k} t_{kl} + \varepsilon_{P_k} \tag{19}$$

$$z_{Q_k} = \sum_{m \in \Omega_k} Q_{km}(\theta_k, \theta_m, V_k, V_{km}) + \sum_{l \epsilon \Gamma_k} u_{kl} + \varepsilon_{Q_k} \quad (20)$$

where:

P_{km} and Q_{km}: are power flows through conventional branch $k - m$;

t_{kl} and u_{kl}: are power flows through switching branch $k - l$;

Ω_k: is the set of conventional branches incident to bus k;

Γ_k: is the set of switch/breaker branches incident to bus k.

The status of CB can be modeled as pseudo measurements (MONTICELLI, 1993b) with high weights, or as operational constraints in an optimization problem (SIMÕES COSTA; LOURENÇO; CLEMENTS, 2002).

If a CB is closed (Figure 3), the angle difference and voltage drop between its nodes are set equal to zero, as presented in the set of Eq. (21). On the other hand, if the CB is open (Figure 6), the power flows through it is set equal to zero, as in the set of Eq. (22).

$$\Delta\theta_{kl}^{p} = \theta_k - \theta_l = 0$$
$$\Delta V_{kl}^{p} = V_k - V_l = 0 \quad (21)$$

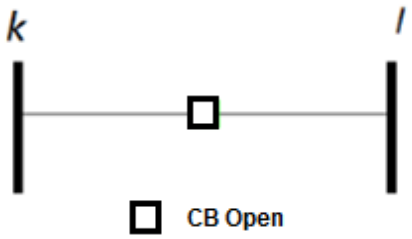

Figure 6 - Open Switch/Breaker from Bus k to

$$t_{kl}^{p} = 0 \quad u_{kl}^{p} = 0 \tag{22}$$

If the status of a CB is unknown, the pseudo measurements of the set of Eq. (21) and (22) cannot be used, and the GSE must calculate the flow through it in order to determine its status.

Moreover, the network configuration also allows the use of pseudo injection measurements in nodes inside the substation or on the boundary, which are very abundant when considering the approach at the substation level. In this way, the injection in those nodes is set equal to zero, as presented in the set of Eq. (23), or it can also be modeled as structural constraints in an optimization problem (SIMÕES COSTA; LOURENÇO; CLEMENTS, 2002).

$$P_{k}^{p} = 0 \quad Q_{k}^{p} = 0 \tag{23}$$

In such case, the measurement function vector and the Jacobian matrix also change, as they reflect the use of the new states and measurements, as shown in. Eq. (24) and Eq. (25), respectively.

$$h(x) = \begin{bmatrix} P_{km} \\ P_{k} \\ Q_{km} \\ Q_{k} \\ V_{k} \\ t_{kl} \\ u_{kl} \\ P_{k}^{p} \\ Q_{k}^{p} \\ \Delta\theta_{kl}^{p} \\ \Delta V_{kl}^{p} \\ t_{kl}^{p} \\ u_{kl}^{p} \end{bmatrix} \tag{24}$$

$$H = \begin{bmatrix} \partial P_{km}/\partial\theta & \partial P_{km}/\partial V & \partial P_{km}/\partial t_{kl} & \partial P_{km}/\partial u_{kl} \\ \partial P_{k}/\partial\theta & \partial P_{k}/\partial V & \partial P_{k}/\partial t_{kl} & \partial P_{k}/\partial u_{kl} \\ \partial Q_{km}/\partial\theta & \partial Q_{km}/\partial V & \partial Q_{km}/\partial t_{kl} & \partial Q_{km}/\partial u_{kl} \\ \partial Q_{k}/\partial\theta & \partial Q_{k}/\partial V & \partial Q_{k}/\partial t_{kl} & \partial Q_{k}/\partial u_{kl} \\ \partial V_{k}/\partial\theta & \partial V_{k}/\partial V & \partial V_{k}/\partial t_{kl} & \partial V_{k}/\partial u_{kl} \\ \partial t_{kl}/\partial\theta & \partial t_{kl}/\partial V & \partial t_{kl}/\partial t_{kl} & \partial t_{kl}/\partial u_{kl} \\ \partial u_{kl}/\partial\theta & \partial u_{kl}/\partial V & \partial u_{kl}/\partial t_{kl} & \partial u_{kl}/\partial u_{kl} \\ \partial P_{k}^{p}/\partial\theta & \partial P_{k}^{p}/\partial V & \partial P_{k}^{p}/\partial t_{kl} & \partial P_{k}^{p}/\partial u_{kl} \\ \partial Q_{k}^{p}/\partial\theta & \partial Q_{k}^{p}/\partial V & \partial Q_{k}^{p}/\partial t_{kl} & \partial Q_{k}^{p}/\partial u_{kl} \\ \partial \Delta\theta_{kl}^{p}/\partial\theta & \partial \Delta\theta_{kl}^{p}/\partial V & \partial \Delta\theta_{kl}^{p}/\partial t_{kl} & \partial \Delta\theta_{kl}^{p}/\partial u_{kl} \\ \partial \Delta V_{kl}^{p}/\partial\theta & \partial \Delta V_{kl}^{p}/\partial V & \partial \Delta V_{kl}^{p}/\partial t_{kl} & \partial \Delta V_{kl}^{p}/\partial u_{kl} \\ \partial t_{kl}^{p}/\partial\theta & \partial t_{kl}^{p}/\partial V & \partial t_{kl}^{p}/\partial t_{kl} & \partial t_{kl}^{p}/\partial u_{kl} \\ \partial u_{kl}^{p}/\partial\theta & \partial u_{kl}^{p}/\partial V & \partial u_{kl}^{p}/\partial t_{kl} & \partial u_{kl}^{p}/\partial u_{kl} \end{bmatrix}. \quad (25)$$

The set of the Eq. (26) present some of the derivatives[3]:

[3] The same equations apply for partial derivatives of pseudo power flows measurements.

$$\frac{\partial t_{kl}}{\partial \theta_k} = \frac{\partial t_{kl}}{\partial \theta_m} = \frac{\partial t_{kl}}{\partial \theta_l} = \frac{\partial t_{kl}}{\partial V_k} = \frac{\partial t_{kl}}{\partial V_m} = \frac{\partial t_{kl}}{\partial V_l} = \frac{\partial t_{kl}}{\partial u_{kl}} = 0, \frac{\partial t_{kl}}{\partial t_{kl}} = 1$$

$$\frac{\partial u_{kl}}{\partial \theta_k} = \frac{\partial u_{kl}}{\partial \theta_m} = \frac{\partial u_{kl}}{\partial \theta_l} = \frac{\partial u_{kl}}{\partial V_k} = \frac{\partial u_{kl}}{\partial V_m} = \frac{\partial u_{kl}}{\partial V_l} = \frac{\partial u_{kl}}{\partial t_{kl}} = 0, \frac{\partial u_{kl}}{\partial u_{kl}} = 1$$

$$\frac{\partial \Delta\theta_{kl}^p}{\partial \theta_m} = \frac{\partial \Delta\theta_{kl}^p}{\partial V_k} = \frac{\partial \Delta\theta_{kl}^p}{\partial V_m} = \frac{\partial \Delta\theta_{kl}^p}{\partial V_l} = \frac{\partial \Delta\theta_{kl}^p}{\partial t_{kl}} = \frac{\partial \Delta\theta_{kl}^p}{\partial u_{kl}} = 0, \frac{\partial \Delta\theta_{kl}^p}{\partial \theta_k} = 1, \frac{\partial \Delta\theta_{kl}^p}{\partial \theta_l} = -1 \quad (26)$$

$$\frac{\partial \Delta V_{kl}^p}{\partial \theta_k} = \frac{\partial \Delta V_{kl}^p}{\partial \theta_m} = \frac{\partial \Delta V_{kl}^p}{\partial \theta_l} = \frac{\partial \Delta V_{kl}^p}{\partial V_m} = \frac{\partial \Delta V_{kl}^p}{\partial t_{kl}} = \frac{\partial \Delta V_{kl}^p}{\partial u_{kl}} = 0, \frac{\partial \Delta V_{kl}^p}{\partial V_k} = 1, \frac{\partial \Delta V_{kl}^p}{\partial V_l} = -1.$$

To estimate the states, the same equation showed in (7) is iteratively solved following the same steps presented in subsection 2.1.1.

GSE approach is similar to the conventional WLS SE, except for the fact that the network model contains switches and circuit breakers, and the power flows through switching branches are state variables. By doing so, the number of states enlarges and so does the size of Jacobian matrix and the measurements function; such changing takes place due to the use of pseudo measurements to represent switch status and null injection nodes (MONTICELLI, 1993a).

The GSE based on the normal equation formulation uses angle difference and voltage drop across zero impedance branches (closed CB), zero power flows across infinite branches (opened CB), and zero injection measurements with high weighting factors, in order to attain acceptable accuracy (MONTICELLI; GARCIA, 1991).

Another approach suggests the use of such pseudo measurements as equality constraints for an optimization problem, as presented in Eq. (27).

$$\begin{aligned} &minimize \quad \frac{1}{2} r^T W r \\ &subject\ to\ r = z - h(\hat{x}) \\ &h_o(\hat{x}) = 0 \\ &h_s(\hat{x}) = 0 \end{aligned} \tag{27}$$

where:

$\hat{x}$: is the vector of estimated states;

h_o: is the vector of operational constraints;

h_s: is the vector of structural constraints.

Operational constraints stand for the status of CB (angle difference, voltage drop, and power flows), and structural constraints stand for null injection measurements and reference bus. The Hacthel´s sparse tableau algorithm (CLEMENTS; SIMÕES COSTA, 1998; GJELSVIK; HOLTEN, 1985) solves this constrained nonlinear problem.

2.2.2 GSE with Phasor Measurements

When voltage and/or current synchronized phasor measurements are available inside the substations, the WLS problem formulated in the subsection 2.2.1 must be adapted. The equations derived ahead consist of one of the contributions of this work, since they are not easily found in papers and books.

Bearing in mind the measurement arrangement in the substation represented in Figure 7, it can be seen that the voltage phasor measurement at busbar 2 provides a voltage magnitude measurement, as well as a phase angle at the same bus. Its implementation is simple and straightforward, as it only needs a voltage angle as a measurement.

The current phasor measurements provide the current magnitude and angle of the current flowing from a busbar to another. As suggested before, these current phasor measurements in the polar form can be converted into a rectangular form (see

Eq. (9)). Thus, two formulations for the WLS SE, complying with those measurements, are offered as follows.

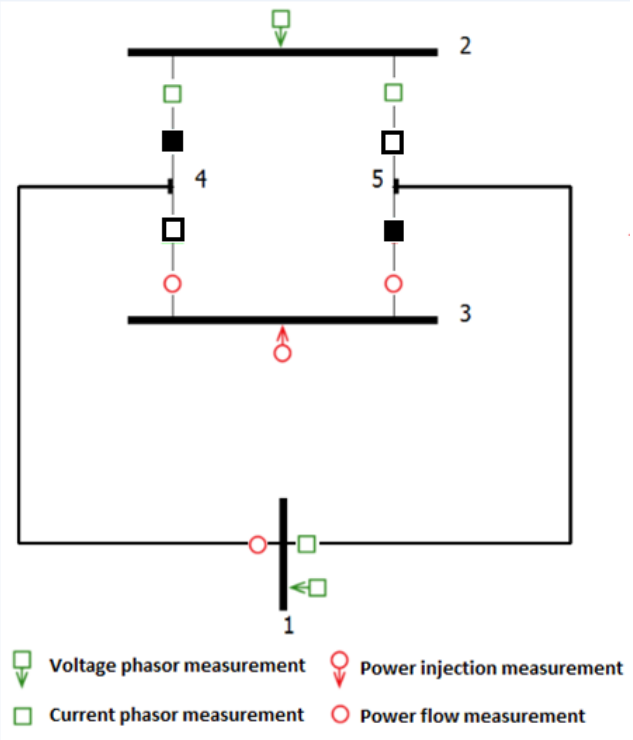

Figure 7 – Substation model with phasor and conventional measurements

(a) Considering power flows through the switching branches as state variables

In such case, the active and reactive power flows through the switching branches are kept as state variables. However, the available current phasor measurements on switching branches 2-4 and 2-5 are no longer power flows, but current flows instead. Then, its corresponding partial derivatives related to power flows are not linear and must be derived as a function of them.

It is preferable to represent the current phasor measurements as a function of the state variables to derive its partial derivatives, as follows.

$$I_{kl}^{Re} = \frac{t_{kl}\cos(\theta_k) + u_{kl}\sin(\theta_k)}{V_k}$$

$$I_{kl}^{Im} = \frac{t_{kl}\sin(\theta_k) - u_{kl}\cos(\theta_k)}{V_k} \quad (28)$$

where:

t_{kl}: refers to the active power flows through the switching branch (state variable);

u_{kl}: refers to the reactive power flows through the switching branch (state variable);

V_k: refers to the voltage magnitude at the measured bus, by the PMU;

θ_k: refers to the voltage angle at the measured bus, by the PMU.

Then, the partial derivatives are easily obtained:

$$\frac{\partial I_{kl}^{Re}}{\partial t_{kl}} = \frac{\cos(\theta_k)}{V_k}$$

$$\frac{\partial I_{kl}^{Re}}{\partial u_{kl}} = \frac{\sin(\theta_k)}{V_k} \quad (29)$$

$$\frac{\partial I_{kl}^{Im}}{\partial t_{kl}} = \frac{\sin(\theta_k)}{V_k}$$

$$\frac{\partial I_{km}^{Im}}{\partial u_{kl}} = -\frac{\cos(\theta_k)}{V_k}$$

The power injection measurement at the busbar 3, and the power flow measurements from the same busbar for nodes 4 and 5, are linearly represented as a function of the state variables.

The Jacobian matrix of the system, presented in Figure 7, takes the form present in Eq. (30) and only the active part is shown, for the sake of simplicity.

It is worth mentioning that in such approach, there is no need to extract a column to provide a reference for the system, once there is at least one synchronized voltage phasor measurement (ZHU; ABUR, 2007).

$$H = \begin{array}{c} \\ P_{1-4} \\ P_{3-4} \\ P_{5-3} \\ P_3 \\ I_{1-5}^{Re} \\ I_{2-4}^{Re} \\ I_{2-5}^{Re} \\ \theta_1 \\ \theta_2 \\ P_4^p \\ P_5^p \\ \Delta\theta_{2-4}^p \\ \Delta\theta_{3-5}^p \\ t_{3-4}^p \\ t_{2-5}^p \end{array} \begin{array}{c} \begin{array}{ccccccccc} \theta_1 & \theta_2 & \theta_3 & \theta_4 & \theta_5 & t_{24} & t_{25} & t_{34} & t_{35} \end{array} \\ \begin{bmatrix} * & & & * & & & & & \\ & & & & & & & 1 & \\ & & & & & & & & -1 \\ & & & & & & & 1 & 1 \\ * & & & & * & & & & \\ & & & & & * & & & \\ & & & & & & * & & \\ 1 & & & & & & & & \\ & 1 & & & & & & & \\ * & & & * & & -1 & & -1 & \\ * & & & & * & & -1 & & -1 \\ & 1 & & -1 & & & & & \\ & & 1 & & -1 & & & & \\ & & & & & & & 1 & \\ & & & & & & 1 & & \end{bmatrix} \end{array} \quad (30)$$

where: * refers to non-zero elements

(b) Considering current flows through the switching branches as state variables

In such alternative, the real and imaginary parts of the currents through switching branches are used as state variables, instead of the active and reactive power flows. Since more phasor measurements will be available in the future, it is assumed that an entire substation is measured only by such devices. For that reason, it is reasonable to make the proposed changes in the formulation of the generalized state estimation, as suggested in Yang, Sun and Bose (2011).

In this case, the current phasor measurements on switching branches are linearly related to the state variables, though the power flow measurements need to be derived as a function of the new state variables.

Equation (31) represents the power flows as a function of the current and the voltage:

$$P_{kl} = V_k[I_{kl}^{Re}\cos(\theta_k) + I_{kl}^{Im}\sin(\theta_k)]$$
$$Q_{kl} = V_k[I_{kl}^{Re}\sin(\theta_k) - I_{kl}^{Im}\cos(\theta_k)]. \quad (31)$$

The derivatives are taken straightforward, as follows:

$$\frac{\partial P_{kl}}{\partial I_{kl}^{Re}} = V_k\cos(\theta_k)$$
$$\frac{\partial P_{kl}}{\partial I_{kl}^{Im}} = V_k\sin(\theta_k)$$
$$\frac{\partial Q_{kl}}{\partial I_{kl}^{Re}} = V_k\sin(\theta_k) \quad (32)$$
$$\frac{\partial Q_{kl}}{\partial I_{kl}^{Im}} = -V_k\cos(\theta_k)$$

By making use of the same system of Figure 7, the Jacobian matrix takes on the form of Equation (33).

$$H = \begin{array}{c} \\ P_{1-4} \\ P_{3-4} \\ P_{5-3} \\ P_{3} \\ I_{1-5}^{Re} \\ I_{2-4}^{Re} \\ I_{2-5}^{Re} \\ \theta_1 \\ \theta_2 \\ P_4^p \\ P_5^p \\ \Delta\theta_{2-4}^p \\ \Delta\theta_{3-5}^p \\ I_{3-4}^{Re,p} \\ I_{2-5}^{Re,p} \end{array} \begin{array}{c} \begin{array}{ccccccccc} \theta_1 & \theta_2 & \theta_3 & \theta_4 & \theta_5 & I_{24} & I_{25} & I_{34} & I_{35} \end{array} \\ \begin{bmatrix} * & & & * & & & & & \\ & & & & & & & * & \\ & & & & & & & & * \\ & & & & & & & * & * \\ * & & & & * & & & & \\ & & & & & 1 & & & \\ & & & & & & 1 & & \\ 1 & & & & & & & & \\ & 1 & & & & & & & \\ * & & & * & & * & & * & \\ * & & & & * & & * & & * \\ & 1 & & -1 & & & & & \\ & & 1 & & -1 & & & & \\ & & & & & & & 1 & \\ & & & & & & 1 & & \end{bmatrix} \end{array} \quad (33)$$

As it can be noticed, on one hand, the phasor current flow measurements through switching branches 2-4 and 2-5 are linearly related to the state variables. On the other hand, the power flow measurements through switching branches 3-4 and 3-5 must be derivative as a function of the currents, accordingly to what had been set on Eq. (32).

In its turn, the power injection measurements at boundary buses/nodes and busbars connecting only switching branches are no longer linearly related to the state variables. They are derived as a function of the current flows of the adjacent switches.

The power injection measurement at busbar 3 is formulated as a summation of the flows through the switching branches 3-4 and 3-5. In the previous approach, they were linearly related to the state variables, but for the sake of the current approach, those power flows must be derived as a function of the current flows, which are the new state variables. The expression for these derivatives is the same from that of the power flows, as presented at the set of Eq.(32).

In the case of pseudo injection measurement at the boundary bus/node 4 and 5, both can be represented as a summation of the power flows through the switching branches and conventional branches. Thus, its derivatives follow the same approach,

with elements referring to conventional state variables (voltage angle and magnitude) and the new ones (current flows through switching branches).

Another difference that can be pinpointed is that the pseudo flow measurements through the opened CB can be directly used as pseudo current flow measurements, once there are set equal to zero.

2.3 SUMMARY OF THE CHAPTER

This chapter has exposed the theory around the State Estimation paradigm when it comes to the Traditional and Generalized approaches. The Traditional approach was first presented in order to demonstrate the classical SE over the WLS method. It was also unfolded the extension of complying with the phasor measurements, which have been benefiting the SE algorithms.

In the sequence, the Generalized approach was discussed, considering both conventional and phasor measurements. It had been illustrated how switching branches can be modeled to perform the state estimation, pondering the new state variables, and the new pseudo measurements, operational and structural constraints. Moreover, the use of phasor measurements was presented considering two different approaches: 1) by changing the state variables from power flows through switching branches to current flows, and 2) by converting the power injection measurement into current injections.

The equations derived here are used in the developed GSE algorithm, which validates the methods proposed on the subsequent chapters.

3 OBSERVABILITY ANALYSIS

The effectiveness of performing state estimation on a power network depends on the availability of enough and well distributed measurements throughout the system (MONTICELLI, 1999). Conventionally, the observability analysis is carried out prior to the state estimation execution, and once the system is observable, it enables to perform further analysis. However, if the system is unobservable, it is yet useful to determine what portions are observable, as well as which parts are unobservable. As a consequence, it is possible to perform a partial state estimation, or use pseudomeasurements to restate the system observability.

This chapter addresses the concepts of Observability analysis in power networks modeled at the bus-branch and bus section levels. It discusses the numerical and topological approaches to determine the system observability along with further numerical methods to find unobservable branches and observable islands. In addition to that, observability methods are explained in tutorial examples, since they are the basis of this work developments.

3.1 TRADITIONAL OBSERVABILITY ANALYSIS: BUS-BRANCH ANALYSIS

In real time modeling, topology processor reduces the network from the bus section level into the bus-branch model, as it processess the status of switches and circuit breakers inside the substations. After that, the Traditional State Estimation is performed.

One of the first papers addressing observability issues calls for a topological approach by making usage of an iterative algorithm whose aim is to find a spanning tree of full rank (KRUMPHOLZ; CLEMENTS; DAVIS, 1980). Conversely, the approach proposed by Monticelli and Wu (1985a, 1985b) claims for a numerical approach to determine the system observability by applying the triangular factorization in the Gain matrix.

3.1.1 Network Observability

For observability purposes, it is convenient to use a simplified linearized model that represents only the active part, and assuming 1.0 p.u. reactances (MONTICELLI; WU, 1985a). The reactive part should also be tested, but since the measurements usually come in pairs, the second part is seldom necessary (MONTICELLI; WU, 1985b).

When it comes to Traditional Observability Analysis (TOA), the first step to be taken is the modeling of the measurements. There are three type of measurements: (i) analog, consisted by power flows, power injections, bus voltage magnitude, current magnitude, and also synchronized voltage and current phasor measurements; (ii) logical, composed by the status of switches and circuit breakers and (iii) pseudomeasurements, consisted by forecasted bus loads and generations (MONTICELLI; WU, 1985a).

Logical information is used for topology processing and it is performed prior the observability analysis. Pseudo measurements become relevant once the system is found unobservable, and are used to restore observability. Therefore, only the first type of measurements is considered for observability analysis and their modeling is addressed as follows (MONTICELLI; WU, 1985a)[4].

(a) Power flow measurements

Figure 8 presents a line model connecting buses k-m, with a power flow measurement on it.

[4] In this chapter, only the conventional measurements are presented. For PMU measurements, see next chapter.

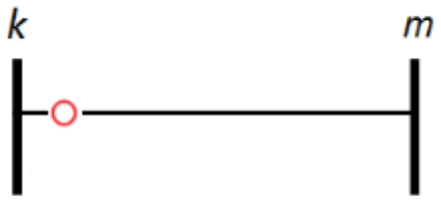

Figure 8 – Power flow measurement on branch $k-m$

Assuming the line reactance (x_{k-m}) equal to 1.0 p.u., the following equation represents the linear power flow measurement.

$$P_{k-m}^{m} = \frac{1}{x_{k-m}}(\theta_k - \theta_m) = \theta_k - \theta_m \tag{34}$$

(b) Power injection measurements

A power injection measurement at a bus is modeled as a summation of all power flows from all adjacent lines. Taking for instance the power injection measurement set at the generic bus t of the 3 bus system in Figure 9, its linear model is given by Eq. (35).

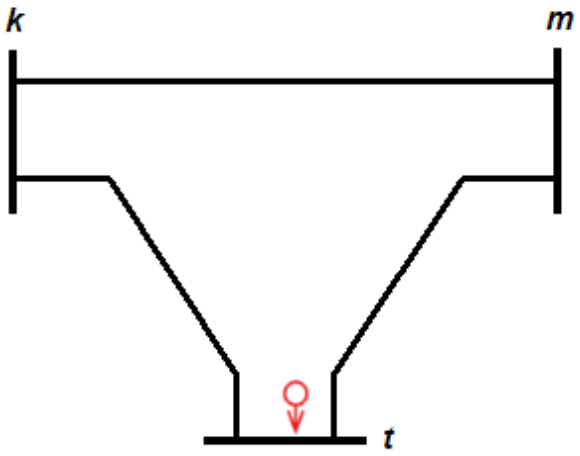

Figure 9 – Power injection measurement at the generic bus t

$$P_t^m = \sum_i^{n_t} P_i = \frac{1}{x_{t-k}}(\theta_t - \theta_k) + \frac{1}{x_{t-m}}(\theta_t - \theta_m) = 2\theta_t - \theta_k - \theta_m \quad (35)$$

where:

n_t: refers to a set of all branches connected to bus t.

The measurements can be grouped in a matrix form to facilitate numerical analysis, such as the one presented ahead. Taking the system in Figure 10 as an example, with the given measurement design, the measurement matrix is formed as follows.

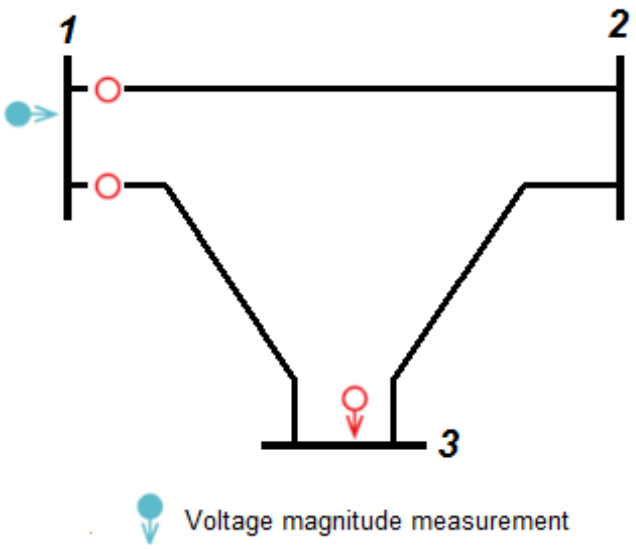

Figure 10 – 3 bus network

3.1.1.1 – Basic Numerical Method

Eq. (36) represents the Jacobian matrix (measurement matrix) of the given measurement design. [5]

$$H_{AA} = \begin{matrix} \\ P_{1-2} \\ P_{1-3} \\ P_3 \end{matrix} \begin{matrix} \begin{matrix} \theta_1 & \theta_2 & \theta_3 \end{matrix} \\ \begin{bmatrix} 1 & -1 & \\ 1 & & -1 \\ -1 & -1 & 2 \end{bmatrix} \end{matrix}. \tag{36}$$

The reactive model requires an additional measurement, that is, the voltage magnitude. The voltage angle, in its turn, corresponds to the same in the active model.

Computing the rank of the Jacobian matrix in Eq. (36) it is possible to determine whether the network is observable or not, regarding the available measurements. If the Jacobian matrix has a full rank (i.e. $rank(H_{AA}) = n = N_b - 1$, where n is the number of states and N_b the number of buses) the system is said observable. In the example of Figure 10, the corresponding rank is full ($rank(H_{AA}) = N_b - 1 = 2$), rendering the system observable.

Another way to determine the system observability is by computing the Gain matrix and performing the triangular factorization, as in Eq. (37) and (38) (MONTICELLI; WU, 1985b).

$$G = {H_{AA}}^T H_{AA} = \begin{matrix} \\ \theta_1 \\ \theta_2 \\ \theta_3 \end{matrix} \begin{matrix} \begin{matrix} \theta_1 & \theta_2 & \theta_3 \end{matrix} \\ \begin{bmatrix} 3 & & -3 \\ & 2 & -2 \\ -3 & -2 & 5 \end{bmatrix} \end{matrix} \tag{37}$$

[5]The Jacobian matrix H_{AA} is the same defined in Eq (6), but in a linearized fashion.

$$U = \begin{array}{c} \\ \theta_1 \\ \theta_2 \\ \theta_3 \end{array} \begin{array}{c} \begin{array}{ccc} \theta_1 & \theta_2 & \theta_3 \end{array} \\ \begin{bmatrix} 1.7 & & -1{,}7 \\ & 1.4 & -1.4 \\ & & 0 \end{bmatrix} \end{array}. \tag{38}$$

The existence of only one zero pivots, i.e. a zero in the diagonal of U matrix, renders the system observable. Such fact indicates that only one angular reference is required, that is, an angle constraint ($\theta_3 = 0$ for instance), and it provides an angular reference. Having more zero pivots, the system is unobservable (MONTICELLI; WU, 1985a).

3.1.1.2 – Basic Topological Method

In the topological approach, the power flow and injection measurements are processed as edges connecting the vertices (representing network buses) so as to form an observable spanning tree (KRUMPHOLZ; CLEMENTS; DAVIS, 1980). Basically, a power flow measurement between buses k and m, such as presented in Figure 8, is processed as an edge connecting the related vertices k and m, as shown in Figure 11.

Figure 11 – Edge of a power flow measurement

Power injection measurements, on the other hand, can form edges with all the adjacent vertices. In Figure 9, for instance, the injection measurement at bus t forms edges connecting vertices k and m. However, only one edge can be used to ensure the network observability. In Figure 12, only one of the two edges can be picked.

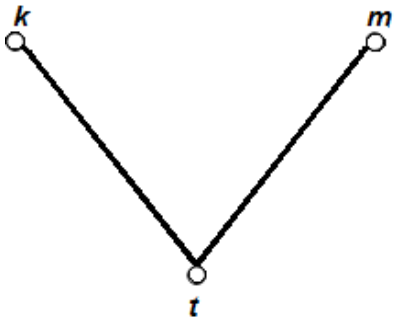

Figure 12 – Edges of a power injection measurement

Observability analysis is carried out considering the $P-\theta/Q-V$ decoupling principle, since the measurements come in pairs. To accomplish the analysis, an angular reference must be provided for $P-\theta$ observability, and at least one voltage magnitude measurement is required to ensure $Q-V$ observability. They are treated as a fictitious flow, which connects a vertex to an extra (ground) node (CLEMENTS; DAVIS; KRUMPHOLZ, 1981). Figure 13 portrays the measurement graph of the network shown in Figure 10, which forms an Observable Spanning Tree (OST).

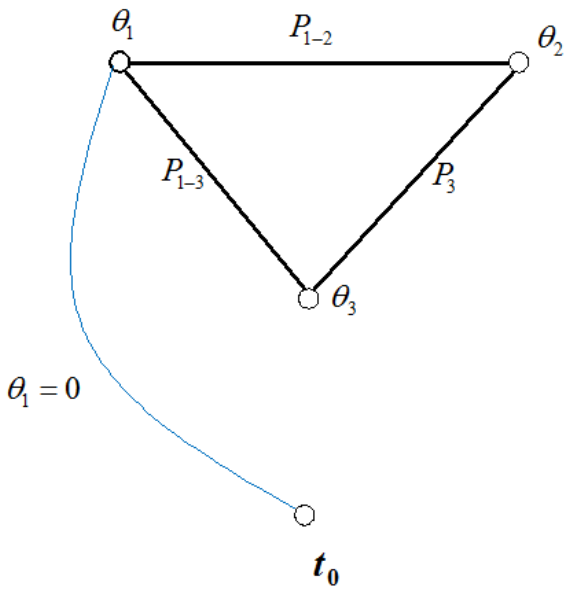

Figure 13 – Measurement graph of 3 bus network

3.1.2 Identification of Observable Islands

Further analysis can be carried out, for instance, measurement criticality, state estimation, bad data and so forth, if a network is observable. On the other hand, if the network is unobservable, it is desirable to find the observable islands and unobservable branches.

The first step consists of identifying and removing the irrelevant branches with the absence of flow measurements, and injection measurements on its adjacent buses. Taking for instance the example of Monticelli and Wu (1985b) presented in Figure 14, the branch 2-3 is found irrelevant and its corresponding row is eliminated from incidence matrix A, in Eq. (39).

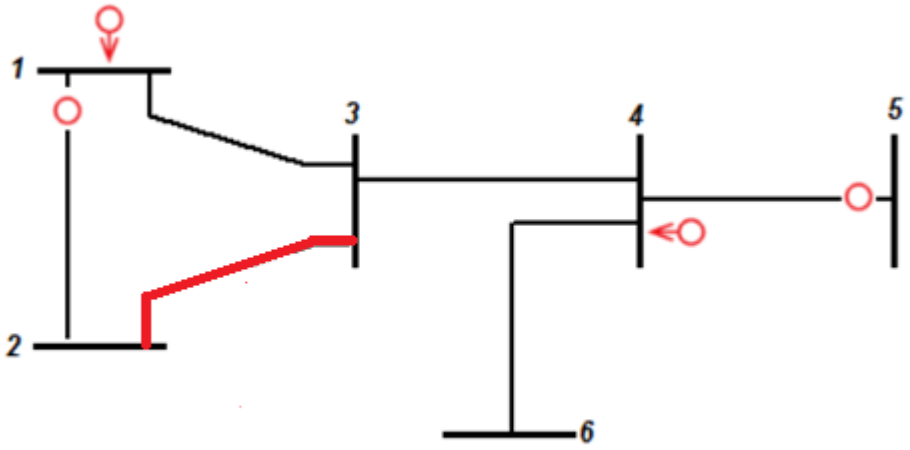

Figure 14 – 6 bus network example
Source: Monticelli and Wu (1985b)

$$A = \begin{array}{c} \\ b_{1-2} \\ b_{1-3} \\ b_{3-4} \\ b_{4-5} \\ b_{6-4} \end{array} \begin{array}{c} \begin{array}{cccccc} \theta_1 & \theta_2 & \theta_3 & \theta_4 & \theta_5 & \theta_6 \end{array} \\ \begin{bmatrix} 1 & -1 & & & & \\ 1 & & -1 & & & \\ & & 1 & -1 & & \\ & & & 1 & -1 & \\ & & & -1 & & 1 \end{bmatrix} \end{array} \tag{39}$$

In the next step, the measurements are processed forming the Jacobian matrix H_{AA} and the corresponding Gain matrix G, as presented in Eq. (40) and (41), respectively.

$$H_{AA} = \begin{array}{c} \\ P_1 \\ P_4 \\ P_{1-2} \\ P_{4-5} \end{array} \begin{array}{c} \begin{array}{cccccc} \theta_1 & \theta_2 & \theta_3 & \theta_4 & \theta_5 & \theta_6 \end{array} \\ \begin{bmatrix} 2 & -1 & -1 & & & \\ & & -1 & 3 & -1 & -1 \\ 1 & -1 & & & & \\ & & & 1 & -1 & \end{bmatrix} \end{array} \tag{40}$$

$$G = \begin{array}{c} \\ \theta_1 \\ \theta_2 \\ \theta_3 \\ \theta_4 \\ \theta_5 \\ \theta_6 \end{array} \begin{array}{c} \begin{array}{cccccc} \theta_1 & \theta_2 & \theta_3 & \theta_4 & \theta_5 & \theta_6 \end{array} \\ \begin{bmatrix} 5 & -3 & -2 & & & \\ -3 & 2 & 1 & & & \\ -2 & 1 & 2 & -3 & 1 & 1 \\ & & -3 & 10 & -4 & -3 \\ & & 1 & -4 & 2 & 1 \\ & & 1 & -3 & 1 & 1 \end{bmatrix} \end{array}. \tag{41}$$

At this point, is possible to evaluate the rank of matrix H and to certify the system unobservability. Performing the triangular factorization of the Gain matrix G, two zero pivots are found, as follows.

$$U = \begin{array}{c} \\ \theta_1 \\ \theta_2 \\ \theta_3 \\ \theta_4 \\ \theta_5 \\ \theta_6 \end{array} \begin{array}{c} \begin{array}{cccccc} \theta_1 & \theta_2 & \theta_3 & \theta_4 & \theta_5 & \theta_6 \end{array} \\ \begin{bmatrix} 2.24 & -1.34 & -0.89 & & & \\ & 0.45 & -0.45 & & & \\ & & 1 & -3 & 1 & 1 \\ & & & 1 & -1 & \\ & & & & 0 & \\ & & & & & 0 \end{bmatrix} \end{array}. \tag{42}$$

Those two zero pivots indicate that the system is divided into two observable islands (MONTICELLI; WU, 1985b), and two angular references must be provided, on buses 5 and 6.

Replacing the zero pivots by “1”s, at positions (5,5) and (6,6) of U matrix, and changing the corresponding number in the right vector t_A by random numbers, one can determine the unobservable state, as in Eq. (43).

$$\hat{\theta} = (U^T U)^{-1} t_A \tag{43}$$

where:

$t_A = [0\ 0\ 0\ 0\ 0\ 1]^T$

The vector t_A is a modified vector, with zeros in the positions related to non-zero pivots, and random numbers on the positions related to zero pivots. Integer numbers such as 0,1,2, etc are usually used (ABUR; EXPÓSITO, 2004).

Multiplying the estimated state $\hat{\theta}$ by the incidence matrix A, it obtains the power flows through the branches, as follows.

$$P_b = A\hat{\theta} = \begin{matrix} b_{1-2} \\ b_{1-3} \\ b_{3-4} \\ b_{4-5} \\ b_{6-4} \end{matrix} \begin{bmatrix} 1 & -1 & & & & \\ 1 & & -1 & & & \\ & & 1 & -1 & & \\ & & & 1 & -1 & \\ & & & -1 & & 1 \end{bmatrix} \begin{bmatrix} 0 \\ 0 \\ 0 \\ 0 \\ 0 \\ 1 \end{bmatrix} = \begin{bmatrix} 0 \\ 0 \\ -1 \\ 0 \\ 1 \end{bmatrix}. \tag{44}$$

where:

b_{k-m}: refers to a branch from generic bus k to m.

The non-zero flows indicate the unobservable branches. In such case, branches 3-4 and 6-4 are unobservable and the corresponding row are removed from matrix A.

After that, the irrelevant injection measurements must be identified and removed from the set of interest. The H_{AA} and A matrices are updated by removing the rows related to the irrelevant injection measurements in H_{AA}, and unobservable branches in A. Therefore, the power flows are computed again, unobservable branches are removed, as well as irrelevant measurements, until no non-zero flows are found.

In the example of Figure 14, the injection measurement at bus 4 is irrelevant, since it has at least one adjacent unobservable branch (MONTICELLI; WU, 1985b).

By adapting the matrix H_{AA}, processing the new Gain matrix and performing the triangular factorization, the new U matrix is obtained, as follows:

$$U = \begin{array}{c} \\ \theta_1 \\ \theta_2 \\ \theta_3 \\ \theta_4 \\ \theta_5 \\ \theta_6 \end{array} \begin{array}{c} \begin{array}{cccccc} \theta_1 & \theta_2 & \theta_3 & \theta_4 & \theta_5 & \theta_6 \end{array} \\ \begin{bmatrix} 2.24 & -1.34 & -0.89 & & & \\ & 0.45 & -0.45 & & & \\ & & 0 & & & \\ & & & 1 & -1 & \\ & & & & 0 & \\ & & & & & 0 \end{bmatrix} \end{array}. \tag{45}$$

Differently, three zero pivots are found and by changing them into one, and applying the Eq. (43) with the following vector $t_A = [0\ 0\ 0\ 0\ 1\ 2]$, gives $\hat{\theta} = [0\ 0\ 0\ 1\ 1\ 2]$ so that the power flows are evaluated as follows.

$$P_b = A\hat{\theta} = \begin{array}{c} \\ b_{1-2} \\ b_{1-3} \\ b_{4-5} \end{array} \begin{bmatrix} 1 & -1 & & & & \\ 1 & & -1 & & & \\ & & & 1 & -1 & \end{bmatrix} \begin{bmatrix} 0 \\ 0 \\ 0 \\ 1 \\ 1 \\ 2 \end{bmatrix} = \begin{bmatrix} 0 \\ 0 \\ 0 \end{bmatrix}. \tag{46}$$

As a consequence, the process stops as all the power flows are null.

Although the process has stopped, it is necessary to determine if the irrelevant branches that were removed at the beginning of the process, are observable or not. In this example, only the branch 2-3 were labeled irrelevant. Updating the A matrix, taking into account the irrelevant branch and removing the already labelled unobservable branches, we have the following matrix, shown in Eq. (47):

$$P_b = A\hat{\theta} = \begin{matrix} b_{1-2} \\ b_{1-3} \\ b_{4-5} \\ b_{2-3} \end{matrix}\begin{bmatrix} 1 & -1 & & & & \\ 1 & & -1 & & & \\ & & & 1 & -1 & \\ & 1 & -1 & & & \end{bmatrix}\begin{bmatrix} 0 \\ 0 \\ 0 \\ 1 \\ 1 \\ 2 \end{bmatrix} = \begin{bmatrix} 0 \\ 0 \\ 0 \\ 0 \end{bmatrix}. \quad (47)$$

Since all the power flows are null, all those branches are labeled observable. The islands are identified by selecting the appropriate buses from the estimated vector $\hat{\theta}$. In this case, θ_1, θ_2 and θ_3 form an island, θ_4 and θ_5 form another, and bus θ_6 forms the last one, as depicted in Figure 15.

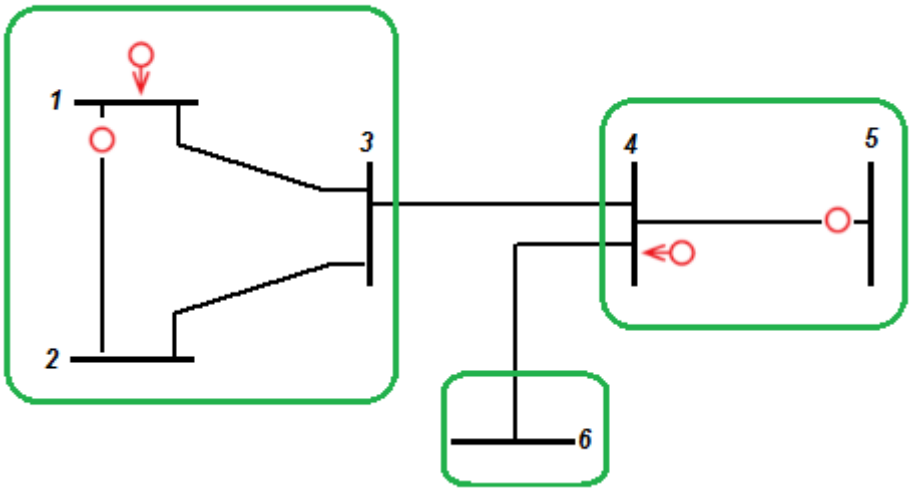

Figure 15 - 6 bus network example, with indication of islands

As one may notice, bus 6 is isolated from the others. Such fact does not necessarily mean that it is not an island. As pointed out in Monticelli and Wu (1985b) even an isolated bus, such as bus 6, is also considered an island.

3.2 GENERALIZED OBSERVABILITY ANALYSIS

When it comes to the problem of representing some substations in the bus section level as a means to perform the Generalized State Estimation, all the fundamental facts of observability analysis remain faithful (MONTICELLI, 1993a). For the sake of this analyses, however, the model must be extended, as presented in this section.

3.2.1 Generalized Network Observability

Although there is no problem in adding power flows through switching branches as state variables, these new states must also be observable (MONTICELLI, 1993b). Taking the network in Figure 16 as an example, it is possible to demonstrate how the observability methods can be extended to power networks modeled at the bus section level.

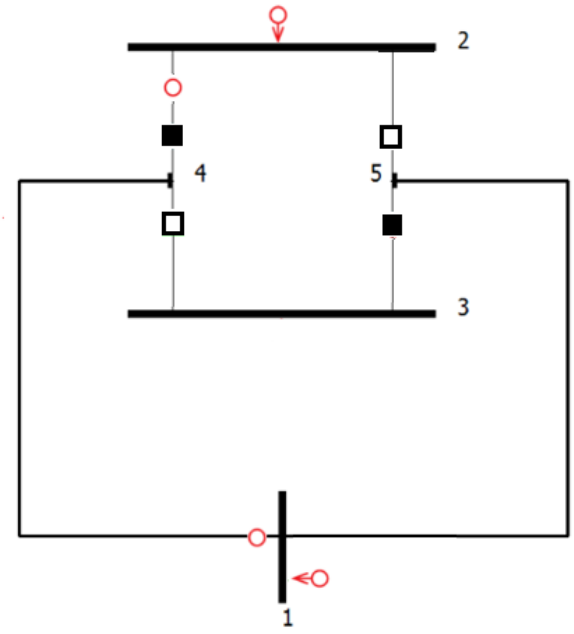

Figure 16 – Example network at bus section level

The Jacobian matrix of the network in Figure 16 is represented in Eq. (48). Notice that only the active part is demonstrated, since it is assumed measurements that come in pairs.

$$H_{AA} = \begin{array}{c} \\ P_{1-4} \\ P_1 \\ P_{2-4} \\ P_2 \\ P_4^p \\ P_5^p \\ \Delta\theta_{2-4}^p \\ \Delta\theta_{3-5}^p \\ t_{3-4}^p \\ t_{2-5}^p \end{array} \begin{array}{c} \begin{array}{ccccccccc} \theta_1 & \theta_2 & \theta_3 & \theta_4 & \theta_5 & t_{24} & t_{25} & t_{34} & t_{35} \end{array} \\ \begin{bmatrix} 1 & & & -1 & & & & & \\ 2 & & & -1 & -1 & & & & \\ & & & & & 1 & & & \\ & & & & & 1 & 1 & & \\ -1 & & & 1 & & -1 & & -1 & \\ -1 & & & & 1 & & -1 & & -1 \\ & 1 & & -1 & & & & & \\ & & 1 & & -1 & & & & \\ & & & & & & & 1 & \\ & & & & & & 1 & & \end{bmatrix} \end{array}. \quad (48)$$

Evaluating the rank of the matrix (48), one realizes that a full rank is achieved (i.e. $rank(H_{AA}) = N - 1 = 8$). This means that the network is fully observable, regarding both the conventional states (θ and V) and the new ones (t and u).

A further analysis proves the system observability, by obtaining the Gain matrix and performing the triangular factorization, as follows.

$$U = \begin{array}{c} \\ \theta_1 \\ \theta_2 \\ \theta_3 \\ \theta_4 \\ \theta_5 \\ t_{24} \\ t_{25} \\ t_{34} \\ t_{35} \end{array} \begin{array}{c} \begin{array}{ccccccccc} \theta_1 & \theta_2 & \theta_3 & \theta_4 & \theta_5 & t_{24} & t_{25} & t_{34} & t_{35} \end{array} \\ \begin{bmatrix} 2.65 & & & -1.51 & -1.13 & 0.38 & 0.38 & 0.38 & 0.38 \\ & 1 & & -1 & & & & & \\ & & 1 & & -1 & & & & \\ & & & 0.85 & -0.85 & -0.51 & 0.68 & -0.51 & 0.68 \\ & & & & 0 & & & & \\ & & & & & 1.61 & 0.74 & 0.37 & 0.12 \\ & & & & & & 1.36 & -0.06 & 0.23 \\ & & & & & & & 1.21 & 0.14 \\ & & & & & & & & 0.56 \end{bmatrix} \end{array}. \quad (49)$$

Only one zero pivot is found, at position (5, 5) referring to bus 5, what means that only one reference is required for the entire system.

In the topological approach, the measurement graph will be composed not only by vertices related to network buses, but also by vertices related to the new state

variables. Conventional measurements are treated in the same way as presented in the last section, though it is necessary to process pseudo measurements related to CB status (also referred as operational and structural constraints).

The measurement graph will be composed of two measurement graphs: the first one related to buses/nodes (G_{M_θ}), and the second related to power flows through switching branches (G_{M_t}). Figure 16 depicts the test system and the measurement graph takes the following form, as shown in Figure 17.

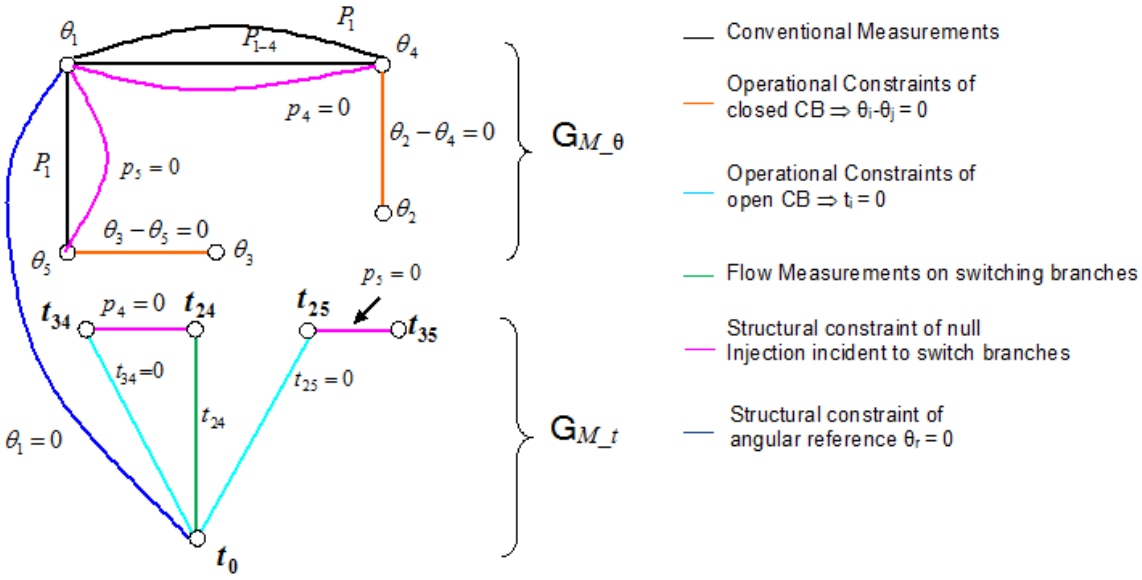

Figure 17 – Generalized measurement graph

The conventional measurement P_{1-4} only connects the vertices related to buses 1,4. The injections measurement P_1 can connect the vertices related to buses 1,4, and 5, but only one edge can be used for observability purposes. In such a case, the edge connecting vertices 1 and 5 must be chosen. The flow measurement on switching branch 2-4 belongs to measurement graph G_{M_t}. and it connects the vertex t_{24} directly to the reference node t_0.

Operational constraints of closed CB belong to G_{M_θ} graph, and operational constraints of open CB take the same form as flow measurements through switching branches. In its turn, structural constraints of null injections can be used to connect conventional states and generalized ones. In such example p_4 can be used to either connect t_{24} - t_{34} or θ_1 - θ_4. Equally, p_5 is used to either connect the vertices related to

states t_{25} - t_{35} or buses θ_1 - θ_5. Nonetheless, for such circumstances is preferable to use them to connect the generalized states t_{24} - t_{34}, and t_{25} - t_{35}, respectively.

The structural constraint of angular reference connects both measurement graphs, enabling the entire network observable and providing a reference for the system. At least one voltage measurement magnitude per observable island is necessary as it plays the same role of the angular reference for the reactive part.

By interpreting the generalized graph in Figure 17, it is possible to analyze measurement/constraint criticality. The operational constraints of closed circuit breaker are critical, since its loss would lead to system unobservability. The same aplies for operational constraint of open CB t_{25}, and structural constraints θ_1 and p_5. The remaining measurements/constraints are all redundant.

3.2.2 Determining Observable Islands in the Generalized Approach

Figure 16 demonstrated a power network fully observable. However, if the network is unobservable, further analysis must be carried out to find both observable islands and unobservable branches.

Taking the example of Figure 16, and assuming the flow measurement on switching branch 2-4 is lost and so does the power injection measurement at bus 2, and also considering the CB 2-5 status as unknown, the Jacobian matrix takes the following form.

$$H_{AA} = \begin{array}{c} \\ P_{1-4} \\ P_1 \\ P_4^p \\ P_5^p \\ \Delta\theta_{2-4}^p \\ \Delta\theta_{3-5}^p \\ t_{3-4}^p \end{array} \begin{array}{c} \begin{array}{ccccccccc} \theta_1 & \theta_2 & \theta_3 & \theta_4 & \theta_5 & t_{24} & t_{25} & t_{34} & t_{35} \end{array} \\ \begin{bmatrix} 1 & & & -1 & & & & & \\ 2 & & & -1 & -1 & & & & \\ -1 & & & 1 & & -1 & & -1 & \\ -1 & & & & 1 & & -1 & & -1 \\ & 1 & & -1 & & & & & \\ & & 1 & & -1 & & & & \\ & & & & & & & 1 & \end{bmatrix} \end{array}. \quad (50)$$

As a result, the rank of the matrix (50) is 7, which renders the network unobservable.

By forming the Gain matrix and by computing the triangular factorization, the following U factor is obtained.

$$U = \begin{array}{c} \\ \theta_1 \\ \theta_2 \\ \theta_3 \\ \theta_4 \\ \theta_5 \\ t_{24} \\ t_{25} \\ t_{34} \\ t_{35} \end{array} \begin{array}{c} \begin{array}{ccccccccc} \theta_1 & \theta_2 & \theta_3 & \theta_4 & \theta_5 & t_{24} & t_{25} & t_{34} & t_{35} \end{array} \\ \begin{bmatrix} 2.65 & & & -1.51 & -1.13 & 0.38 & 0.38 & 0.38 & 0.38 \\ & 1 & & -1 & & & & & \\ & & 1 & & -1 & & & & \\ & & & 0.85 & -0.85 & -0.51 & 0.68 & -0.51 & 0.68 \\ & & & & 0 & & & & \\ & & & & & 0.77 & 0.26 & 0.77 & 0.26 \\ & & & & & & 0.58 & & 0.58 \\ & & & & & & & 1 & \\ & & & & & & & & 0 \end{bmatrix} \end{array}. \quad (51)$$

Two zero pivots are found, at positions (5,5) and (9,9), corresponding to bus 5 and switching branch 3-5. Such finding means the system needs two references, an angle and a power flow. Reference flow measurements are associated with switching branches state variables; in the same way, angular references are attached to network islands (MONTICELLI, 1993b).

By changing the zero pivots by one, and the respective elements of the vector t_A, the estimated state $\hat{\theta}$ is evaluated. Then, the unobservable branches are found as follows.

$$P_b = A\hat{\theta} = \begin{matrix} b_{1-4} \\ b_{1-5} \\ s_{2-4} \\ s_{2-5} \\ s_{3-4} \\ s_{3-5} \end{matrix}\begin{bmatrix} 1 & & & -1 & & & & & \\ 1 & & & & -1 & & & & \\ & & & & & 1 & & & \\ & & & & & & 1 & & \\ & & & & & & & 1 & \\ & & & & & & & & 1 \end{bmatrix}\begin{bmatrix} 0 \\ 0 \\ 0 \\ 0 \\ 0 \\ 0 \\ -1 \\ 0 \\ 1 \end{bmatrix} = \begin{bmatrix} 0 \\ 0 \\ 0 \\ -1 \\ 0 \\ 1 \end{bmatrix}. \quad (52)$$

where:

s_{k-l}: refers to a switching branch from generic node k to l.

This first analysis reveals that switching branches 2-5 and 3-5 are unobservable, and as a consequence, the pseudo-injection measurement at node 5 is irrelevant. When the Jacobian matrix H_{AA} is updated by taking out the row corresponding the pseudo injection measurement at node 5 and applying the triangular factorization again, it gives the following U factor.

$$U = \begin{matrix} \\ \theta_1 \\ \theta_2 \\ \theta_3 \\ \theta_4 \\ \theta_5 \\ t_{24} \\ t_{25} \\ t_{34} \\ t_{35} \end{matrix}\begin{matrix} \begin{matrix} \theta_1 & \theta_2 & \theta_3 & \theta_4 & \theta_5 & t_{24} & t_{25} & t_{34} & t_{35} \end{matrix} \\ \begin{bmatrix} 2.45 & & & -1.63 & -0.82 & 0.41 & & 0.41 & \\ & 1 & & -1 & & & & & \\ & & 1 & & -1 & & & & \\ & & & 0.58 & -0.58 & -0.58 & & -0.58 & \\ & & & & 0 & & & & \\ & & & & & 0.71 & & 0.71 & \\ & & & & & & 0 & & \\ & & & & & & & 1 & \\ & & & & & & & & 0 \end{bmatrix} \end{matrix}. \quad (53)$$

Accordingly, three zero pivots are found at (5,5), (7,7), and (9,9). Following the same procedure, the flows are obtained as follows.

$$P_b = A\hat{\theta} = \begin{matrix} b_{1-4} \\ b_{1-5} \\ s_{2-4} \\ s_{3-4} \end{matrix}\begin{bmatrix} 1 & & -1 & & & \\ 1 & & & -1 & & \\ & & & & 1 & \\ & & & & & 1 \end{bmatrix}\begin{bmatrix} 0 \\ 0 \\ 0 \\ 0 \\ 0 \\ 0 \\ 1 \\ 0 \\ 2 \end{bmatrix} = \begin{bmatrix} 0 \\ 0 \\ 0 \\ 0 \end{bmatrix}. \quad (54)$$

From the above, one can notice that if the flows are null, all the remaining branches and switching branches are observable. In such case, the conventional branches from bus 1 to 4 and 5, and switching branches 2-4 and 3-4 form an observable island. Switching branches 2-5 and 3-5 are unobservable and form two unobservable islands.

3.3 SUMMARY OF THE CHAPTER

This chapter have represented the observability methods for power systems modeled at the bus-branch and bus-section levels. The numerical and topological approaches were demonstrated, and as consequence it has been shown how a power network can be found observable, by determining the rank of Jacobian matrix and by finding and Observable Spanning Tree. In case of unobservability, it was demonstrated how to find unobservable branches, observable islands and irrelevant measurement by post-processing the Jacobian matrix.

For power systems modeled at the substation level, the same numerical algorithms could be applied, as the new state variables are considered in the Jacobian matrix. For the topological approach, the same is true, since the new states from a new measurement graph, which also must form an Observable Spanning Tree.

The numerical algorithm unfolded here are used in the proposed method to evaluate the system observability in the presence of PMUs, in a pre-processing step.

4 OBSERVABILITY AND CRITICALITY ANALYSIS FOR GENERALIZED STATE ESTIMATION CONSIDERING PHASOR MEASUREMENTS

This chapter presents the above mentioned methodology when coping with GPS synchronized phasor measurements in the Generalized approach of State Estimation.

The proposed approach is an extension of the method presented in the paper named “Observability and criticality analyses for power systems measured by phasor measurements” (GOL; ABUR, 2013). Such paper offered observability and criticality analysis methods for two different kinds of current phasor measurement configurations. However, is focused only for systems modeled at the bus-branch level.

The method is described for two current phasor measurement configurations. In the first one, named measurement configuration type-1, current phasor measurements have a corresponding voltage phasor measurement at the sending end bus. Thus, it allows the deployment of the traditional methods for observability and criticality analysis as it converts the current phasor measurement into power flow measurements. On its turn, measurement configuration type-2 is applicable in case of loss or bad data, when current phasor measurement may be available without the corresponding voltage phasor measurement, therefore forbidding the conversion for power flow measurements and the use of traditional methods.

4.1 OBSERVABILITY AND CRITICALITY METHODS FOR MEASUREMENT CONFIGURATION TYPE-1

In general, one of the PMU’s channels measures the voltage phasor of its bus while the remaining ones measure the current phasors of connected branches, as depicted in Figure 18.

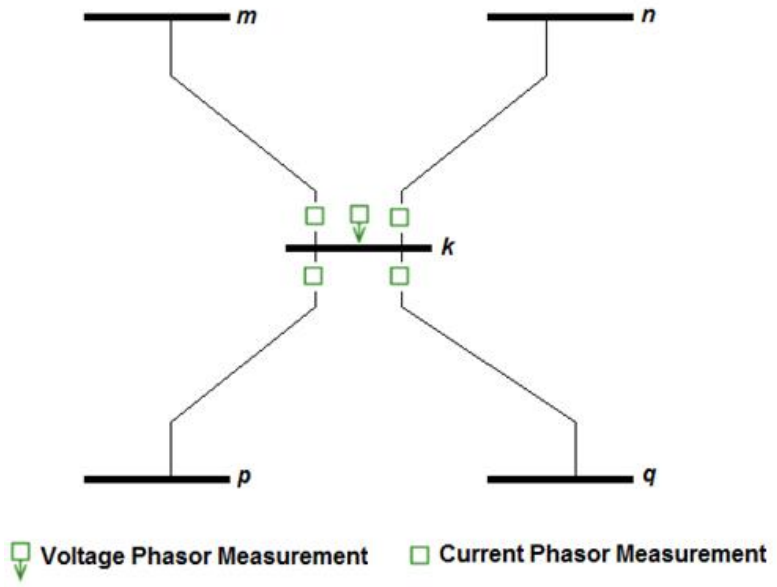

Figure 18 – Bus and branches measured by a PMU

With both voltage and current measurements available, it is possible to compute the active and reactive power flows in those branches, turning the current phasor measurements into power flow ones, as follows:

$$V_k I_{km}^* = P_{km} + jQ_{km} \tag{55}$$

In the example of Figure 18, all the current phasor measurement can be converted into power flow ones by using the Eq. (55). This is a common practice in industry (ATANACKOVIC *et al.*, 2008) and it permits the use of the traditional observability and criticality methods.

In order to show these properties for GSE, the 3 bus/5 nodes system shown in Figure 19 is used as an example.

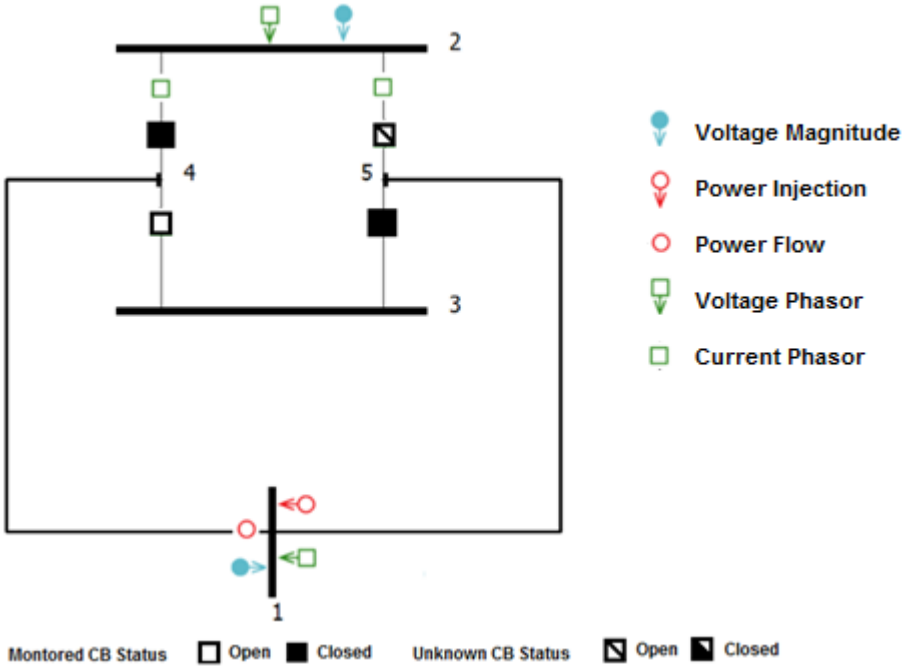

Figure 19 – 3 bus / 5 nodes system – Example 1

In this case, there is a PMU at the busbar 2, where one channel measures the voltage phasor, and the other two channels measure the current phasors on the switching branches 2 – 4 and 2 – 5. The actual status of the circuit breaker 2 – 5 is opened, but unknown for purposes of demonstration.

The current phasor measurements have a voltage measurement at the corresponding bus, so that they can be converted into power flow measurements. The current phasor measurements, however, are placed on switching branches, where the equation takes the following form for conversion:

$$V_k I_{kl}^* = t_{kl} + j u_{kl} \tag{56}$$

Therefore, the current phasor measurements are converted as measurements of the generalized states to be estimated, being usable directly in the Jacobian matrix, which takes the following form:

$$H_{AA} = \begin{array}{c} \\ P_{1-4} \\ P_1 \\ I_{2-4}^{PMU}/t_{2-4} \\ I_{2-5}^{PMU}/t_{2-5} \\ \theta_1^{PMU} \\ \theta_2^{PMU} \\ P_4^p \\ P_5^p \\ \Delta\theta_{2-4}^p \\ \Delta\theta_{3-5}^p \\ t_{3-4}^p \end{array} \begin{array}{c} \begin{array}{ccccccccc} \theta_1 & \theta_2 & \theta_3 & \theta_4 & \theta_5 & t_{24} & t_{25} & t_{34} & t_{35} \end{array} \\ \begin{bmatrix} 1 & & & -1 & & & & & \\ 2 & & & -1 & -1 & & & & \\ & & & & & 1 & & & \\ & & & & & & 1 & & \\ 1 & & & & & & & & \\ & 1 & & & & & & & \\ -1 & & & 1 & & -1 & & -1 & \\ -1 & & & & 1 & & -1 & & -1 \\ & 1 & & -1 & & & & & \\ & & 1 & & -1 & & & & \\ & & & & & & & 1 & \end{bmatrix} \end{array} \quad (57)$$

The voltage phasor measurements are also used as measurements of the states, and in the corresponding column is represented by “1”.

Since circuit breaker 2-5 status is unknown, its operational constraint, or pseudo measurement ($\Delta\theta_{2-5}^p$), is not included in the Jacobian matrix.

The matrix H_{AA} in Eq. (57) has a full rank, rendering the network observable. When the triangular factorization is performed, none zero pivots are found. Figure 20 shows the measurement graph of the system, which yields a spanning tree.

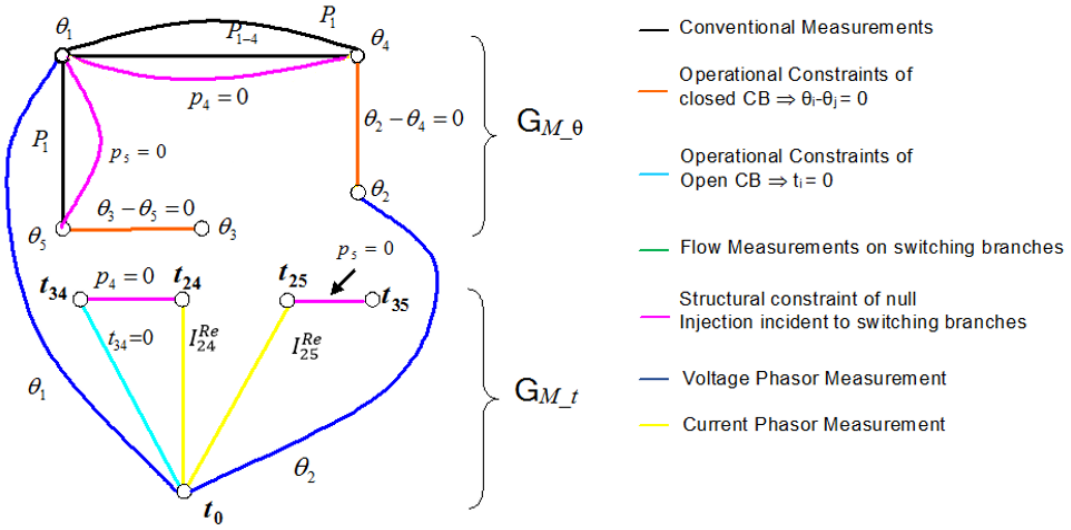

Figure 20 – Measurement graph of the 3 bus / 5 nodes system – Example 1

The criticality analysis can be carried out using the traditional method, as described in Gol and Abur (2013). The Sensitivity matrix (S) is computed as described in Eq. (58).

$$S = I - H_{AA}(H_{AA}^{T}H_{AA})^{-1}H_{AA}^{T} \tag{58}$$

where:

I: is an mxm identify matrix

The zero diagonals entries in matrix S represent critical measurements. Since the proposed extension includes operational and structural constraints (pseudo measurements related to CB status and null injection nodes), which models the status of switching branches, matrix S (zero diagonal entries) also indicates critical constraints. In the example case of Figure 19, two measurements and two constraints (or pseudo measurements) are flagged critical, as follows: injection measurements at bus 1; the current phasor measurement on switching branch 2-5; the operational constraint of CB 3-5; and structural constraint of null injection at node 5.

This result is verified by analyzing the measurement graph in Figure 20, where it is possible to verify that if each critical measurement and constraint is lost, an observable spanning tree is no longer formed.

An important result that is worth being pointed out here is that the voltage phasor measurement at busbar 2 is able to prevent criticality of an operational constraint, and it corresponds to the closed position of circuit breaker 2-4. Furthermore, the graph in Figure 20 indicates that the direct measure of the state θ_2 clearly creates an additional connection with the reference node t_o through “node” θ_2. Consequently, this PMU also avoids the criticality of phasor measurement at bus 1, claiming the relevance of analyzing the observability and criticality of systems with PMU at the bus-section level, as proposed in this thesis.

4.2 OBSERVABILITY AND CRITICALITY METHODS FOR MEASUREMENT CONFIGURATION TYPE -2

The case of configuration measurement type-2 can be illustrated with the same example of Figure 19, but removing the voltage phasor measurement at busbar 2, as shown in Figure 21.

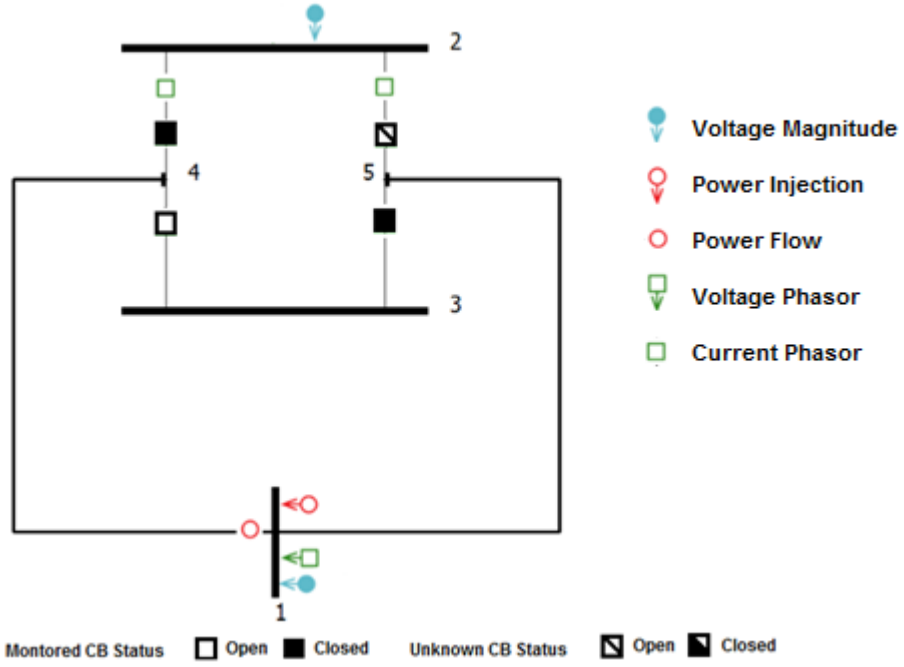

Figure 21 - 3 bus / 5 nodes system – Example 2

In such a case, the current phasor measurements cannot be decoupled, and the traditional approach cannot be carried out. The proposed method in Gol and Abur (2013), extended here to process switching branch states, consists of the following steps:

1. Disregard all the phasor measurement and process the conventional measurement making use of the traditional method;
2. If the system is found not observable, the observable islands should be found and each of them must be considered as super-nodes;
3. Place the non-processed phasor measurements in the simplified system consisted of super-nodes, and check the observability again.

In step 1, by removing the voltage phasor measurement at bus 1 and current phasor measurements on switch branches 2-4 and 2-5, the system is processed only with the conventional measurements. The same system is found unobservable. After that, step 2, applies the method shown in chapter 3, and it forms the observable islands. The resulting system is exemplified in Figure 22.

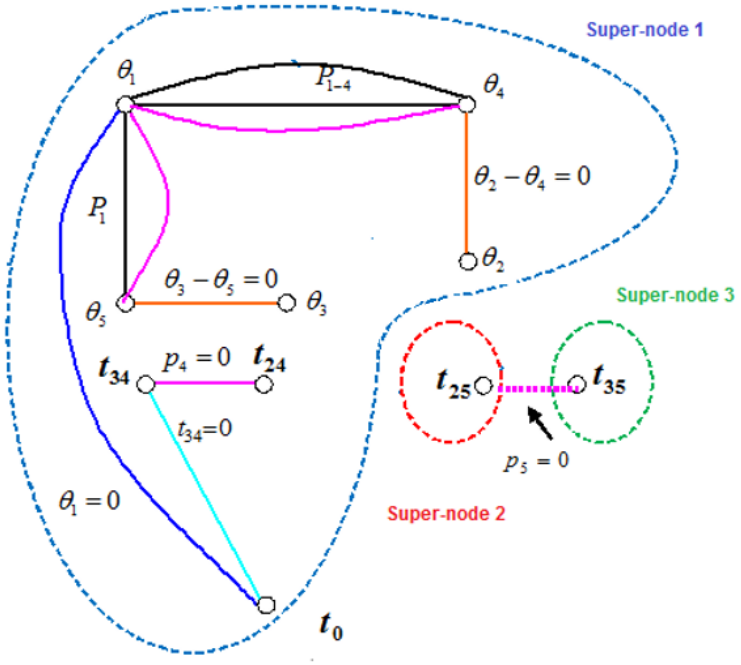

Figure 22 - Measurement graph of the 3 bus / 5 nodes system disregarding PMU – First Step – Example 2

Bearing the picture in mind, the super-node 1 is formed by all the conventional states and switching branches t_{34} and t_{24}. Super-nodes 2 and 3 are formed by switching branch states t_{25} and t_{35}, respectively. The structural constraint of null injection at bus 5 is a boundary injection, flagged as irrelevant. As mentioned before, the phasor measurement at bus 1 is not being considered in this first analysis, though an angular reference is adopted at this stage.

Step 3 processes phasor measurements on the new system, which is made up by super-nodes. Figure 23 illustrates such system:

Figure 23 – Subsystem formed with Super-nodes of PMU – Example 2

In the figure above, the voltage phasor measurement at bus 1 is represented by a phasor at super-node 1. Current phasor measurement on switching branch 2-4 is inside the super-node 1. Since the state can be estimated, it corresponds to a voltage phasor measurement in terms of observability (GOL; ABUR, 2013).

Finally, the current phasor measurement on switching branch 2-5 is also represented as a voltage phasor, as it is placed on a switching branch, which is a state to be estimated.

In order to numerically process the phasor measurements, an incidence matrix relating the states to phasor measurements is formed. The matrix's columns represent the super-nodes and the rows the phasor measurements, as follows:

$$A = \begin{array}{c} \\ I_{2-4} \\ I_{2-5} \\ V_1 \end{array} \begin{array}{c} \begin{array}{ccc} 1 & 2 & 3 \end{array} \\ \begin{bmatrix} 1 & & \\ & 1 & \\ 1 & & \end{bmatrix} \end{array}. \tag{59}$$

Voltage phasor at bus 1 and current phasor on switching branch 2-4 are "1"s in the column corresponding to super-node 1. Current phasor on switching branch 2-5 is a "1" in the column corresponding to super-node 2.

Performing the row reduced echelon form of matrix A, it provides the identification of the anchored and floating super-nodes. In its turn, the columns including linearly independent “1”s stand for anchored super-nodes (GOL; ABUR, 2013). Eq. (60) elucidates such identification:

$$\begin{array}{c} \\ I_{2-4} \\ I_{2-5} \\ \theta_1 \end{array} \begin{array}{c} \begin{array}{ccc} 1 & 2 & 3 \end{array} \\ \begin{bmatrix} 1 & & \\ & 1 & \\ & & 1 \end{bmatrix} \end{array} \Rightarrow \begin{array}{c} \begin{array}{ccc} 1 & 2 & 3 \end{array} \\ \begin{bmatrix} 1 & & \\ & 1 & \\ & & \end{bmatrix} \end{array}. \tag{60}$$

In example 2, the super-nodes 1 and 2 form an anchored super-node and the super-node 3 is a floating super-node. After processing the phasor measurements, the system is still identified as unobservable.

On the other hand, the structural constraint of null injection at node 5, which was flagged irrelevant in the first step of the proposed analysis, must be considered to finalize the process. The structural constraint at node 5 ensures the system observability, as shown in Figure 24.

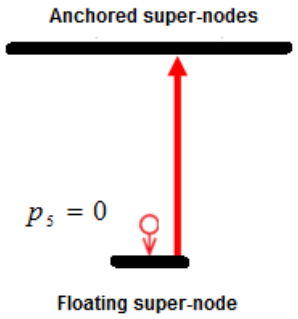

Figure 24 – Anchored and floating super-nodes – Example 2

This boundary injection/constraint allows the connections of super-nodes 2 and 3, as shown in the dotted line in Figure 22. This constraint was flagged irrelevant in the first step of the analysis; however, after considering the phasor measurements,

it must be reconsidered to finalize the observability analysis. Figure 25 depicts this situation in a graph illustration.

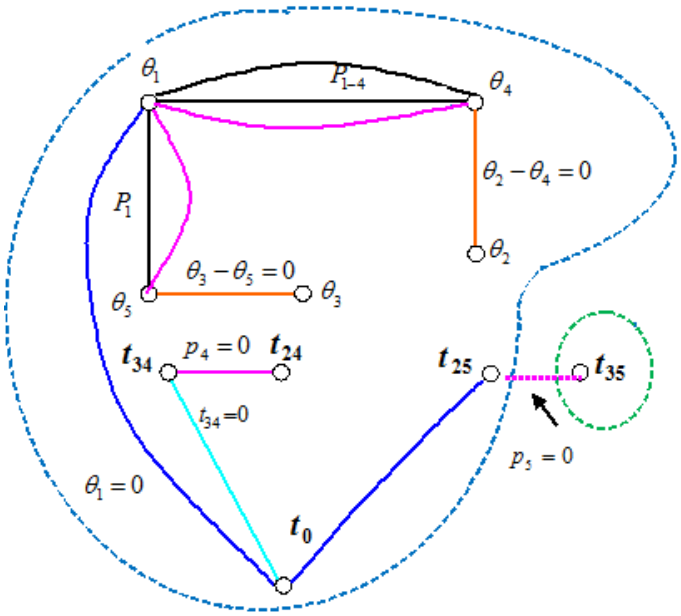

Figure 25 - Measurement graph of the 3 bus / 5 nodes system disregarding PMU –Effect of irrelevant injection measurement/constraint– Example 2

Another possible case is when an irrelevant boundary injection is not necessary to render the system observable. In its turn, it allows the use of Sensitivity matrix to find critical measurements, as discussed ahead. Consider the new situation depicted in Figure 26.

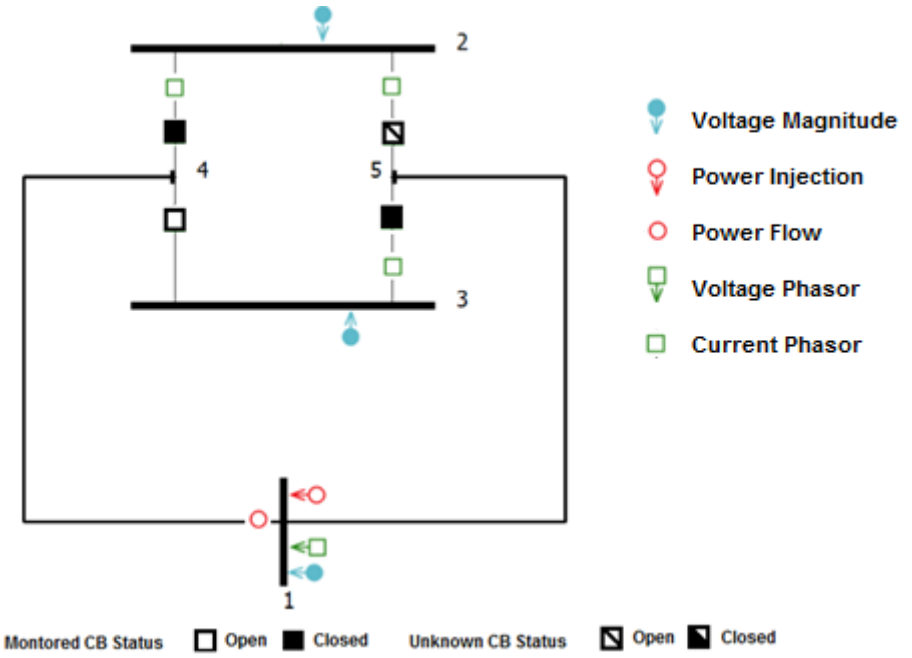

Figure 26 - 3 bus / 5 nodes system – Example 3

Conventional measurements process reveals the same results from the previous example, and it has the same super-nodes shown in Figure 23. Super node 3, however, also has a voltage phasor measurement associated to it, corresponding to the current phasor on switching branch 3-5, as shown in Figure 27.

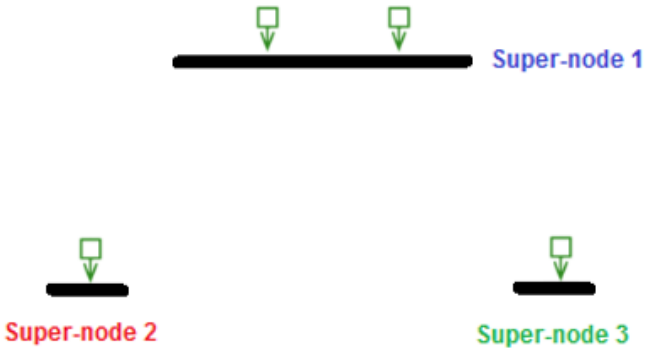

Figure 27 - Subsystem formed with Super-nodes – Example 3

The A matrix and its corresponding row reduced echelon form take the following form, as demonstrated in Eq. (61).

$$A = \begin{array}{c} \\ I_{2-4} \\ I_{2-5} \\ I_{3-5} \\ \theta_1 \end{array} \begin{array}{c} \begin{array}{ccc} 1 & 2 & 3 \end{array} \\ \begin{bmatrix} 1 & & \\ & 1 & \\ & & 1 \\ 1 & & \end{bmatrix} \end{array} \Rightarrow \begin{array}{c} \begin{array}{ccc} 1 & 2 & 3 \end{array} \\ \begin{bmatrix} 1 & & \\ & 1 & \\ & & 1 \\ & & \end{bmatrix} \end{array}. \quad (61)$$

The row reduced echelon form shows that the system is only found observable when phasor measurements are taken into account, by having “1”s at each linearly independent column of the matrix. Once the system is observable, it is possible to use the A matrix to compute the Sensitivity matrix S, as demonstrated in Eq. (62) (GOL; ABUR, 2013).

$$S = I - A(A^T A)^{-1} A^T \quad (62)$$

The null elements in the diagonal of the matrix S correspond to critical phasor measurements.

In the presence of irrelevant injection, however, it is necessary to go back one step and consider the boundary injection/constraint. This is the case of Example 3, in which the effect of the structural constraint of null injection at node 5 was not considered yet. Considering such example, the boundary injection connects the super-nodes 2 and 3, which corresponds to switching branches 2-5 and 3-5, as shown in Figure 22. Thus, at this stage, only two super-nodes must be formed to analyze the effect of phasor measurements, as outlined in Figure 28.

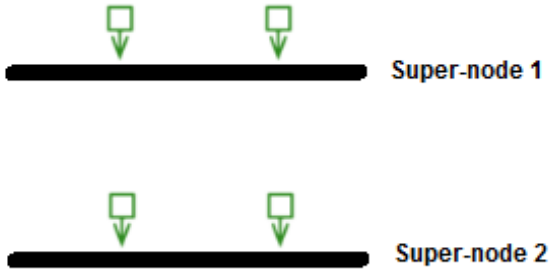

Figure 28- Subsystem formed with Super-nodes, considering the boundary injection – Example 3

Therefore, the actual A matrix, its corresponding row reduced echelon form, and the Sensitivity matrix S take the following forms.

$$A = \begin{array}{c} \\ I_{2-4} \\ I_{2-5} \\ I_{3-5} \\ \theta_1 \end{array} \begin{array}{c} \begin{array}{cc} 1 & 2 \end{array} \\ \begin{bmatrix} 1 & \\ & 1 \\ & 1 \\ 1 & \end{bmatrix} \end{array} \Rightarrow \begin{array}{c} \begin{array}{cc} 1 & 2 \end{array} \\ \begin{bmatrix} 1 & \\ & 1 \\ & \\ & \end{bmatrix} \end{array} \tag{63}$$

$$S = \begin{array}{c} \\ I_{2-4} \\ I_{2-5} \\ I_{3-5} \\ \theta_1 \end{array} \begin{array}{c} \begin{array}{cccc} & & & \end{array} \\ \begin{bmatrix} 0.5 & & & -0.5 \\ & 0.5 & -0.5 & \\ & -0.5 & 0.5 & \\ -0.5 & & & 0.5 \end{bmatrix} \end{array}. \tag{64}$$

From those, none of the phasor measurements are flagged critical.

This numerical criticality analysis only allows the identification of critical phasor measurements. The critical conventional measurements and constraints can be identified by applying the conventional analysis separately for each super-node. The step-by-step procedure of the proposed algorithm is presented as follows:

1 Disregard all phasor measurements and perform the Traditional Observability Analysis (TOA);
2 If the system is Observable, proceed to step 12; otherwise find the observable islands and form super-nodes;
3 Set the phasor measurements in the corresponding simplified system composed by super-nodes; form the A matrix, and find its echelon reduced form;
4 Check the observability by looking if there are “1”s in all columns, which are at linearly independent rows. Despite of the result, also check if there is/are irrelevant measurements/constraints;
5 If the system is observable and there is/are irrelevant measurements/constraints proceed to step 6; if the system is observable and there are no irrelevant measurements/constraints proceed to step 8; if the system is unobservable and there is/are irrelevant measurements/constraints proceed to step 9; otherwise, proceed to step 11;
6 Find all connections among super-nodes that might be provided by irrelevant measurements/constraints and merge them, thereby structuring a new simplified system;
7 Set the phasor measurements in the new subsystem, and form the A matrix;
8 Form the S matrix with A matrix; find critical phasor measurements and proceed to step 12;
9 Find the anchored and floating super-nodes, form a new simplified system, and process the irrelevant measurements/constraints;
10 If the irrelevant measurements render the system observable proceed to step 12; otherwise, proceed to step 11;
11 Find observable islands, unobservable branches and stop the analysis;
12 Proceed for SE.

The proposed algorithm can be summarized in the flow chart in Figure 29. The Highlighted boxes refer to the contribution of this work.

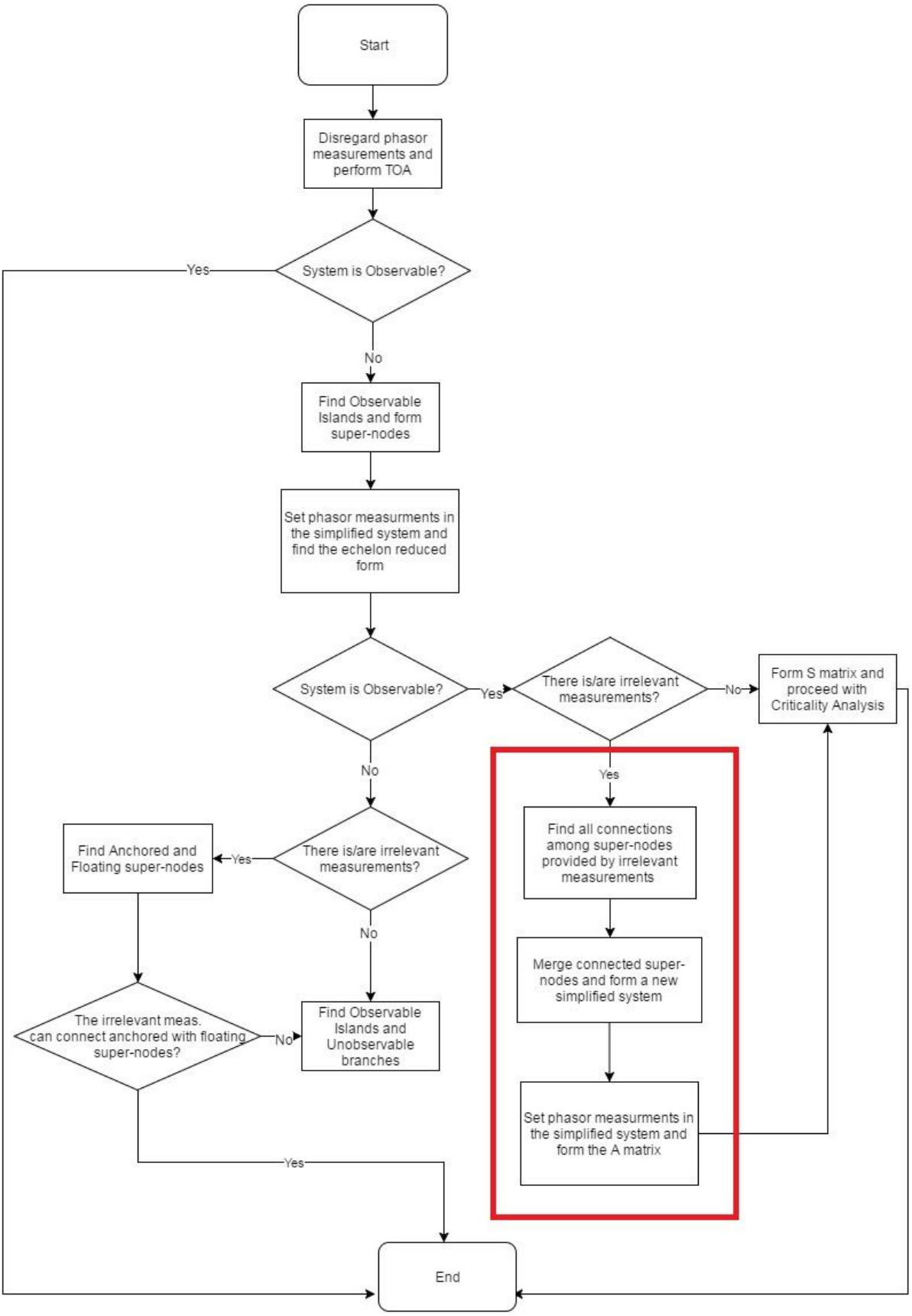

Figure 29 – Algorithm Flowchart for Observability and Criticality Analysis for Measurements Type-2

4.3 SUMMARY OF THE CHAPTER

This chapter presented the proposed method to treat phasor measurements for systems modeled at the substation level, considering two kinds of measurement configuration. In the first one, traditional methods could be applied as current phasor measurements were converted into power flow measurements. In the second case, however, phasor measurements were processed after the conventional measurements, in a simplified system of super-nodes.

The impact of irrelevant measurements was also discussed and it was able to show their capability to render a system fully observable when phasor measurements are considered. Along with that, the proposed algorithm was presented in a step-by-step procedure as well as summarized in a flow chart.

Subsequently, it was pointed out how phasor measurements present themselves as a great advantage to be used in GSE. For such cases, the operational constraint of closed CB is no longer critical, providing a redundancy for logical measurements.

5 TESTS AND RESULTS ANALYSIS

This chapter presents the results of the developed algorithm, which was implemented in MATLAB. The Power Education Toolbox (PET) software (ABUR; MAGNAGO; KRIZAN, 2014) was also used as a means to simplify the way the system is modelled, and to generate the system data and measurements. The well-known IEEE 14 bus benchmark system was used as a base case, with three substations modeled in detail.

The next sections of this chapter present the base case, the modeled substations, and the different measurement designs deployed to validate the proposed method of Observability and Criticality methods for power networks modeled at the substation level with PMU.

5.1 BASE CASE

Figure 30 discloses three buses, 10, 11 and 14, of the IEEE 14 bus system adopted to be modeled in detail at the substation level:

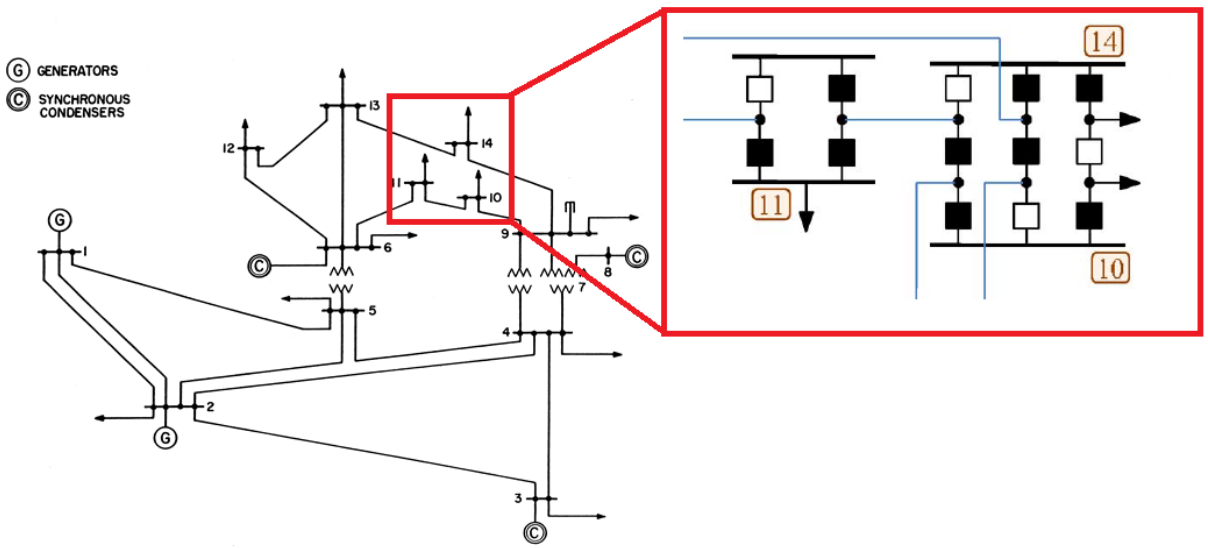

Figure 30 – IEEE 14 Bus system with Modeled Substations

With those substations modeled in detail, it has been assumed the status of two circuit breakers as unknown, and an initial set of conventional measurements, as shown in Figure 31.

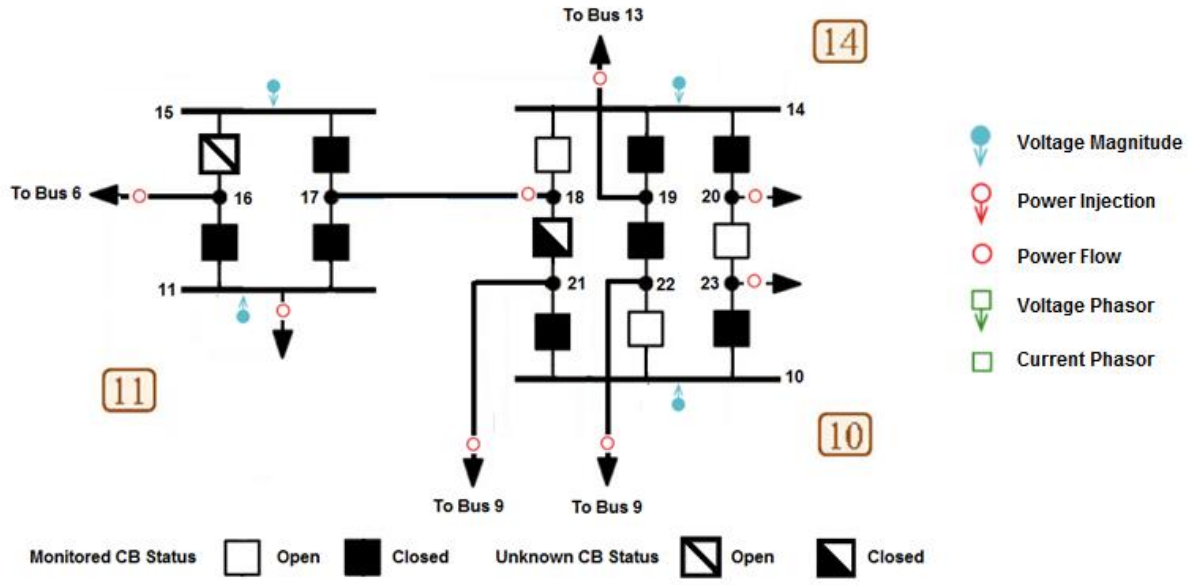

Figure 31 – Substation modeled in detail – Base Case

The new buses/nodes were numerated according to an increase of the system size, that is, from 14 buses to 23 buses/nodes. CB 15-16 status is open but unknown by the system operator, and the status of CB 18-21 is closed and also unknown, so as to simulate a communication failure. The unknown situation aims to simulate a situation of communication failure, where the system operator does not know the actual CB status. The base set of measurements, i.e. the measurement set in the system modeled at the bus-branch level, is composed by several measurements such that no one is critical in the bus-branch level, and it provides a clear analysis for the substation level[6].

[6] For more details, please refer to Appendix B

Running the GSE algorithm, the system is found unobservable, as described ahead. All the conventional states (θ, V) and conventional branches are observable, as well as switching branch states (t, u) of substations 10 and 14. The switching states of substation 11 though, are unobservable, as they form four unobservable islands. According to the proposed algorithm, the system is reduced into five super-nodes, as it can be seen in Figure 32.

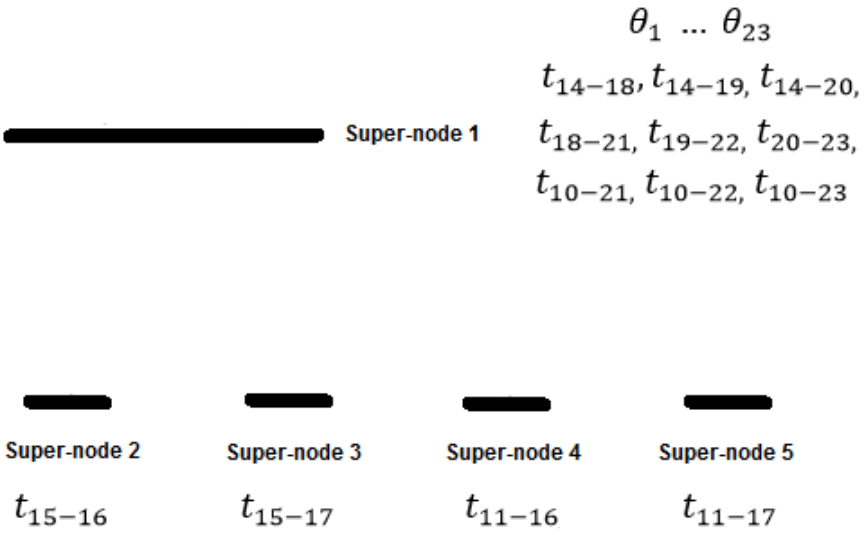

Figure 32 – Super-nodes of base case

Furthermore, the injection measurement at bus 11, and the structural constraints of null injection at buses 15, 16, and 17 are flagged irrelevant by the proposed approach.

5.2 CASE A – MEASUREMENT CONFIGURATION TYPE 1

The first case illustrates the use of measurement configuration type-1, described in section 4.1 of Chapter 4. Figure 33 shows the set of measurements for this case:

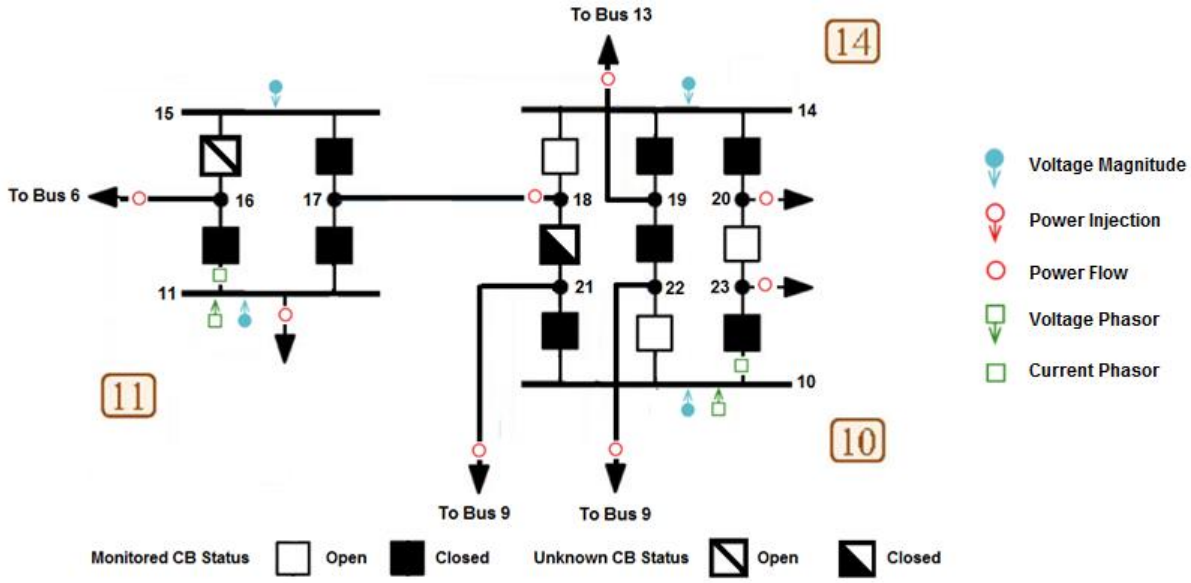

Figure 33 – Modeled Substations – Case Study A

In comparison to the base case, in this very one there are two voltage phasor measurements set at busbars 10 and 11, and two current phasor measurements set on switching branches 10-23 and 11-16. These current phasor measurements can be converted into power flow measurements, allowing the use of traditional methods for observability and criticality analysis.

The use of current phasor measurement on switching branch 11-16, is enough to render the system observable when combined with the voltage phasor at the corresponding busbar. The irrelevant injection measurements/constraints at busbars 11, 15, 16 and 17 play an important role here, since they allow the connection among the super-nodes 2 to 5, rendering a full observability.

The criticality analysis reveals that current phasor measurement on switching branch 11-16 is critical, as well as the operation constraints of closed CB 11-17, 15-17, 10-23, 14-19, and 14-20.

Although the pair of phasor measurements at busbar 10 and switching branch 10-23 are redundant, they make the operational constraint of closed CB 10-21, which was initially critical, but it turned out to be non-critical. The current phasor measurement also makes all the operational constraints of open circuit breakers redundant as well.

Running the GSE algorithm, a final solution was found after 4 iterations. See appendix B for more details.

5.3 CASE B – MEASUREMENT CONFIGURATION TYPE 2

In case B, the current phasor measurement on switching branch 11-16 is lost, as well as the voltage phasor measurement at busbar 10, as shown in Figure 34.

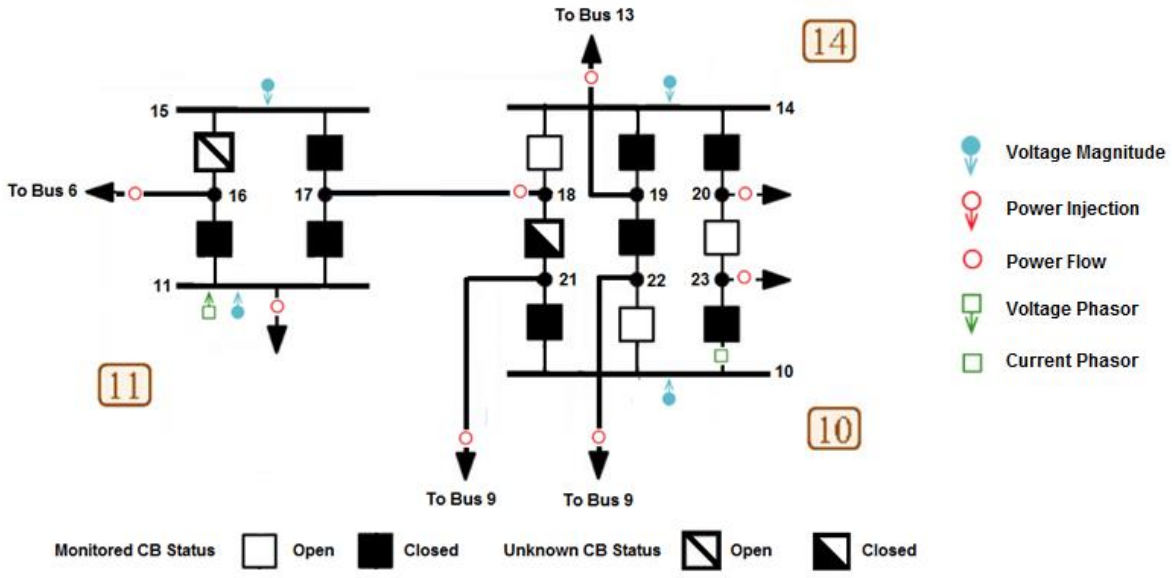

Figure 34 - Modeled Substations – Case Study B

In this case, the current phasor measurement on switching branch 10-23 cannot be converted into a power flow measurement, and the traditional approach cannot be applied.

In this situation, the proposed algorithm first processes the conventional measurements using the traditional observability method, that is, all the phasor measurements are disregarded in the first moment as described in Step 1 of the proposed algorithm (please refer to Section 4.2, of Chapter 4).

At the end of Step 1, the system is reduced to the simplified system. The results are the same as shown in subsection 5.1, and depicted in Figure 32.

The phasor measurement at busbar 11 directly measures a state to be estimated (θ_{11}), and current phasor measurement on switching branch 10-23 is a function of another state to be estimated (t_{10-23}). Therefore, according to the proposed algorithm, both measurements can be represented in the same way as voltage phasor measurements on super-node 1, as shown in Figure 35[7].

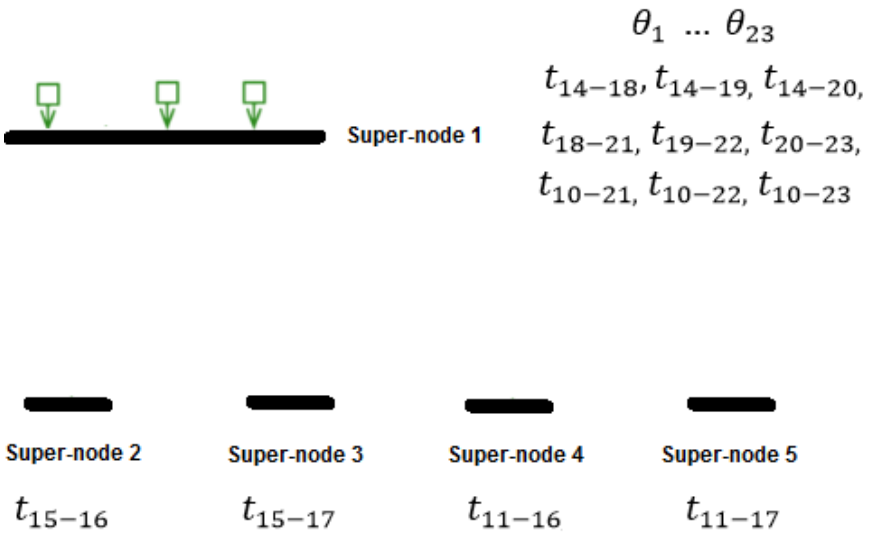

Figure 35 - Super-nodes of case study B

This measurement set is not able of rendering the system fully observable. Both phasor measurements are redundant and they only make the conventional states and switching states of substation 10 and 14 observable. The switching states of substation 11 remains unobservable, and as a consequence, injection measurement at busbar 11 and the structural constraints of null injection at nodes 15, 16 and 17 remains irrelevant.

[7] The third voltage phasor at super-node 1 is a voltage phasor measurement placed at bus 1

Running the GSE algorithm, a final solution was not found, since it does not converge due to system unobservability.

5.4 CASE C – MEASUREMENT CONFIGURATION TYPE 2

In the case C, a current phasor measurement is placed on switching branch 15-16, as exhibited in Figure 36.

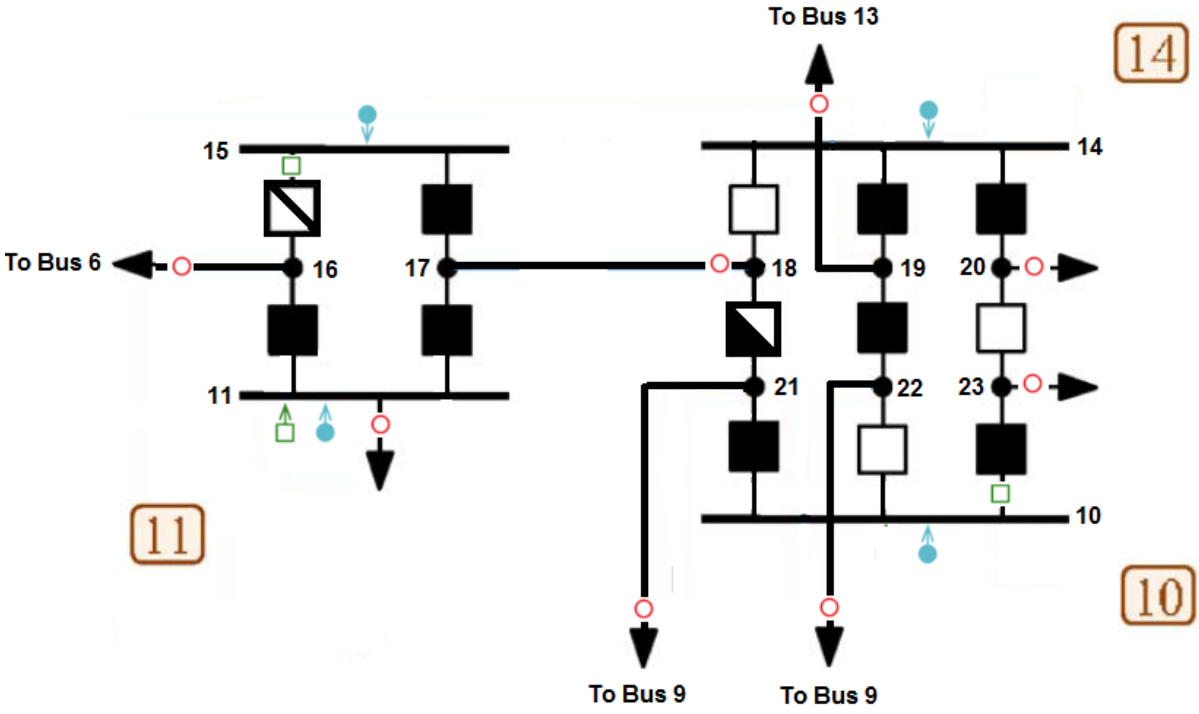

Figure 36 - Modeled Substations – Case Study C

This new current phasor measurement cannot be converted into power flow measurement, since busbar 15 has no voltage phasor measurement. Following the proposed algorithm, this current phasor is represented as a voltage phasor on super-node 2, and it corresponds to switching states t_{15-16}, as shown in Figure 37.

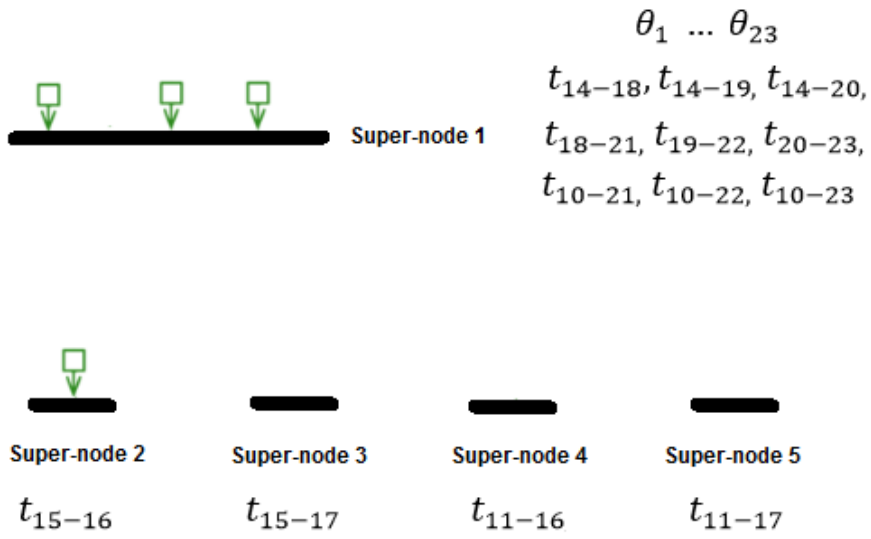

Figure 37 - Super-nodes of case study C

Now, the super-nodes 1 and 2 form an anchored super-node, and those remained form three floating super-nodes, as shown in Figure 38.

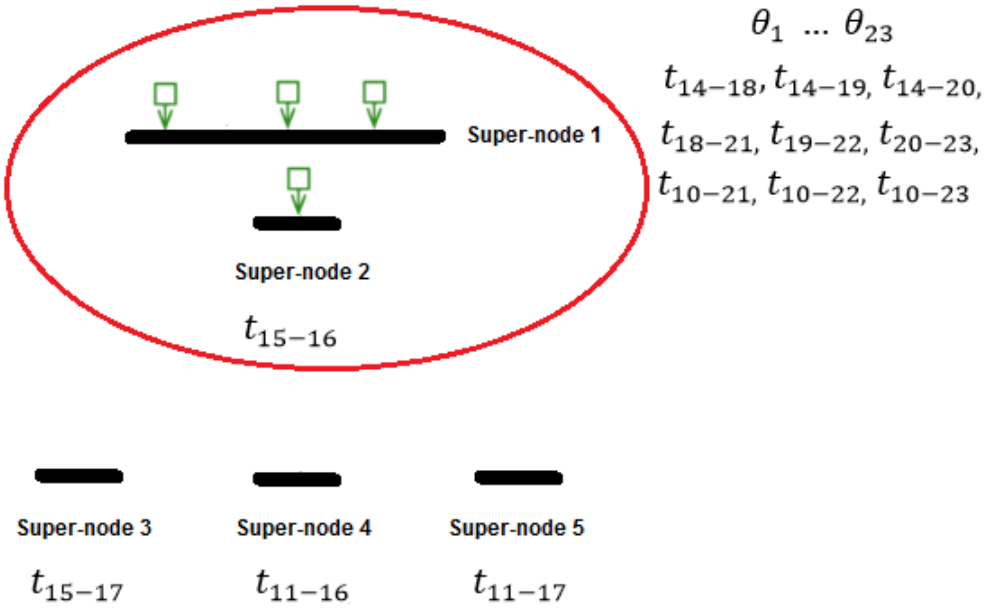

Figure 38 – Anchored and Floating super-nodes – Case C

At this point, the system is unobservable. However, there are injection measurements/constraints ($P_{11}^m, P_{15}^c,\ P_{16}^c,$ and P_{17}^c) which were flagged irrelevant and,

according to the proposed algorithm, they should be re-evaluated at this point (see Step 9 of the algorithm). Figure 39 offers the possible connections.

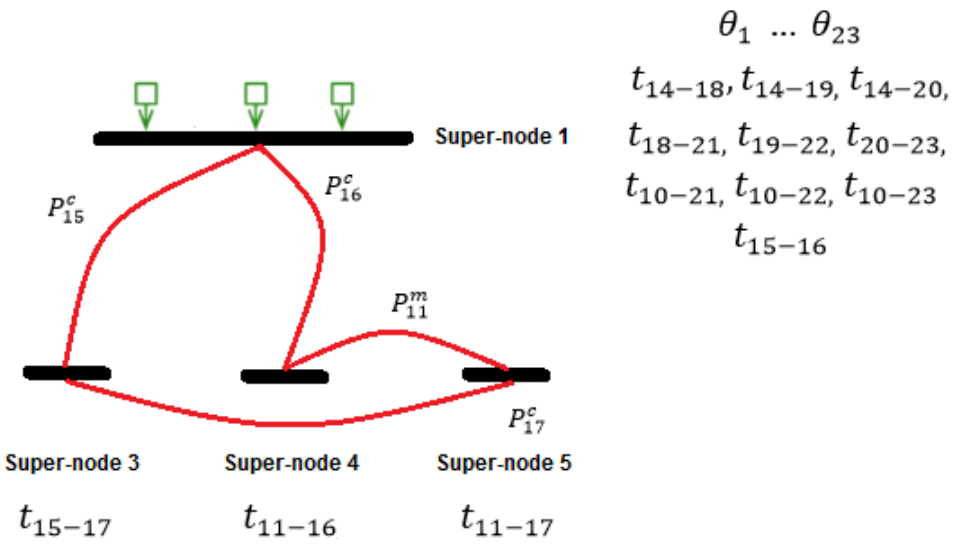

Figure 39 - Anchored and Floating super-nodes and injection measurement connections – Case C

It can be noticed that the injection measurement at busbar 11 connects super-nodes 4 and 5, and the structural constraint of null injection at node 17 connects super-nodes 3 and 5. The remaining structural constraints of null injection at nodes 15 and 16 connect the super-node 3 and 4 with super-node, rendering the system fully observable.

Running the GSE algorithm, a final solution was found after 5 iterations. See appendix B for more details.

5.5 CASE D – MEASUREMENT CONFIGURATION TYPE 2

In the case D, all the switching branches of substation 11 are measured by current phasor measurements, though without a voltage phasor one, as portrayed in Figure 40.

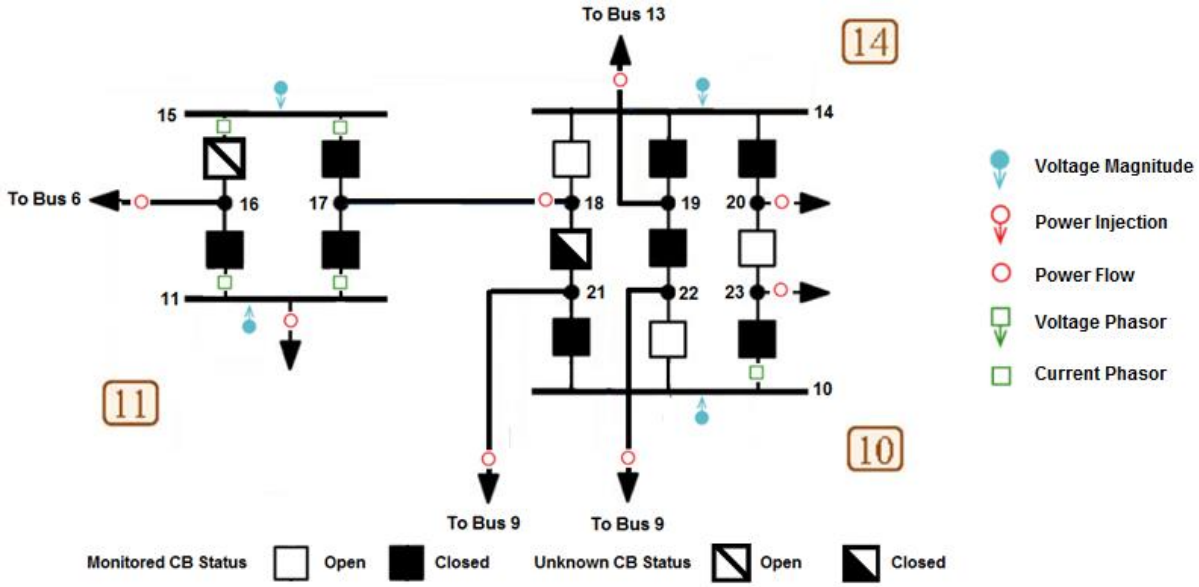

Figure 40 - Modeled Substation – Case Study D

In this case, all the current phasor measurements in substation 11 render observability for all switching states, which were unobservable in the base case. The current phasor measurements are represented in the proposed approach in the same way as voltage phasor in super-nodes 2 to 5, as depicted in Figure 41.

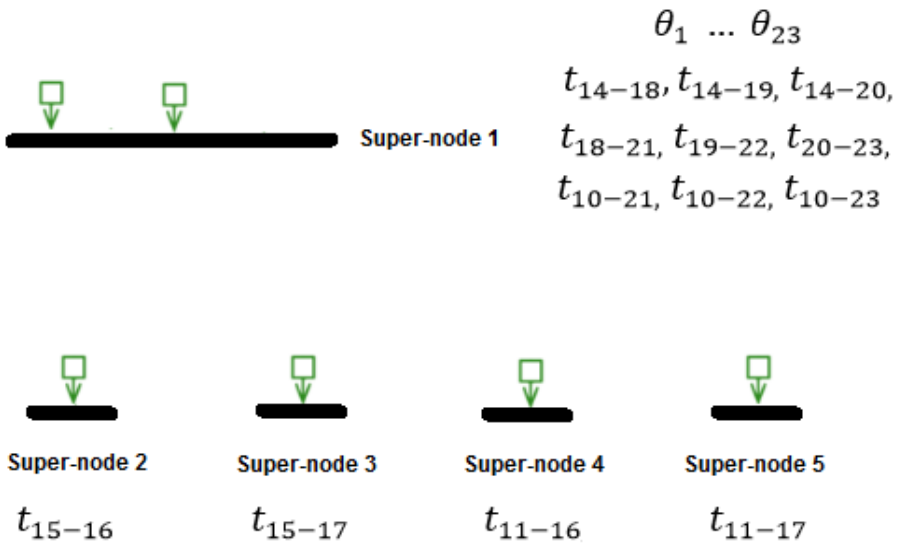

Figure 41 - Super-nodes of case study D

Since the phasor measurements render the system fully observable by making no use of irrelevant measurements, an application of the criticality analysis using the

matrix A, is suitable. The irrelevant measurements, in its turn, must be considered before such analysis is carried out, as described in Step 4 of the algorithm.

Step 6 points out the procedure for this case, that is, to find all connections among super-nodes provided by irrelevant measurements and merge them so as to form a new simplified system. The result of this analysis indicates that super-nodes 2 to 5 are all connected, as in Figure 42.

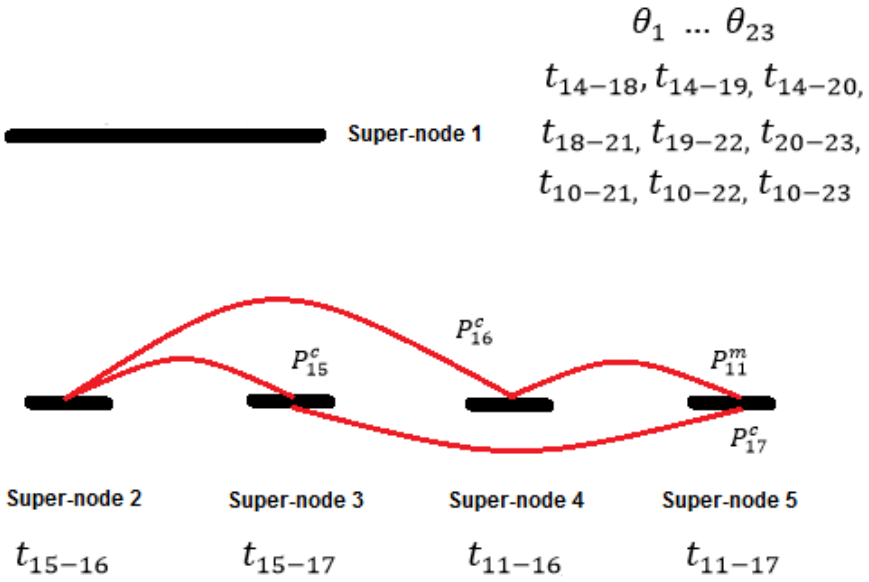

Figure 42 - Super-nodes of case study D with irrelevant measurements and constraints

Therefore, the phasor measurements are processed considering two super-nodes when it comes to criticality analysis, as detailed in Figure 43.

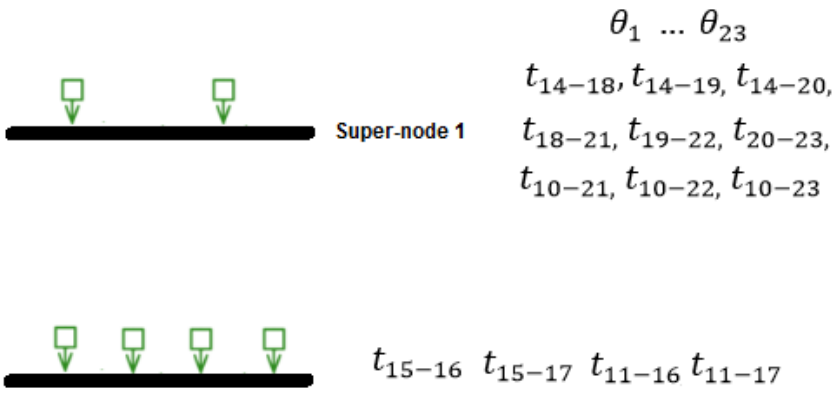

Figure 43 – Super-node of case study D for Criticality Analysis

Matrix A is assembled considering only two super-nodes and six phasor measurements (see Step 7 of the algorithm), as follows:

$$A = \begin{array}{c} \\ \theta_1 \\ I_{10-23} \\ I_{11-16} \\ I_{11-17} \\ I_{15-16} \\ I_{15-17} \end{array} \begin{array}{c} \begin{array}{cc} 1 & 2 \end{array} \\ \begin{bmatrix} 1 & \\ 1 & \\ & 1 \\ & 1 \\ & 1 \\ & 1 \end{bmatrix} \end{array}. \tag{65}$$

Therefore, the Sensitivity matrix S_A (determined in Step 8) takes the following form:

$$S_A = \begin{array}{c} \\ \theta_1 \\ I_{10-23} \\ I_{11-16} \\ I_{11-17} \\ I_{15-16} \\ I_{15-17} \end{array} \begin{array}{c} \begin{array}{cccccc} \theta_1 & I_{10-23} & I_{11-16} & I_{11-17} & I_{15-16} & I_{15-17} \end{array} \\ \begin{bmatrix} 0.5 & -0.5 & & & & \\ -0.5 & 0.5 & & & & \\ & & 0.75 & -0.25 & -0.25 & -0.25 \\ & & -0.25 & 0.75 & -0.25 & -0.25 \\ & & -0.25 & -0.25 & 0.75 & -0.25 \\ & & -0.25 & -0.25 & -0.25 & 0.75 \end{bmatrix} \end{array}. \tag{66}$$

As it has not been found any zero elements in the S_A matrix, none of the phasor measurements are flagged critical.

Running the GSE algorithm, a final solution was found after 5 iterations. See appendix B for more details.

5.6 CASE E – ISLAND NODE

In case E, the status of CB 10-21 is unknown, causing the islanding of nodes 10 and 23, as seen in Figure 44.

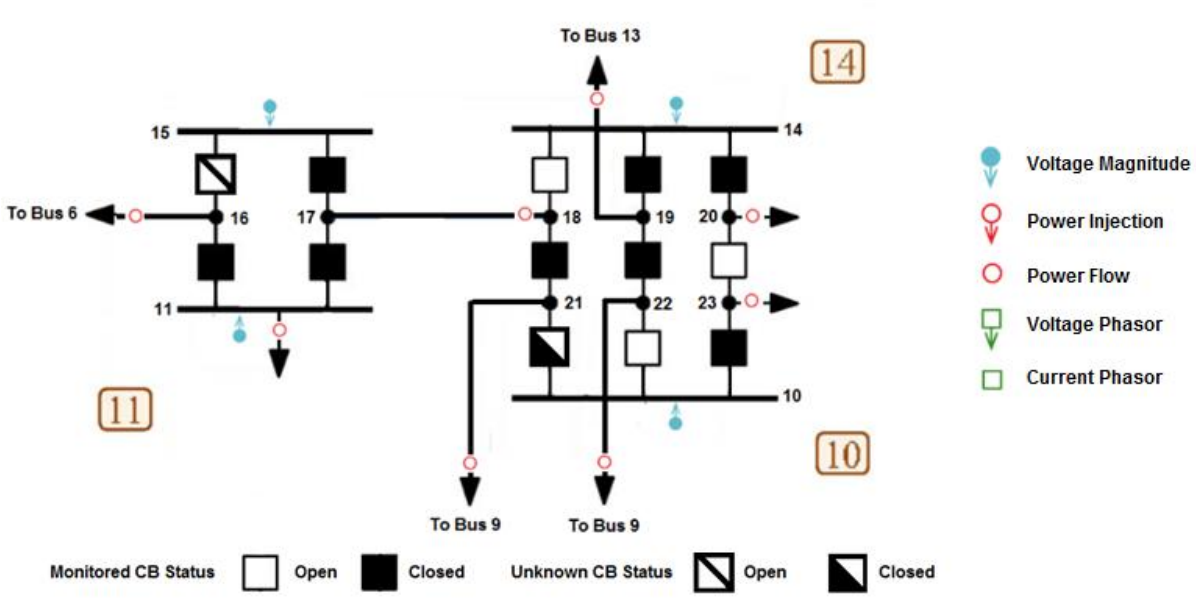

Figure 44 – Modeled substation – Case E

For such circumstances, the traditional numerical algorithm was not capable of identifying the observable and unobservable portions of the system, and as a consequence was not able to form the super-nodes. Since it failed to provide a satisfactory result in this first step, this case could not be fully investigated in the light of the proposed method. Although the analysis could not be carried out, this case serves to highlight the impact of an operational constraint of closed CB.

5.7 SUMMARY OF THE CHAPTER

This chapter presented the results of the proposed method in systems modeled at the substation level. A base case was disclosed whose composition consisted of only conventional measurements and two unknown CB status, which rendered the system unobservable. Thus, four situations combining measurements configurations type 1 and 2 were presented for analysis. The results have shown that the method could be extended for systems in substation level. Moreover, it is worth mentioning that all the results were validated by using the Topological approach, proposed in Simões Costa, Lourenço and Clements (2002), and also by running the developed GSE algorithm. The results achieved by the developed GSE algorithm are thoroughly presented in Appendix B.

6 CONCLUDING REMARK AND FUTURE STUDY

This chapter presents the concluding remarks of this work by reassessing the proposed objectives, singling out the achievements and main results. In addition, it also presents suggestions for future studies.

6.1 CONCLUDING REMARKS

This Master's thesis presented the theory of the well-known WLS Traditional and Generalized State Estimation related to conventional measurements. The inclusion of synchronized phasor measurements was discussed, addressing the use of voltage and current phasor measurements in the bus-branch and bus-section levels. The equations used in two different approaches of the GSE with phasor measurements were derived, providing an easy way to implement them, and providing satisfactory results once included in the already developed GSE algorithm.

The theory of observability analysis, including the topological and numerical approaches were also presented. The numerical approach was deeply investigated as its use was paramount for the proposed method, since it was used to identify observable and unobservable portions of the system, forming the super-nodes in the proposed methods.

The proposed methods of Observability and Criticality Analysis were based on the work of Gol and Abur (2013), which have suggested two approaches for dealing with different measurement configurations for systems modeled at the bus-branch model. In the same way, the proposed methods were implemented and tested for those two measurement configurations, though taking into account the system modeled at substation level.

In addition to that, an algorithm was developed in MATLAB and it was validated via tests over an IEEE system. The results have revealed that the observability method could be extended for substation level, enabling a determination whether the system is observable or not, as well as unobservable switching branches.

Notwithstanding, a specific situation of failure was pointed out in case of node islanding when an operational constraint of closed CB is unknown.

Additionally, the measurement criticality analysis presented some drawbacks, since it was not possible to make use of it in cases where irrelevant injection measurements/constraints had been used to render the system observability.

Besides the drawbacks found, the results have shown a great advantage of using phasor measurements inside the substations. The PMUs were capable of providing a greater level of redundancy for operational constraints. It was observed that critical constraints of closed CB were no longer critical after the usage of voltage phasor measurements in some busbars. Current phasor measurements also provided more redundancy for operational constraints of opened CB, since they directly measure the state to be estimated.

6.2 FURTHER STUDY

This work has acknowledged the applicability of Observability and Criticality methods for power systems modeled at the bus-section level. However, the proposed method of measurement criticality for measurements in configuration type-2 was applicable only for cases where irrelevant injection measurements had not been used to ensure the system observability. As a further study, this method can be improved in order to cope with such situations, and provide an analysis of critical measurements for all cases.

In addition to that, an improvement of the numerical algorithm to deal with island situations would as well be developed. A way to approach it would be pre-processing the system, separating the island portions from the rest, to apply the proposed method afterwards. Another way would be using a hybrid algorithms leveraging the benefits of the topological approach.

The proposed method of measurement criticality analysis could also be attached in the objective function of an optimization algorithm, aiming to find an optimal design of PMUs allocation, and avoiding critical measurements and operational constraints.

REFERENCES

ABUR, A.; EXPÓSITO, A. G. **Power System State Estimation: Theory and Implementation**. New York: Marcel Dekker, 2004.

ABUR, A.; KIM, H.; CELIK, M. K. Identifying the Unknown Circuit Breaker Statuses in Power Networks. **IEEE Transactions on Power Systems**, v. 10, n. 4, 1995.

ABUR, A.; MAGNAGO; KRIZAN. **Power Education Toolbox - PET**. Available in: < http://www1.ece.neu.edu/~abur/pet.html >. Acessed in April 4th 2015.

ALMEIDA, M. C. DE; ASADA, E. N.; GARCIA, A. V. Power System Observability Analysis Based on Gram Matrix and Minimum Norm Solution. **IEEE Transactions on Power Systems**, v. 23, n. 4, p. 1611–1618, 2008.

ALSAC, O.; VEMPATI, N.; STOTT, B.; MONTICELLI, A. Generalized State Estimation. **IEEE Transactions on Power Systems**, v. 13, n. 3, p. 1069–1075, 1998.

ATANACKOVIC, D.; CLAPAUCH, G.; DWERNYCHUCK, G.. First Steps to Wide Area Control. **IEEE Power and Energy Magazine**, p. 61–68, 2008.

BALDWIN, T.; MILI, L.; BOISEN JR, M.; ADAPA, R.. Power System Observability With Minimal Phasor Measurement Placement. **IEEE Transactions on Power Systems**, v. 8, n. 2, p. 707–715, 1993.

BENEDITO, R. A. S.; MOREIRA, E. M.; JR, J. B. A. L.; BRETAS, N. G. Observability Analysis Based on Path Graph Concepts and Triangular Factorization of the Jacobian Matrix. Transmission and Distribution Conference and Exposition: Latin America. **Proceedings...** . p.1–7, 2008.

CARO, E.; CONEJO, A. J.; ABUR, A. Breaker Status Identification. **IEEE Transactions on Power Systems**, v. 25, n. 2, p. 694–702, 2010.

CHEN, J.; ABUR, A. Placement of PMUs to Enable Bad Data Detection in State Estimation. **IEEE Transactions on Power Systems**, v. 21, n. 4, p. 1608–1615, 2006.

CLEMENTS, K. A.; DAVIS, P. W.; KRUMPHOLZ, G. R. Power System State Estimation Residual Analysis: An Algorithm Using Network Topology. **IEEE Transactions on Power Apparatus and Systems**, n. 4, p. 1779–1787, 1981.

CLEMENTS, K. A.; KRUMPHOLZ, G. R.; DAVIS, P. W. Power System State Estimation with Measurement Deficiency: An Algorithm that Determines the Maximal Observable Subnetwork. **IEEE Transactions on Power Apparatus and Systems**, v. PAS-101, n. 9, p. 3044–3052, 1982.

CLEMENTS, K. A.; KRUMPHOLZ, G. R.; DAVIS, P. W. Power System State Estimation with Measurement Deficiency: An Observable/Measurement Placement Algorithm. **IEEE Transactions on Power Apparatus and Systems**, v. PAS-102, n. 7, p. 2012–2020, 1983.

CLEMENTS, K. A.; SIMÕES COSTA, A. Topology Error Identification Using Normalized Lagrange Multipliers. **IEEE Transactions on Power Systems**, v. 13, n. 2, p. 347–353, 1998.

EMAMI, R.; ABUR, A. Robust Measurement Design by Placing Synchronized Phasor Measurements on Network Branches. **IEEE Transactions on Power Systems**, v. 25, n. 1, p. 38–43, 2010.

EXPÓSITO, A. G.; ABUR, A. Generalized Observability Analysis and Measurement Classification. **IEEE Transactions on Power Systems**, v. 13, n. 3, p. 1090–1095, 1998.

EXPÓSITO, A. G.; ABUR, A.; RAMOS, E. R. On the Use of Loop Equations in Power System Analysis. IEEE International Symposium on Circuits and Systems. **Proceedings...** . p.1504–1507, 1995.

EXPÓSITO, A. G.; JAÉN, A. DE LA V. Reduced Substation Models for Generalized State Estimation. **IEEE Transactions on Power Systems**, v. 16, n. 4, p. 839–846, 2001.

FALCÃO, D. M.; ARIAS, M. A. State Estimation and Observability Analysis Based on Echelon Forms of the Linearized Measuremet Models. **IEEE Transactions on Power Systems**, v. 9, n. 2, p. 979–987, 1994.

GJELSVIK, A.; HOLTEN, L. Hachtel´s Augmented Matrix Method - A Rapid Method Improving Numerical Stability in Power System Static Estimation. **IEEE Transactions on Power Apparatus and Systems**, n. 11, p. 2987–2993, 1985.

GOL, M.; ABUR, A. Observability and criticality analyses for power systems measured by phasor measurements. **IEEE Transactions on Power Systems**, v. 28, n. 3, p. 3319–3326, 2013.

GOU, B. Jacobian matrix-based observability analysis for state estimation. **IEEE Transactions on Power Systems** , v. 21, n. 1, p. 348–356, 2006.

GOU, B.; ABUR, A. A Direct Numerical Method for Observability. **IEEE Transactions on Power Systems**, v. 15, n. 2, p. 625–630, 2000.

GOU, B.; ABUR, A. An Improved Measurement Placement Algorithm for Network Observability. **IEEE Transactions on Power Systems**, v. 16, n. 4, p. 819–824, 2001.

IRVING, M. R.; STERLING, M. J. H. Substation data validation **IET Generation, Transmission and Distribution**. 1982.

JAÉN, A. DE LA V.; EXPÓSITO, A. G. Including Ampere Measurements in Generalized State Estimators. **IEEE Transactions on Power Systems**, v. 20, n. 2, p. 603–610, 2005.

JAÉN, A. DE LA V.; ROMERO, P. C.; EXPÓSITO, A. G. Substation data validation by a local three-phase generalized state estimator. **IEEE Transactions on Power Systems**, v. 20, n. 1, p. 264–271, 2005.

KATSIKAS, P. J.; KORRES, G. N. Unified Observability Analysis and Measurement Placement in Generalized State Estimation. **IEEE Transactions on Power Systems**, v. 18, n. 1, p. 324–333, fev. 2003.

ZHU, J.; ABUR, A. Effect of Phasor Measurements on the Choice of Reference Bus for State Estimation. IEEE Power Engineering Society General Meeting. **Proceedings...** . p.1–5, 2007.

KORRES, G. N. KATSIKAS, P.; CLEMENTS, K. DAVIS, P. Numerical Observability Analysis Based on Network Graph Theory. **IEEE Transactions on Power Systems**, v. 18, n. 3, p. 1035–1045, ago. 2003.

KORRES, G. N.; KATSIKAS, P. J. A hybrid Method for Observability Analysis Using a Reduced Network Graph Theory. **IEEE Transactions on Power Systems**, v. 18, n. 1, p. 295–304, fev. 2003.

KORRES, G. N.; KATSIKAS, P. J. Reduced Model for Numerical Observability Analysis in Generalised State Estimation. **IEE - Generation, Transmission and Distribution**, v. 152, n. 1, p. 99–108, 2005.

KORRES, G. N.; MANOUSAKIS, N. M. State estimation and bad data processing for systems including PMU and SCADA measurements. **Electric Power Systems Research**, v. 81, n. 7, p. 1514–1524, jul. 2011.

KORRES, G. N.; MANOUSAKIS, N. M. State estimation and observability analysis for phasor measurement unit measured systems. **IET Generation, Transmission & Distribution**, v. 6, n. 9, p. 902, 2012.

KOUTSOUKIS, N.; MANOUSAKIS, N.; KORRES, G.; GEORGILAKIS, P. Numerical observability method for optimal phasor measurement units placement using recursive Tabu search method. **IET Generation, Transmission & Distribution**, v. 7, n. 4, p. 347–356, 1 abr. 2013.

KRUMPHOLZ, G. R.; CLEMENTS, K. A.; DAVIS, P. W. Power System Observability: A Practical Algorithm Using Network Topology. **IEEE Transactions on Power Apparatus and Systems**, v. PAS-99, n. 4, p. 1534–1542, 1980.

LONDON, J.; PIERETI,S.; BENEDITO, R.; BREATAS, N. Redundancy and Observability Analysis of Conventional and PMU Measurements. **IEEE Transactions on Power Systems**, v. 24, n. 3, p. 1629–1630, ago. 2009.

LONDON, J. B. A.; ALBERTO, L. F. C.; BRETAS, N. G. Analysis of measurement-set qualitative characteristics for state-estimation purposes. **Generation, Transmission & Distribution, IET**, v. 1, n. 1, p. 39–45, 2007.

LOURENÇO, E. M. **Análise de Observabilidade e Identificação de Erros de Topologia na Estimação de Estados Generalizada**. (PhD Thesis) - Universidade Federal de Santa Catarina, 2001.

LOURENÇO, E. M.; SIMÕES COSTA, A.; CLEMENTS, K. A. Bayesian-Based Hypothesis Testing for Topology Error Identification in Generalized State Estimation. **IEEE Transactions on Power Systems**, v. 19, n. 2, p. 1206–1215, 2004.

MANOUSAKIS, N. M.; KORRES, G. N.; ALIPRANTIS, J. N.; VAVOURAKIS, G. P.; MAKRINAS, G. C. J. A two-stage state estimator for power systems with PMU and SCADA measurements. IEEE Grenoble Conference PowerTech, POWERTECH 2013. **Procedings...** , 2013.

MONTICELLI, A. Modeling Circuit Breakers in Weighted Least Squares State Estimation. **IEEE Transactions on Power Systems**, v. 8, n. 3, p. 1143–1149, 1993a.

MONTICELLI, A. The Impact of Modeling Short Circuit Branches in State Estimation. **IEEE Transactions on Power Systems**, v. 8, n. 1, p. 364–370, 1993b.

MONTICELLI, A. **State Estimation in Electric Power Systems: A Generalized Approach**. Boston: Kluwer Academic Publishers, 1999.

MONTICELLI, A. Testing equality constraint hypotheses in weighted least squares state estimators. **IEEE Transactions on Power Systems**, v. 15, n. 3, p. 950–954, 2000.

MONTICELLI, A.; GARCIA, A. Modeling Zero Impedance Branches in Power System State Estimation. **IEEE Transactions on Power Systems**, v. 6, n. 4, 1991.

MONTICELLI, A.; WU, F. F. Network Observability: Theory. **IEEE Transactions on Power Apparatus and Systems**, v. PAS-104, n. 5, p. 1042–1048, 1985a.

MONTICELLI, A.; WU, F. F. Network Observability: Identification of Observable Islands and Measurement Placement. **IEEE Transactions on Power Apparatus and Systems**, v. PAS-104, n. 5, 1985b.

MONTICELLI, A.; WU, F. F. Observability Analysis for Orthogonal Transformation Based State Estimation. **IEEE Transactions on Power Apparatus and Systems**, v. PWRS-1, n. 1, p. 201–206, 1986.

NUCERA, R. R.; GILLES, M. L. Observability Analysis : A New Topological Algorithm. **IEEE Transactions on Power Systems**, v. 6, n. 2, p. 466 – 475, 1991.

NUQUI, R. F.; PHADKE, A. G. Hybrid linear state estimation utilizing synchronized phasor measurements. 2007 IEEE Lausanne POWERTECH, Proceedings. **Proceedings...** . p.1665–1669, 2007.

NUQUI, R. F.; PHADKE, A. G. Phasor Measurement Unit Placement Techniques for Complete and Incomplete Observability. **IEEE Transactions on Power Systems**, v. 20, n. 4, p. 2381–2388, 2005.

PHADKE, A. G.; IBRAHIM, M.; HLIBKA, T. Fundamental Basis for Distance Relaying with Symmetrical Components. **IEEE Transactions on Power Apparatus and Systems**, v. PAS-96, n. 2, p. 635–646, 1977.

PHADKE, A. G.; THORP, J. S. State estimation with phasor measurements. **IEEE Transactions on Power Systems**, v. PWRS-1, n. 1, p. 233–238, 1986.

QUINTANA, V. H.; SIMÕES COSTA, A.; MANDEL, A. Power System Topological Observability Using a Direct Graph-Theoretic Approach. **IEEE Transactions on Power Apparatus and Systems**, v. PAS-101, n. 3, p. 617–626, 1982.

SCHWEPPE, F. C. Power System Static-State Estimation, Part III : Implementation. **IEEE Transactions on Power Apparatus and Systems**, n. 1, p. 130–135, 1970.

SCHWEPPE, F.; ROM, D. Power System Static-State Estimation, Part II: Approximate Model. **IEEE Transactions on Power Apparatus and Systems**, v. PAS-89, n. 1, p. 125–130, jan. 1970.

SCHWEPPE, FRED C; WILDES, J. Power System Static-State, Part I: Exact Model. **IEEE Transactions on Power Apparatus and Systems**, v. PAS-89, n. 1, p. 120–125, 1970.

SILVA, N. S. DA; SIMÕES COSTA, A.; LOURENÇO, E. M. A Numerical Method for Observability Analysis Based on Givens Rotations. NAPS 2011 - 43rd North American Power Symposium. **Proceedings...** , 2011.

SIMÕES COSTA, A.; LOURENÇO, E. M.; CLEMENTS, K. A. Power System Topological Observability Analysis Including Switching Branches. **IEEE Transactions on Power Systems**, v. 17, n. 2, p. 250–256, 2002.

SIMÕES COSTA, A.; PIAZZA, T. S.; MANDEL, A. Qualitative Methods to Solve Qualitative Problems in Power System State Estimation. **IEEE Transactions on Power Systems**, v. 5, n. 3, 1990.

THORP, J. S.; PHADKE, A. G.; KARIMI, K. J. Real Time Voltage-Phasor Measurement for Static State Estimation. **IEEE Transactions on Power Apparatus and Systems**, v. PAS-104, n. 11, p. 3098–3106, 1985.

UNIVERSITY OF WASHINGTON. **Power Systems Test Case Archive**. Disponível em: <https://www.ee.washington.edu/research/pstca/>. Acessed in March 16th . 2015.

ZHU, J.; ABUR, A. Effect of Phasor Measurements on the Choice of Reference Bus for State Estimation. IEEE Power Engineering Society General Meeting. **Proceedings...** . p.1–5, 2007.

YANG, T.; SUN, H.; BOSE, A. Transition to a two-level linear state estimator - Part I: Architecture. **IEEE Transactions on Power Systems**, v. 26, n. 1, p. 54–62, 2011a.

YANG, T.; SUN, H.; BOSE, A. Transition to a two-level linear state estimator - Part II: Algorithm. **IEEE Transactions on Power Systems**, v. 26, n. 1, p. 54–62, 2011b.

ZHOU, M.; CENTENO, V.; THORP, J.; PHADKE, A. An Alternative for Including Phasor Measurements in State Estimators. **IEEE Transactions on Power Systems**, v. 21, n. 4, p. 1930–1937, 2006.

ZHU, J.; ABUR, A. Effect of Phasor Measurements on the Choice of Reference Bus for State Estimation. IEEE Power Engineering Society General Meeting. **Proceedings...** . p.1–5, 2007.

APPENDIX A – POWER FLOW AND INJECTION EQUATIONS

This appendix presents all the referred equations cited in the previous chapters.

(A) Power Flow Equations

Considering the unified branch model (MONTICELLI, 1999) presented at Figure 45, in which there are two phase shifting transformers, one of each side of the line, it is possible to derive all the power flow equations.

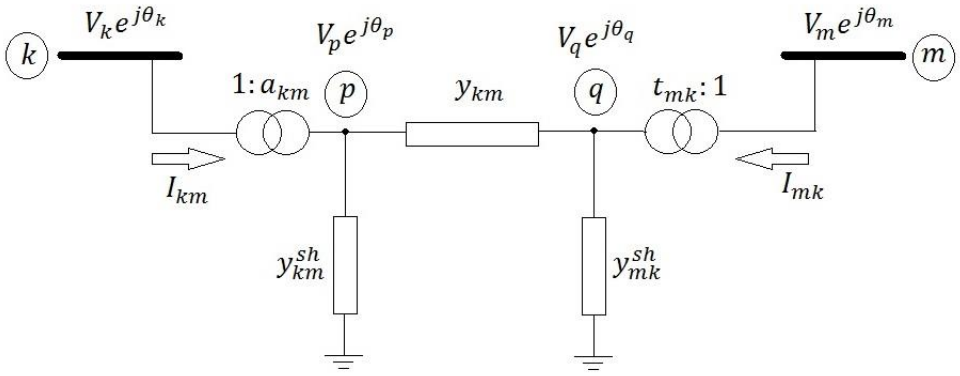

Figure 45 – Unified branch Model
Source: Monticelli (1999)

Active and reactive power flows from bus k to bus m:

$$P_{km} = |a_{km}|^2 V_k^2 g_{km} - |a_{km}||t_{mk}|V_k V_m(g_{km}\cos(\theta_{km} + \varphi_{km} - \varphi_{mk}) + b_{km}\sin(\theta_{km} + \varphi_{km} - \varphi_{mk}))$$

$$Q_{km} = -|a_{km}|^2 V_k^2 (b_{km} + b_{km}^{sh}) - |a_{km}||t_{mk}|V_k V_m(g_{km}\sin(\theta_{km} + \varphi_{km} - \varphi_{mk}) - b_{km}cos(\theta_{km} + \varphi_{km} - \varphi_{mk}))$$

where:

$a_{km} = |a_{km}|e^{j\varphi_{km}}$;

$t_{km} = |t_{mk}|e^{j\varphi_{mk}}$;

g_{km}: is the series conductance;

b_{km}: is the series susceptance.

Active and reactive power flows from bus m to bus k:

$$P_{mk} = |t_{mk}|^2 V_m^2 g_{km} - |a_{km}||t_{mk}|V_k V_m(g_{km}\cos(\theta_{km} + \varphi_{mk} - \varphi_{km}) + b_{km}\sin(\theta_{km} + \varphi_{mk} - \varphi_{km}))$$

$$Q_{mk} = -|t_{mk}|^2 V_m^2 (b_{mk} + b_{mk}^{sh}) - |a_{km}||t_{mk}|V_k V_m(g_{km}\sin(\theta_{km} + \varphi_{mk} - \varphi_{km}) - b_{km}cos(\theta_{km} + \varphi_{mk} - \varphi_{km}))$$

(B) Power Injection Equations

By only given a bus k, the power injection equations can also be derived:

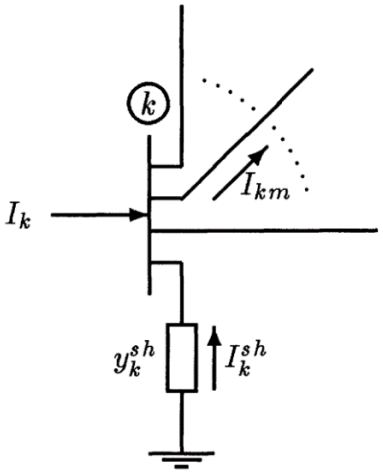

Figure 46 – Generic Bus
Source: Monticelli (1999)

By applying Kirchholff´s Current Law (KCL) yields:

$$P_k = V_k \sum_{m \in N_k} V_j (G_{km} \cos\theta_{km} + B_{km} \sin\theta_{km})$$

$$Q_k = V_k \sum_{m \in N_k} V_m (G_{km} \sin\theta_{km} - B_{km} \cos\theta_{km})$$

where:

G_{km} and B_{km}: are the real and imaginary parts of the admittance nodal matrix;

N_k: is the set of buses connected to bus k.

(C) Jacobian Matrix Equations

Once the power flows and injection equations were derived, the Jacobian matrix equations are given as follow.

$$\frac{\partial P_{km}}{\partial \theta_k} = |a_{km}||t_{mk}|V_k V_m(g_{km}\sin(\theta_{km}+\varphi_{km}-\varphi_{mk})b_{km}-\cos(\theta_{km}+\varphi_{km}-\varphi_{mk}))$$

$$\frac{\partial P_{km}}{\partial \theta_m} = -|a_{km}||t_{mk}|V_k V_m(g_{km}\sin(\theta_{km}+\varphi_{km}-\varphi_{mk})-b_{km}(\cos(\theta_{km}+\varphi_{km}-\varphi_{mk})))$$

$$\frac{\partial P_{km}}{\partial V_k} = 2|a_{km}|^2 g_{km}V_k - |a_{km}||t_{mk}|V_m(g_{km}\cos(\theta_{km}+\varphi_{km}-\varphi_{mk}) + b_{km}\sin(\theta_{km}+\varphi_{km}-\varphi_{mk}))$$

$$\frac{\partial P_{km}}{\partial V_m} = -|a_{km}||t_{mk}|V_k(g_{km}\cos(\theta_{km}+\varphi_{km}-\varphi_{mk})+b_{km}\sin(\theta_{km}+\varphi_{km}-\varphi_{mk}))$$

$$\frac{\partial Q_{km}}{\partial \theta_k} = -|a_{km}||t_{mk}|V_k V_m(g_{km}\cos(\theta_{km}+\varphi_{km}-\varphi_{mk})+b_{km}\sin(\theta_{km}+\varphi_{km}-\varphi_{mk}))$$

$$\frac{\partial Q_{km}}{\partial \theta_m} = |a_{km}||t_{mk}|V_k V_m(g_{km}\cos(\theta_{km}+\varphi_{km}-\varphi_{mk})+b_{km}\sin(\theta_{km}+\varphi_{km}-\varphi_{mk}))$$

$$\frac{\partial Q_{km}}{\partial V_k} = -2|a_{km}|^2\left(b_{km}+b_{km}^{sh}\right)V_k - |a_{km}||t_{mk}|V_j(g_{km}\sin(\theta_{km}+\varphi_{km}-\varphi_{mk}) - b_{km}\cos(\theta_{km}+\varphi_{km}-\varphi_{mk}))$$

$$\frac{\partial Q_{km}}{\partial V_m} = -|a_{km}||t_{mk}|V_k(g_{km}\sin(\theta_{km}+\varphi_{km}-\varphi_{mk})-b_{km}cos(\theta_{km}+\varphi_{km}-\varphi_{mk}))$$

$$\frac{\partial P_k}{\partial \theta_k} = -V_k^2 B_{kk} + \sum_{m=1}^{N} V_k V_m(-G_{km}\,\text{sen}\,\theta_{km} + B_{km}\cos\theta_{km})$$

$$\frac{\partial P_k}{\partial \theta_m} = V_k V_m(G_{km}\,\text{sen}\,\theta_{km} - B_{km}\cos\theta_{km})$$

$$\frac{\partial P_k}{\partial V_k} = V_k G_{kk} + \sum_{m=1}^{N} V_m(G_{km}\cos\theta_{km} + B_{km}\,\text{sen}\,\theta_{km})$$

$$\frac{\partial k}{\partial V_m} = V_k(G_{km}\cos\theta_{km} + B_{km}\,\text{sen}\,\theta_{km})$$

$$\frac{\partial Q_k}{\partial \theta_k} = -V_k^2 G_{kk} + \sum_{m=1}^{N} V_k V_m(G_{km}\cos\theta_{km} + B_{km}\,\text{sen}\,\theta_{km})$$

$$\frac{\partial Q_k}{\partial \theta_m} = V_k V_m(-G_{km}\cos\theta_{km} - B_{km}\,\text{sen}\,\theta_{km})$$

$$\frac{\partial Q_k}{\partial V_k} = -V_k B_{kk} + \sum_{m=1}^{N} V_m(G_{km}\,\text{sen}\,\theta_{km} - B_{km}\cos\theta_{km})$$

$$\frac{\partial Q_k}{\partial V_m} = V_k(G_{km}\,\text{sen}\,\theta_{km} - B_{km}\cos\theta_{km})$$

Voltage magnitude measurements

$$\frac{\partial V_k}{\partial \theta_k} = 0, \frac{\partial V_k}{\partial \theta_m} = 0, \frac{\partial V_k}{\partial V_k} = 1, \frac{\partial V_k}{\partial V_m} = 0$$

APPENDIX B – SYSTEM DETAILS AND RESULTS OF GSE ALGORITHM

This appendix presents a description of the modeled system and the results from the developed GSE algorithm.

(A) System Modeling

The entire system was modeled at PET (Power Education Toolbox), with the switching branches modeled as transmission lines with low and high impedance values for open and closed CB, respectively. Having a few branches modeled with atypical impedance values, the software was able to run a power flow and generate the measurements for state estimation, thereby providing similar results compared to the system modeled at the bus-branch level. Figure 47 shows the entire system modeled in PET, with the conventional measurements spread all over it.

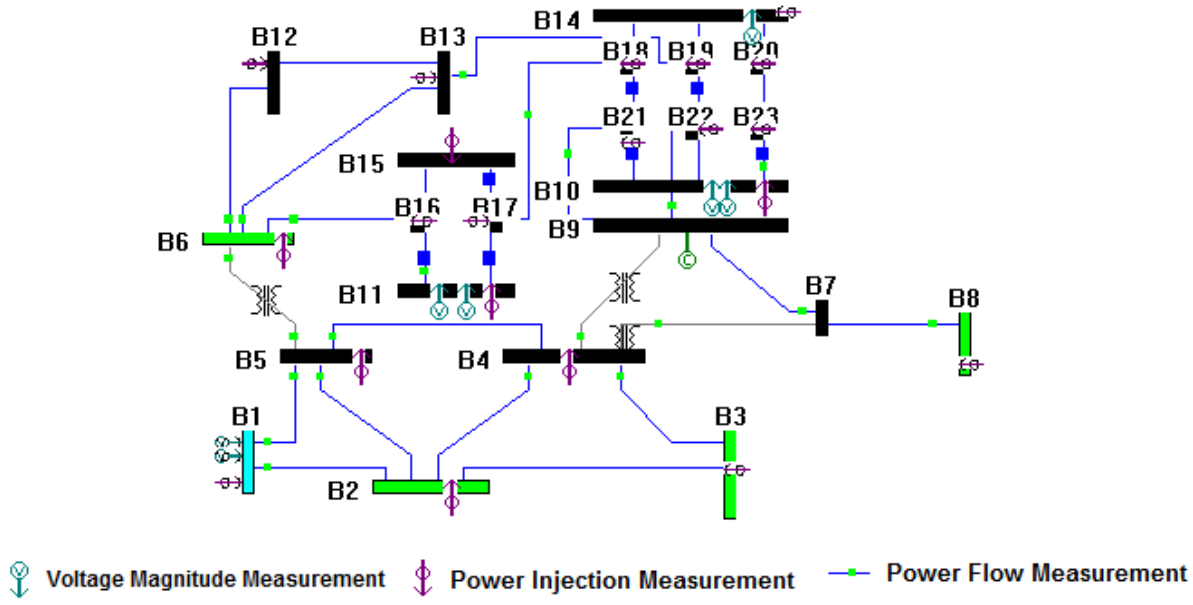

Figure 47 – IEEE 14 bus system modeled in PET

The double voltage magnitude measurement at buses B1, B10, and B11 stands for a voltage magnitude and phasor measurements. These last, in their turn, were emulated by converting some power flow measurements into current ones.

The measurements were generated by a power flow algorithm, with a mismatch of $1x10^{-3}$. Gaussian noise was added to all measurements in order to emulate a real condition. Conventional measurements were considered with standard deviations of $1x10^{-3}$ (power flow and injections) and $1x10^{-4}$ for phasor measurements (voltage and current). The State Estimation was performed with a mismatch of $1x10^{-5}$.

(B) Results from GSE Algorithm

After carrying out the observability and measurement criticality analyses, presented in chapter 5, the developed GSE algorithm was run for all cases in order to check if the state estimation process was possible and the results are shown in the form of screen shots of the outputs from the algorithm.

Test Case A
Converged in 4 iterations

Estimated Bus Data Values					
Bus #	True States V(pu)	True States Ang(deg)	Estimated States V(pu)	Estimated States Ang(deg)	Errors(percent) V(perc)	Errors(percent) Ang(perc)
1	1.060	0.000	1.060	0.000	0.01	0.00
2	1.045	-4.980	1.045	-4.980	0.01	0.00
3	1.010	-12.720	1.010	-12.720	0.01	0.00
4	1.018	-10.310	1.018	-10.320	0.01	0.10
5	1.020	-8.770	1.020	-8.780	0.00	0.11
6	1.070	-14.220	1.070	-14.220	0.01	0.00
7	1.062	-13.360	1.062	-13.360	0.01	0.00
8	1.090	-13.360	1.090	-13.360	0.01	0.00
9	1.056	-14.940	1.056	-14.940	0.01	0.00
10	1.051	-15.100	1.051	-15.100	0.01	0.00
11	1.057	-14.780	1.057	-14.790	0.01	0.07
12	1.055	-15.070	1.055	-15.080	0.01	0.07
13	1.051	-15.150	1.050	-15.160	0.01	0.07
14	1.036	-16.030	1.036	-16.040	0.00	0.06
15	1.057	-14.790	1.057	-14.790	0.01	0.00
16	1.057	-14.790	1.057	-14.790	0.01	0.00
17	1.057	-14.780	1.057	-14.790	0.01	0.07
18	1.051	-15.090	1.051	-15.100	0.02	0.07
19	1.036	-16.030	1.036	-16.040	0.00	0.06
20	1.036	-16.030	1.036	-16.040	0.01	0.06
21	1.051	-15.090	1.051	-15.100	0.01	0.07
22	1.036	-16.030	1.036	-16.040	0.00	0.06
23	1.051	-15.100	1.051	-15.100	0.01	0.00

Objective Function (J(x)-index): 0.589

Estimated Branch Data

Line #	From Bus	To Bus	Power Flow P (MW)	Power Flow Q (Mvar)	Power Flow P (MW)	Power Flow Q (Mvar)	Power Losses P (MW)	Power Losses Q (Mvar)
1	1	2	156.82	-20.39	-152.52	27.65	4.29	7.26
2	1	5	75.52	3.65	-72.76	2.43	2.76	1.22
3	2	5	41.51	0.91	-40.60	-1.85	0.90	0.93
4	2	4	56.12	-1.80	-54.45	3.26	1.68	1.47
5	2	3	73.21	3.56	-70.88	1.59	2.32	1.98
6	3	4	-23.31	4.22	23.68	-4.59	0.37	0.37
7	5	6	44.07	12.68	-44.07	-8.25	0.00	4.42
8	4	5	-61.19	15.15	61.71	-14.86	0.51	0.29
9	4	9	16.09	-0.38	-16.09	1.68	0.00	1.30
10	4	7	28.08	-9.55	-28.08	11.25	0.00	1.70
11	7	8	-0.00	-17.05	0.00	17.50	0.00	0.45
12	7	9	28.08	5.79	-28.08	-4.98	0.00	0.80
13	6	12	7.79	2.50	-7.71	-2.35	0.07	0.15
14	6	13	17.75	7.19	-17.53	-6.77	0.21	0.42
15	12	13	1.61	0.75	-1.60	-0.74	0.01	0.01
16	16	15	-0.01	-0.01	0.01	0.01	0.00	0.00
17	17	15	0.01	0.00	-0.01	-0.00	0.00	0.00
18	16	11	7.30	3.41	-7.30	-3.41	0.00	0.00
19	17	11	-3.79	-1.61	3.79	1.61	0.00	0.00
20	6	16	7.34	3.51	-7.28	-3.40	0.05	0.11
21	21	18	-3.76	-1.57	3.76	1.57	0.00	0.00
22	21	10	8.99	5.79	-8.99	-5.79	0.00	0.00
23	22	19	9.30	3.38	-9.30	-3.38	0.00	0.00
24	19	14	14.89	5.00	-14.89	-5.00	0.00	0.00
25	20	14	-14.90	-5.01	14.90	5.01	0.00	0.00
26	23	10	-9.00	-5.79	9.00	5.79	0.00	0.00
27	18	14	0.01	0.01	-0.01	-0.01	0.00	0.00
28	22	10	0.00	-0.00	-0.00	0.00	0.00	0.00
29	20	23	0.00	0.01	-0.00	-0.01	0.00	0.00
30	17	18	3.79	1.60	-3.77	-1.57	0.01	0.03
31	9	21	5.23	4.26	-5.22	-4.22	0.01	0.03
32	22	9	-9.31	-3.38	9.42	3.63	0.12	0.25
33	19	13	-5.59	-1.61	5.64	1.72	0.05	0.11
							13.381099	23.30

Test Case C
Converged in 5 iterations

Estimated Bus Data Values					
Bus #	True States V(pu)	True States Ang(deg)	Estimated States V(pu)	Estimated States Ang(deg)	Errors(percent) V(perc)	Errors(percent) Ang(perc)
1	1.060	0.000	1.060	0.000	0.01	0.00
2	1.045	-4.980	1.045	-4.980	0.01	0.00
3	1.010	-12.720	1.010	-12.720	0.01	0.00
4	1.018	-10.310	1.018	-10.320	0.01	0.10
5	1.020	-8.770	1.020	-8.780	0.00	0.11
6	1.070	-14.220	1.070	-14.220	0.01	0.00
7	1.062	-13.360	1.062	-13.360	0.01	0.00
8	1.090	-13.360	1.090	-13.360	0.01	0.00
9	1.056	-14.940	1.056	-14.940	0.01	0.00
10	1.051	-15.100	1.051	-15.100	0.01	0.00
11	1.057	-14.790	1.057	-14.790	0.01	0.00
12	1.055	-15.070	1.055	-15.080	0.01	0.07
13	1.051	-15.150	1.050	-15.160	0.01	0.07
14	1.036	-16.030	1.036	-16.040	0.00	0.06
15	1.057	-14.790	1.057	-14.790	0.01	0.00
16	1.057	-14.790	1.057	-14.790	0.01	0.00
17	1.057	-14.790	1.057	-14.790	0.02	0.00
18	1.051	-15.090	1.051	-15.100	0.02	0.07
19	1.036	-16.030	1.036	-16.040	0.01	0.06
20	1.036	-16.030	1.036	-16.040	0.01	0.06
21	1.051	-15.100	1.051	-15.100	0.01	0.00
22	1.036	-16.030	1.036	-16.040	0.01	0.06
23	1.051	-15.100	1.051	-15.100	0.01	0.00

Objective Function (J(x)-index): 0.735

Estimated Branch Data

Line #	From Bus	To Bus	Power Flow P (MW)	Power Flow Q (Mvar)	Power Flow P (MW)	Power Flow Q (Mvar)	Power Losses P (MW)	Power Losses Q (Mvar)
1	1	2	156.82	-20.40	-152.52	27.65	4.29	7.26
2	1	5	75.52	3.65	-72.76	2.43	2.76	1.22
3	2	5	41.51	0.91	-40.60	-1.85	0.90	0.93
4	2	4	56.12	-1.80	-54.45	3.26	1.68	1.47
5	2	3	73.20	3.56	-70.88	1.59	2.32	1.97
6	3	4	-23.31	4.22	23.68	-4.59	0.37	0.37
7	5	6	44.07	12.68	-44.07	-8.26	0.00	4.42
8	4	5	-61.19	15.15	61.71	-14.86	0.51	0.29
9	4	9	16.09	-0.38	-16.09	1.68	0.00	1.30
10	4	7	28.08	-9.56	-28.08	11.25	0.00	1.70
11	7	8	-0.00	-17.05	0.00	17.50	0.00	0.45
12	7	9	28.09	5.79	-28.09	-4.99	0.00	0.80
13	6	12	7.78	2.50	-7.71	-2.35	0.07	0.15
14	6	13	17.74	7.19	-17.53	-6.77	0.21	0.42
15	12	13	1.61	0.75	-1.61	-0.74	0.01	0.01
16	16	15	-0.00	0.00	0.00	-0.00	0.00	0.00
17	17	15	0.00	-0.01	-0.00	0.01	0.00	0.00
18	16	11	7.30	3.41	-7.30	-3.41	0.00	0.00
19	17	11	-3.79	-1.59	3.79	1.59	0.00	0.00
20	6	16	7.34	3.51	-7.28	-3.40	0.05	0.12
21	21	18	-3.77	-1.57	3.77	1.57	0.00	0.00
22	21	10	9.00	5.80	-9.00	-5.80	0.00	0.00
23	22	19	9.30	3.37	-9.30	-3.37	0.00	0.00
24	19	14	14.89	4.99	-14.89	-4.99	0.00	0.00
25	20	14	-14.91	-5.01	14.91	5.01	0.00	0.00
26	23	10	-9.01	-5.80	9.01	5.80	0.00	0.00
27	18	14	0.01	0.01	-0.01	-0.01	0.00	0.00
28	22	10	0.00	0.00	-0.00	-0.00	0.00	0.00
29	20	23	0.00	0.00	-0.00	-0.00	0.00	0.00
30	17	18	3.79	1.60	-3.78	-1.57	0.01	0.03
31	9	21	5.24	4.25	-5.22	-4.22	0.01	0.03
32	22	9	-9.31	-3.38	9.42	3.63	0.12	0.25
33	19	13	-5.58	-1.61	5.64	1.72	0.05	0.11
							13.380584	23.30

Test Case D
Converged in 5 iterations

Estimated Bus Data Values						
Bus #	True States V(pu)	True States Ang(deg)	Estimated States V(pu)	Estimated States Ang(deg)	Errors(percent) V(perc)	Errors(percent) Ang(perc)
1	1.060	0.000	1.060	0.000	0.00	0.00
2	1.045	-4.980	1.045	-4.980	0.01	0.00
3	1.010	-12.710	1.010	-12.720	0.00	0.08
4	1.018	-10.310	1.018	-10.320	0.01	0.10
5	1.020	-8.770	1.020	-8.780	0.00	0.11
6	1.070	-14.210	1.070	-14.220	0.01	0.07
7	1.062	-13.360	1.062	-13.360	0.00	0.00
8	1.090	-13.360	1.090	-13.360	0.00	0.00
9	1.056	-14.930	1.056	-14.940	0.00	0.07
10	1.051	-15.100	1.051	-15.100	0.00	0.00
11	1.057	-14.790	1.057	-14.790	0.00	0.00
12	1.055	-15.070	1.055	-15.080	0.01	0.07
13	1.051	-15.150	1.050	-15.160	0.01	0.07
14	1.036	-16.030	1.036	-16.040	0.01	0.06
15	1.057	-14.790	1.057	-14.790	0.00	0.00
16	1.057	-14.780	1.057	-14.790	0.01	0.07
17	1.057	-14.780	1.057	-14.790	0.01	0.07
18	1.051	-15.090	1.051	-15.100	0.01	0.07
19	1.036	-16.030	1.036	-16.040	0.00	0.06
20	1.036	-16.020	1.036	-16.040	0.01	0.12
21	1.051	-15.090	1.051	-15.100	0.01	0.07
22	1.036	-16.030	1.036	-16.040	0.00	0.06
23	1.051	-15.090	1.051	-15.100	0.01	0.07

Objective Function (J(x)-index): 1.830

Estimated Branch Data								
Line #	From Bus	To Bus	Power Flow P (MW)	Power Flow Q (Mvar)	Power Flow P (MW)	Power Flow Q (Mvar)	Power Losses P (MW)	Power Losses Q (Mvar)
1	1	2	156.82	-20.39	-152.52	27.65	4.29	7.26
2	1	5	75.52	3.65	-72.76	2.43	2.76	1.22
3	2	5	41.51	0.91	-40.60	-1.85	0.90	0.93
4	2	4	56.12	-1.80	-54.45	3.26	1.68	1.47
5	2	3	73.21	3.57	-70.89	1.59	2.32	1.98
6	3	4	-23.31	4.22	23.68	-4.59	0.37	0.37
7	5	6	44.07	12.68	-44.07	-8.25	0.00	4.42
8	4	5	-61.20	15.15	61.71	-14.86	0.51	0.29
9	4	9	16.09	-0.37	-16.09	1.68	0.00	1.30
10	4	7	28.08	-9.55	-28.08	11.25	0.00	1.70
11	7	8	0.00	-17.05	-0.00	17.50	0.00	0.45
12	7	9	28.09	5.79	-28.09	-4.99	0.00	0.80
13	6	12	7.78	2.49	-7.71	-2.35	0.07	0.15
14	6	13	17.74	7.19	-17.53	-6.77	0.21	0.42
15	12	13	1.61	0.75	-1.61	-0.74	0.01	0.01
16	16	15	-0.01	-0.00	0.01	0.00	0.00	0.00
17	17	15	0.00	0.00	-0.00	-0.00	0.00	0.00
18	16	11	7.29	3.41	-7.29	-3.41	0.00	0.00
19	17	11	-3.79	-1.61	3.79	1.61	0.00	0.00
20	6	16	7.34	3.51	-7.28	-3.40	0.05	0.11
21	21	18	-3.77	-1.58	3.77	1.58	0.00	0.00
22	21	10	9.00	5.79	-9.00	-5.79	0.00	0.00
23	22	19	9.29	3.38	-9.29	-3.38	0.00	0.00
24	19	14	14.89	5.00	-14.89	-5.00	0.00	0.00
25	20	14	-14.90	-5.01	14.90	5.01	0.00	0.00
26	23	10	-9.01	-5.79	9.01	5.79	0.00	0.00
27	18	14	0.01	0.01	-0.01	-0.01	0.00	0.00
28	22	10	0.00	-0.01	-0.00	0.01	0.00	0.00
29	20	23	-0.00	0.01	0.00	-0.01	0.00	0.00
30	17	18	3.79	1.61	-3.78	-1.58	0.01	0.03
31	9	21	5.23	4.25	-5.22	-4.21	0.01	0.03
32	22	9	-9.30	-3.38	9.42	3.63	0.12	0.25
33	19	13	-5.58	-1.61	5.64	1.72	0.05	0.11
							13.381952	23.30

Only the results of test cases A, C, and D are shown here, as they refer to observable systems. The GSE algorithm did not converge for test cases B and E.